FUNGAL LACTAMASES: TESTING AN INDUCTION/FUNCTION HYPOTHESIS

by

MINGLU GAO

(Under the Direction of Scott E. Gold and Anthony E. Glenn)

ABSTRACT

Fusarium verticillioides is one of the most prevalent seed- and wind-borne fungal pathogens on maize, causing severe ear rot symptoms. Alternative to its pathogenic effect, *F. verticillioides* often exists as a symptomless endophyte. Living inside maize tissues, *F. verticillioides* has to cope with antimicrobial phytochemicals such as 2-benzoxazolinone (BOA), which the fungus tolerates better than other fungi due to its ability to hydrolyze the γ-lactam ring via a lactamase encoding gene, *MBL1*. Inspired by the hydrolytic function of MBL1, I examined genomes from across the fungal kingdom for lactamase encoding genes. A strong positive correlation was clearly evident between environmental niche complexity and the number of lactamase encoding genes in a fungal species. A resulting central hypothesis is that many fungal hydrolytic lactamases are responsible for the degradation of, and thus resistance to, plant or microbial xenobiotic lactam compounds encountered in their respective niches (Chapter 2). Pyrrocidine A and B are two lactam-containing antimicrobial compounds produced by a protective maize endophyte, *Sarocladium zeae*, which co-inhabits maize kernels with *F. verticillioides* but maintains tissue specificity (i.e., *S. zeae* in the embryonic area, and *F. verticillioides* in the pedicel). RNA-seq experiments were carried out to elucidate *F. verticillioides'* responses to pyrrocidine exposure and its tolerance mechanism(s). Among 10

pyrrocidine up-regulated genes selected for functional characterization, an ABC transporter gene (FVEG_11089, *FvABC3*) was a primary determinant of pyrrocidine tolerance. Further, a pyrrocidine induced zinc-binding dehydrogenase encoding gene (FVEG_00314, *FvZBD1*) appears to be a heretofore unidentified repressor of fumonisin biosynthesis and lies immediately adjacent to the fumonisin biosynthetic gene cluster. This may be a mechanism by which *S. zeae* pyrrocidines silence *F. verticillioides* secondary metabolism during sympatric interactions in the plant (Chapter 3). Lastly, BOA, 2-oxindole, 2-coumaranone, and chlorzoxazone are four lactam and/or lactone-containing compounds with similar chemical structures, and RNA-seq analysis of *F. verticillioides* exposed to these compounds identified gene clusters responsive to each of the four compounds, indicating substrate and enzymatic specificity (Chapter 4). Overall, this work represents the first in-depth exploration of fungal lactamases and antifungal lactams, underlying their relevance to fitness and resistance to antimicrobials in the environment.

INDEX WORDS: *Fusarium verticillioides*, beta-lactams, beta-lactamases, bioinformatics, molecular antagonisms, pyrrocidine, RNA-seq, fumonisin

FUNGAL LACTAMASES: TESTING AN INDUCTION/FUNCTION HYPOTHESIS

by

MINGLU GAO

BE, Dalian University of Technology, China, 2012

A Dissertation Submitted to the Graduate Faculty of The University of Georgia in Partial Fulfillment of the Requirements for the Degree

DOCTOR OF PHILOSOPHY

ATHENS, GEORGIA

2018

FUNGAL LACTAMASES: TESTING AN INDUCTION/FUNCTION HYPOTHESIS

by

MINGLU GAO

Major Professors:	Scott Gold
	Anthony Glenn
Committee:	Ronald Walcott
	Phillip Brannen
	Zachary Lewis

Electronic Version Approved:

Suzanne Barbour

Dean of the Graduate School

The University of Georgia

August 2018

DEDICATION

This work is dedicated to my parents and my sister, who support me throughout my personal and professional life and encourage me to follow my heart and pursue my goal. To my lovely girlfriend Xi, for your great accompany and emotional comfort. Your kind personality and clear pursuit of life have inspired me to be a better person, and I cannot wait to enjoy more life adventures together.

ACKNOWLEDGEMENTS

I am really fortunate and grateful to acknowledge the following people at UGA and USDA.

I first have to thank my co-major advisor, Dr. Scott Gold, whom I've had a blast working with. Your characteristic yet entertaining Scottism embarks my hidden interest in American politics and "breaking news". I would doubt the success of my research, were it not for your willingness to take me as your student as well as the unique combination of encouragement and pressure. I was granted with freedom to independently pursue interesting research findings, and I surely benefit tremendously as I advance towards my intended profession. I appreciate your strategic wisdom and precautious help in manuscript editing to ensure publishing in an on-time manner. Your thorough and profound speculation on students' behaviors and decent support of students' career prove you a dedicated mentor. I hope someday I would be as perfection-driven, perceptive, and emotional intelligent as you are.

I would also like to thank my co-major advisor, Dr. Anthony Glenn. It's been a pleasure working and publishing with you. I appreciate your professionalism, fairness, meticulousness, assertiveness, and scientific judgment along the way, especially during my degree completion. I am also grateful for the introduction of promising resources and collaboration. Your attention to details have inspired and influenced me a lot, which I hope to carry over in my future career.

Thank you to Dr. Ronald Walcott for your kind suggestions and confidence when I need them the most. Thank you to Dr. Phillip Brannen for your kinds words and help. Your focus on the context of plant pathology is what I want to maintain as I move forward. Thank you to Dr.

Zachary Lewis for bringing up the crucial RNA-seq idea for my experiment design, which I could not imagine without. Thank you to Dr. Scherm for your help throughout the years. We witness and benefit from the changes you bring to the department. Thank you to Dr. Shavannor Smith for the life lessons. The one-hour on the phone prepared me to face the toughness in life. Thank you to Dr. Woodward for the full diagnostic experience. I root for plant pathology. Thank you, Dr. Bacon for supporting me and sharing lab equipment, and my interaction with you has always been joyful and rewarding. My appreciation is also extended to Ms. Dorothy Hinton, and you have always been cheerful and interested in hearing us talking about our lives.

Thank you, Ms. Nicole Crenshaw, for providing us students with exceptional lab support and assistance. My stress and frustration magically disappeared every time you shared your sweet family moment. It means so much to me! I was deeply inspired by how you balance your professional and personal life. I would also like to extend my gratitude to Mr. Trevor Mitchell for the gracious help in developing research methods, without which my work would not proceed thus far. Thank you to Dr. Maurice Snook for your expertise in chemistry and kindness. I am truly motivated by your dedication to extension. It has always been a pleasant experience sharing your hobbies in astronomy, science, post stamps, and trains. You are a role model to me. Thank you to Melinda and Shawn for the fun and laughter we shared.

I would also like to thank my fellow lab mates (past and current), Alex, Manisha, Shan, Stephanie, Garrett, Blake, Felicia, and many more, for the culture talks, academic help, fun time together (Trivia at Johnny's Pizza), and emotional support. Thank you to the Fungal Group at UGA for the informative talks. I would also like to thank my fellow graduate students and UGA emerging leaders, particularly Cynthia Chan, Jessica Chappell and Ansuya Jogi. I really enjoy

hanging out with you. Thank you to my Chinese friends, especially Chang Liu, Gong Chen, and Wujun Zhao, for the diverse activities we experienced together.

Special thanks to the Plant Pathology office staff, Mary Ann, Kisha, Brooke, Judy, Betty and anyone I've missed, who assist the running of the department and ensure us graduate students to get reimbursed and forms submitted. Thank you UGA for providing me with a vision of the reality and future world, from which I master how to adapt.

TABLE OF CONTENTS

Page

LIST OF TABLES

Page

CHAPTER 1

INTRODUCTION AND LITERATURE REVIEW

Fusarium verticillioides is an important pathogen of maize

The large genus *Fusarium* contains soil-borne, plant pathogenic, generally necrotrophic filamentous fungi. *Fusarium* species are important as world-wide cereal pathogens causing severe diseases such as head blight, kernel or ear rot, crown rot, scab, etc., and have led to dramatic economic losses (Nelson et al., 1994). *Fusarium* species are widely distributed in soil, water, aerial plant parts, plant debris and other organic substrates (Elvers et al., 1998; Nelson et al., 1994). *Fusarium verticillioides* is one of the most prevalent fungal plant pathogens of maize. Alternative to severe crop damage such as ear rot, *F. verticillioides* is capable of causing very common symptomless maize infections. Although the seed-borne *F. verticillioides* generally persists as a symptomless endophyte across all reproductive stages, it can be a source for root, stalk and kernel infections (Bacon and Hinton, 1996; Blacutt et al., 2017; Munkvold et al., 1997).

Fusarium verticillioides has been associated with human and animal toxicoses

Contamination of cereals with *F. verticillioides* has been associated with several human and animal diseases (Gelderblom et al., 1991; Marasas et al., 1988; Nir-Paz et al., 2004; Rock, 1997; Ross et al., 1990; Sydenham et al., 1990). Under experimental conditions, cultures of this fungus can lead to leukoencephalomalacia (ELEM) in horses and toxic pulmonary effects in swine (Marasas et al., 1988; Ross et al., 1990). In addition, *F. verticillioides* cultures are hepatotoxic to horses, swine, and rats, and were proven to cause liver cancer in lab rodents after long-term exposure (Gelderblom et al., 1991).

F. verticillioides can be an opportunistic human pathogen, and infection is mainly through inhalation of air-borne conidia or via wounds in the skin due to trauma or burns (Guarro and Gené, 1995). Sporadic cases of fusariosis have been reported, where contamination of hospital water systems resulted in the dispersal of air-borne conidia, and patients undergoing immunosuppressive therapy or haematopoietic stem cell transplantation were more prone to infection (Nucci and Anaissie, 2007; Suleyman and Alangaden, 2016). In 1994, a nosocomial pseudo-outbreak was reported in Italy, when hospital reconstruction and renovation introduced *F. verticillioides,* and led to bloodstream infections among severely immunocompromised patients (Suleyman and Alangaden, 2016).

***Fusarium verticillioides* can produce fumonisin and several other types of mycotoxins**

An outbreak of esophageal cancer as well as ELEM in the Transkei region in South Africa drew attention to the fungus *F. verticillioides*, since its occurrence was prevalent in high-incidence areas of moldy home-grown corn (Marasas et al., 1984, 1988; Sydenham et al., 1990). In subsequent toxicological investigations of *F. verticillioides* isolates from corn in the Transkei, one of these isolates, designated MRC 826, was found to cause esophageal cancer and ELEM in feeding experiments (Marasas et al., 1988). In 1988, fumonisins, a family of secondary metabolites contributing to the same pathological changes with those of ELEM, were first isolated from MRC 826 and chemically characterized during the same year by a group of South African scientists (Bezuidenhout et al., 1988). It was a landmark in food safety research because *F. verticillioides* was not previously considered a major concern until its production of fumonisins was discovered.

While *F. verticillioides* can also produce other mycotoxins and biologically active metabolites such as fusaric acid, fusarin C, and naphthoquinones (Bacon et al., 1996; Steyn et al.,

1979; Wiebe and Bjeldanes, 1981), fumonisins are of highest importance due to their toxicity to animals and humans. Since their discoveries, numerous strains have been reported to produce high levels of B-series fumonisins and low levels of their derivatives, but only fumonisin B1, B2, B3 and B4 have been found in naturally contaminated foods, with B1 being the most toxic and abundant (Covarelli et al., 2012; Soriano and Dragacci, 2004). The chemical structure of fumonisin B1 (FB1) resembles sphinganine, and the primary mechanism of action of this mycotoxin is through its competitive inhibition of ceramide synthase resulting in the disruption of *de novo* biosynthesis of ceramide and of sphingolipid metabolism (Bezuidenhout et al., 1988; Soriano et al., 2005). Since sphingolipids are found in cell membranes, particularly nerve cells and brain tissues, their disruption could lead to altered cell growth, apoptosis, differentiation, carcinogenicity, and cell injury (Soriano et al., 2005).

Detoxification of plant benzoxazinones correlates with *F. verticillioides* colonization of maize and wheat

The production of mycotoxins by *F. verticillioides* is viewed as a food safety issue and has given rise to significant concern worldwide. The importance of reducing fumonisin levels by inhibiting the growth of *F. verticillioides* has been addressed. Fortunately, plants possess various defensive mechanisms to respond to pathogenic challenges, and in some cases, antibiosis is adopted to antagonize invading pathogens. Several important cereal crops such as maize, rye and wheat can constitutively produce benzoxazinones DIMBOA (2,4-dihydroxy-7-methoxy-2H-1, 4-benzoxazin-3-one) and DIBOA (2,4-dihydroxy-2H-1, 4-benzoxazin-3-one) that confer resistance towards certain bacterial or fungal pathogens (Niemeyer, 1988). Free DIMBOA and DIBOA can spontaneously degrade to the corresponding benzoxazolinones, the MBOA (6-methoxy-2-benzoxazolinone) and BOA (2-benzoxazolinone), respectively (Woodward et al., 1978), which

show fungistatic effects against many *Fusarium* species (Glenn et al., 2001). However, *F. verticillioides* can tolerate MBOA or BOA by converting them into non-toxic metabolites (Glenn et al., 2001, 2002, 2016; Glenn and Bacon, 2009; Saunders and Kohn, 2008; Yue et al., 1998) (Fig. 1.1). The capability of bio-transforming plant toxins enhances the survival of *F. verticillioides* and provides the basis for its colonization of this ecological niche.

Beta-lactamases are functionally involved in hydrolysis, biosynthesis, DNA repair, etc.

In 2002, Glenn et al. genetically analyzed *F. verticillioides* strains based on segregation analysis and UV mutagenesis. The segregation results indicated two loci, *FDB1* and *FDB2*, were involved in detoxification, and mutation at either locus would result in sensitivity to MBOA/BOA (Glenn et al., 2002). We now know from genomic and transcriptional analyses that these two loci constitute lactamase-containing gene clusters. Deletion of the metallo-beta-lactamase gene (FVEG_08291, *MBL1*) in the *FDB1* cluster resulted in failure to hydrolyze the BOA lactam ring, and mutant strains showed significantly elevated *in vitro* sensitivity to BOA (Glenn et al., 2016). The above functional characterization of fungal lactamases and the identification of 45 additional putative lactamase encoding genes inspired me to investigate functional analyses of fungal lactamases. Importantly for the studies described in this dissertation, *MBL1* transcription is highly induced by BOA, its toxic substrate, to which the *MBL1* encoded lactamase confers resistance. Leveraging this paradigm, a central hypothesis of the work described here is that xenobiotic induction of xenobiotic remediating enzyme encoding genes will lead us to the identification of those genes. This hypothesis can be described as an "Induction/Function" hypothesis.

β-lactamases are important in bacteria for their roles in resisting bactericidal lactam antibiotics. The substrates, β-lactams, disrupt synthesis of the bacterial peptidoglycan cell wall

and have been a cornerstone of modern medicine. However, fungal cell walls are structurally unrelated to those of bacteria, and β-lactam antibiotics generally have no effect on fungal growth. This indicates gaps in current knowledge: why do fungi have β-lactamases if β-lactams have no effect upon them? Observation of fungal genomes indicates that β-lactamase genes are abundant in fungi. Comparison of related fungi from relatively axenic environments versus soil-borne species indicates that soil inhabitants are dramatically enriched in these enzymes (as much as 15-fold). This reveals another knowledge gap: What is the function of the amplified gene families encoding β-lactamase enzyme in soil inhabiting fungi?

In addition to lactam hydrolysis, beta-lactamases were also reported with other functions, such as biosynthesis, DNA repair, and RNA processing. A physically discrete MBL type thioesterase in *Aspergillus fumigatus* was also found to be indispensable for endocrocin biosynthesis, when its deletion abolished endocrocin production (Lim et al., 2012). Another beta-lactamase motif in *S. cerevisiae* designated as Snm1 was required for DNA double-strand break (DSB) repair, and it appeared to act in processing DSB repair intermediates (Li and Moses, 2003). Some members of beta-lactamases are also related to redox processes, DNA uptake, and RNA processing (Aravind, 1999). Although beta-lactamases take on various functions in different biological processes, we focus our research on the observed MBOA/BOA degradation model and their ability to hydrolyze toxic compounds.

To address these questions above, my research aimed to 1) explore the occurrence and abundance of fungal beta-lactamase encoding genes in fungi, with *Fusarium verticillioides* as the paradigm; 2) investigate the transcriptomic responses of *F. verticillioides* upon exposure to pyrrocidines and several lactam-containing compounds, and 3) explore the role of lactam moieties in antifungals and elucidate the microbial antagonistic interactions between two maize

endophytes, *F. verticillioides* and *S. zeae*. Overall, the work presented in this dissertation was guided by the following objectives:

1. Bioinformatically characterize beta-lactamase-encoding genes in fungi, with *F. verticillioides* serving as a paradigm (Chapter 2)
2. Assess the impact of pyrrocidine lactam challenge on the *F. verticillioides* transcriptome and functionally characterize select interesting induced genes (Chapter 3)
3. Compare the transcriptomic responses of lactam or lactone-containing benzoxazolinone-like compounds in *F. verticillioides* (Chapter 4)

What do RNA sequencing and functional characterization tell us?

RNA-seq has become one of the major strategies to evaluate expression levels upon drug exposure, since the experiment design does not necessarily rely on prior knowledge. RNA-seq possesses several advantages over microarray technologies in that 1) RNA-seq can identify unknown transcripts quantitatively; 2) RNA-seq is more cost-effective; 3) RNA-seq has a high level of data reproducibility (Agarwal et al., 2010). Messenger RNA conveys information from DNA to the ribosome, and its brief existence begins with transcription and ends with degradation. Generally, the abundance of mature mRNA represents the level of transcription. Thus, numerous research experiments have been designed to alter the mRNA expression levels in order to reveal the function of relevant genes. In this dissertation, I proposed to the identify the *F. verticillioides* genes involved in resistance to lactam-containing xenobiotic compounds. Based on the Induction/Function hypothesis suggested by the *MBL1* paradigm in objectives 2 and 3 above, we exposed the fungus in lactam-treated and non-treated control groups. Following the bioinformatics analyses, responsive genes of interest were selected for conventional functional

characterization by generating single deletion mutants and observing phenotypes elicited by gene deletions.

REFERENCES

Agarwal, A., Koppstein, D., Rozowsky, J., Sboner, A., Habegger, L., Hillier, L. W., et al. (2010). Comparison and calibration of transcriptome data from RNA-Seq and tiling arrays. *BMC Genomics* 11. doi:10.1186/1471-2164-11-383.

Aravind, L. (1999). An evolutionary classification of the metallo-beta-lactamase fold proteins. *Silico Biol* 1, 69–91. Available at: http://www.ncbi.nlm.nih.gov/pubmed/11471246%5Cnhttp://iospress.metapress.com/content/7wu0chexlj69nwmt/?genre=article&issn=1386-6338&volume=1&issue=2&spage=69.

Bacon, C. W., and Hinton, D. M. (1996). Symptomless endophytic colonization of maize by *Fusarium moniliforme*. *Can. J. Bot.* 74, 1195–1202. doi:10.1139/b96-144.

Bacon, C. W., Porter, J. K., Norred, W. P., and Leslie, J. F. (1996). Production of fusaric acid by *Fusarium* species. *Appl. Environ. Microbiol.* 62, 4039–4043. Available at: http://aem.asm.org/content/62/11/4039.full.pdf.

Bezuidenhout, S. C., Gelderblom, W. C. A., Gorst-Allman, C. P., Horak, R. M., Marasas, W. F. O., Spiteller, G., et al. (1988). Structure elucidation of the fumonisins, mycotoxins from *Fusarium moniliforme*. *J. Chem. Soc. Chem. Commun.*, 743. doi:10.1039/c39880000743.

Blacutt, A. A., Gold, S., Voss, K. A., Gao, M., and Glenn, A. E. (2017). *Fusarium verticillioides* : Advancements in understanding the toxicity, virulence, and niche adaptations of a model mycotoxigenic pathogen of maize. *Phytopathology*, PHYTO-06-17-0203-RVW. doi:10.1094/PHYTO-06-17-0203-RVW.

Covarelli, L., Stifano, S., Beccari, G., Raggi, L., Lattanzio, V. M. T., and Albertini, E. (2012). Characterization of *Fusarium verticillioides* strains isolated from maize in Italy: Fumonisin production, pathogenicity and genetic variability. *Food Microbiol.* 31, 17–24. doi:10.1016/j.fm.2012.02.002.

Elvers, K. T., Leeming, K., Moore, C. P., and Lappin-Scott, H. M. (1998). Bacterial-fungal biofilms in flowing water photo-processing tanks. *J.Appl.Microbiol.* 84, 607–618. doi:10.1046/j.1365-2672.1998.00388.x.

Gelderblom, W. C. A., Kriek, N. P. J., Marasas, W. F. O., and Thiel, P. G. (1991). Toxicity and carcinogenicity of the *Fusarium moniliforme* metabolite, fumonisin-B1, in rats. *Carcinogenesis* 12, 1247–1251. doi:Doi 10.1093/Carcin/12.7.1247.

Glenn, a E., Gold, S. E., and Bacon, C. W. (2002). *Fdb1* and *Fdb2*, *Fusarium verticillioides* loci necessary for detoxification of preformed antimicrobials from corn. *Mol. Plant. Microbe. Interact.* 15, 91–101. doi:10.1094/MPMI.2002.15.2.91.

Glenn, A. E., and Bacon, C. W. (2009). *FDB2* encodes a member of the arylamine N-acetyltransferase family and is necessary for biotransformation of benzoxazolinones by *Fusarium verticillioides*. *J. Appl. Microbiol.* 107, 657–671. doi:10.1111/j.1365-2672.2009.04246.x.

Glenn, A. E., Davis, C. B., Gao, M., Gold, S. E., Mitchell, T. R., Proctor, R. H., et al. (2016). Two horizontally transferred xenobiotic resistance gene clusters associated with detoxification of benzoxazolinones by *Fusarium* species. *PLoS One* 11, e0147486. doi:10.1371/journal.pone.0147486.

Glenn, A. E., Hinton, D. M., Yates, I. E., and Bacon, C. W. (2001). Detoxification of corn antimicrobial compounds as the basis for isolating *Fusarium verticillioides* and some other *Fusarium* species from corn. *Appl Env. Microbiol* 67, 2973–2981. doi:10.1128/AEM.67.7.2973-2981.2001.

Guarro, J., and Gené, J. (1995). Opportunistic fusarial infections in humans. *Eur. J. Clin. Microbiol. Infect. Dis.* 14, 741–754. doi:10.1007/BF01690988.

Kettle, A. J., Carere, J., Batley, J., Benfield, A. H., Manners, J. M., Kazan, K., et al. (2015). A γ-lactamase from cereal infecting *Fusarium* spp. catalyses the first step in the degradation of the benzoxazolinone class of phytoalexins. *Fungal Genet. Biol.* 83, 1–9. doi:10.1016/j.fgb.2015.08.005.

Li, X. R., and Moses, R. E. (2003). The beta-lactamase motif in Snm1 is required for repair of DNA double-strand breaks caused by interstrand crosslinks in S-cerevisiae. *DNA Repair (Amst)*. 2, 121–129. doi:Pii S1568-7864(02)00192-1Doi 10.1016/S1568-7864(02)00192-1.

Lim, F. Y., Hou, Y., Chen, Y., Oh, J. H., Lee, I., Bugni, T. S., et al. (2012). Genome-based cluster deletion reveals an endocrocin biosynthetic pathway in *Aspergillus fumigatus*. *Appl. Environ. Microbiol.* 78, 4117–4125. doi:10.1128/AEM.07710-11.

Marasas, W. F., Kellerman, T. S., Gelderblom, W. C., Coetzer, J. a, Thiel, P. G., and van der Lugt, J. J. (1988). Leukoencephalomalacia in a horse induced by fumonisin B1 isolated from *Fusarium moniliforme*. *Onderstepoort J. Vet. Res.* 55, 197–203.

Marasas, W. F. O., Nelson, P. E., and Toussoun, T. A. (1984). *Toxigenic Fusarium species, identity and mycotoxicology*. University Park, Pa.: Pennsylvania State University Press.

Munkvold, G. P., McGee, D. C., and Carlton, W. M. (1997). Importance of different pathways for maize kernel infection by *Fusarium moniliforme*. *Phytopathology* 87, 209–217. doi:10.1094/PHYTO.1997.87.2.209.

Nelson, P. E., Dignani, M. C., and Anaissie, E. J. (1994). Taxonomy, biology, and clinical aspects of *Fusarium* species. *Clin. Microbiol. Rev.* 7, 479–504. doi:10.1128/CMR.7.4.479.Updated.

Niemeyer, H. M. (1988). Hydroxamic acids (4-hydroxy-1,4-benzoxazin-3-ones), defence chemicals in the gramineae. *Phytochemistry* 27, 3349–3358. doi:10.1016/0031-9422(88)80731-3.

Nir-Paz, R., Strahilevitz, J., Shapiro, M., Keller, N., Goldschmied-Reouven, A., Yarden, O., et al. (2004). Clinical and epidemiological aspects of infections caused by *Fusarium* species: a collaborative study from Israel. *J Clin Microbiol* 42, 3456–3461. doi:10.1128/JCM.42.8.3456-3461.2004.

Nucci, M., and Anaissie, E. (2007). *Fusarium* infections in immunocompromised patients. *Clin.Microbiol.Rev.* 20, 695–704. doi:10.1128/CMR.00014-07.

Rock, L. (1997). *Fusarium*, a significant emerging pathogen in patients with hematologic malignancy: ten years' experience at a cancer center and implications for management. *Blood* 90, 999–1008. Available at: http://www.bloodjournal.org/content/bloodjournal/90/3/999.full.pdf.

Ross, P. F., Nelson, P. E., Richard, J. L., Osweiler, G. D., Rice, L. G., Plattner, R. D., et al. (1990). Production of fumonisins by *Fusarium moniliforme* and *Fusarium proliferatum* isolates associated with equine leukoencephalomalacia and a pulmonary-edema syndrome in swine. *Appl. Environ. Microbiol.* 56, 3225–3226.

Saunders, M., and Kohn, L. M. (2008). Host-synthesized secondary compounds influence the *in vitro* interactions between fungal endophytes of maize. *Appl Env. Microbiol* 74, 136–142. doi:10.1128/AEM.01538-07.

Soriano, J. M., and Dragacci, S. (2004). Occurrence of fumonisins in foods. *Food Res. Int.* 37, 985–1000. doi:Doi 10.1016/J.Foodres.2004.06.009.

Soriano, J. M., Gonzalez, L., and Catala, A. I. (2005). Mechanism of action of sphingolipids and

their metabolites in the toxicity of fumonisin B1. *Prog. Lipid Res.* 44, 345–356. doi:Doi 10.1016/J.Plipres.2005.09.001.

Steyn, P. S., Wessels, P. L., and Marasas, W. F. O. (1979). Pigments from *Fusarium moniliforme* sheldon. Structure and 13C nuclear magnetic resonance assignments of an azaanthraquinone and three naphthoquinones. *Tetrahedron* 35, 1551–1555. doi:10.1016/0040-4020(79)80043-5.

Suleyman, G., and Alangaden, G. J. (2016). Nosocomial fungal infections: Epidemiology, infection control, and prevention. *Infect. Dis. Clin. North Am.* 30, 1023–1052. doi:10.1016/j.idc.2016.07.008.

Sydenham, E. W., Thiel, P. G., Marasas, W. F. O., Shephard, G. S., Van Schalkwyk, D. J., and Koch, K. R. (1990). Natural occurrence of some *Fusarium* mycotoxins in corn from low and high esophageal cancer prevalence areas of the Transkei, Southern Africa. *J. Agric. Food Chem.* 38, 1900–1903. doi:10.1021/jf00100a004.

Wiebe, L. A., and Bjeldanes, L. F. (1981). Fusarin C, a mutagen from *Fusarium moniliforme* grown on corn. *J. Food Sci.* 46, 1424–1426. doi:Doi 10.1111/J.1365-2621.1981.Tb04189.X.

Woodward, M. D., Corcuera, L. J., Helgeson, J. P., and Upper, C. D. (1978). Decomposition of 2,4-dihydroxy-7-methoxy-2H-1,4-benzoxazin-3(4H)-one in aqueous solutions. *Plant Physiol.* 61, 796–802. Available at: http://www.plantphysiol.org/cgi/content/abstract/61/5/796.

Yue, Q., Bacon, C. W., and Richardson, M. D. (1998). Biotransformation of 2-benzoxazolinone and 6-methoxy-benzoxazolinone by *Fusarium moniliforme*. *Phytochemistry* 48, 451–454. doi:10.1016/S0031-9422(98)00013-2.

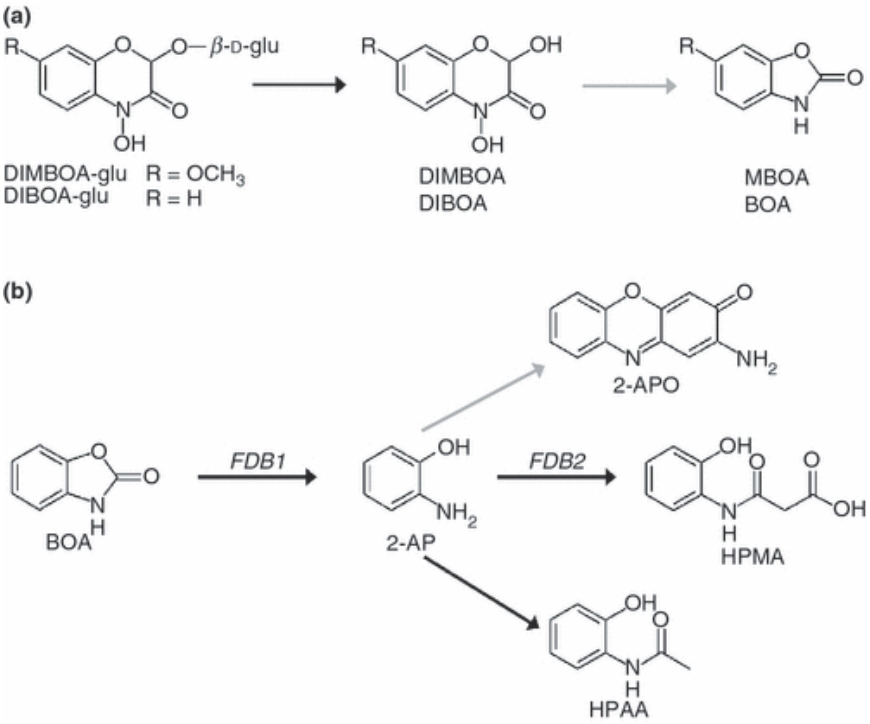

Figure 1.1. Production pathway of DIMBOA, **DIBOA**, **MBOA**, **and BOA and the *F. verticillioides* biotransformation pathway of BOA into various metabolites.** (a) Maize initially produces DIMBOA (2,4-dihydroxy-7-methoxy-2H-1, 4-benzoxazin-3-one) and DIBOA (2,4-dihydroxy-2H-1,4-benzoxazin-3-one) as glucosides, which are released as free metabolites by a beta-glucosidase upon cellular damage. These two compounds have inherent instability and naturally convert into MBOA (6-methoxy-2-benzoxazolinone) and BOA (2-benzoxazolinone), respectively (gray arrow indicates nonenzymatic reaction). (b) BOA is hydrolyzed by *F. verticillioides* into the intermediate 2-aminophenol (2-AP) by one or more genes encoded at the *FDB1* locus. 2-AP is acylated by the *FDB2* locus to produce *N*-(2-hydroxyphenyl)malonamic acid (HPMA). A branch in the pathway is most evident in *fdb2* mutant strains, which have limited accumulation of *N*-(2-hydroxyphenyl)acetamide (HPAA) owing to acetylation of 2-AP. The gray arrow indicates nonenzymatic oxidation of 2-AP producing 2-amino-3*H*-phenoxazin-3-one (2-APO) (Glenn and Bacon, 2009).

CHAPTER 2

FUNGAL LACTAMASES, THEIR OCCURRENCE AND FUNCTION

Gao, M., Glenn, A. E., Blacutt, A. A., & Gold, S. E. (2017). Fungal lactamases: their occurrence and function. *Frontiers in microbiology*, *8*, 1775. Reprinted with permission from the publisher

ABSTRACT

Fungi are absorptive feeders and thus must colonize and ramify through their substrate to survive. In so doing they are in competition, particularly in the soil, with myriad microbes. Additionally, these microbes use xenobiotic compounds as offensive weapons to compete for nutrition, and fungi must be sufficiently resistant to these xenobiotics. One prominent mechanism of xenobiotic resistance is through production of corresponding degrading enzymes. As typical examples, bacterial β-lactamases are well known for their ability to degrade and consequently confer resistance to β-lactam antibiotics, a serious emerging problem in health care. We have identified many fungal genes exhibiting a high degree of similarity to β-lactamases. However, fungal cell walls are structurally unrelated to the bacterial peptidoglycan target of β-lactams. This raises the question, why do fungi have lactamases and what are their functions? Previously, we identified and characterized one *Fusarium verticillioides* lactamase gene (FVEG_08291) that confers resistance to the benzoxazinoid phytoanticipins produced by maize and several other grain crop species. Since benzoxazinoids are γ-lactams with five-membered rings rather than the four-membered β-lactams, we refer to the predicted enzymes simply as lactamases, rather than β-lactamases. An overview of fungal genomes suggests a strong positive correlation between environmental niche complexity and the number of fungal lactamase encoding genes, with soil-borne fungi showing dramatic amplification of lactamase genes compared to those fungi found in less biologically complex environments. Remarkably, *Fusarium* species frequently possess large numbers of (>40) lactamase genes. We hypothesize that many fungal hydrolytic lactamases are responsible for the degradation of plant or microbial xenobiotic lactam compounds. Phylogenic studies of the lactamase-encoding genes in *F. verticillioides* indicate most are consistent with vertical inheritance while two may have a history of horizontal gene transfer. Alignment of protein

sequences revealed two conserved patterns resembling bacterial β-lactamases, specifically those possessing PFAM domains PF00753 or PF00144. Structural predictions of *F. verticillioides* lactamases also suggested similar catalytic mechanisms to those of their bacterial counterparts. Overall, we present the first in-depth analysis of both "metallo-β-lactamases" (PF00753) and "serine-based β-lactamases" (PF00144) in fungi, and we discuss their potential relevance to fitness and resistance to antimicrobials in the environment.

INTRODUCTION

The soil is one of the most complex habitats on earth due primarily to the diversity of microorganisms that inhabit it and the myriad biochemical products they secrete. Experiments utilizing metagenomic technologies estimate up to several million species of bacteria per gram in some naturally occurring soils (Gans, 2006). The majority of these species are, to date, uncultured. For fungi, less information is available, but global estimates of 6 million soil fungi were suggested based on comprehensive molecular studies (Taylor et al., 2014). This microbial diversity creates a dynamic environment for microorganisms to communicate and compete for limited resources. Further, metabolic processes of microbes together with plants act as significant sources of chemical diversity, and microbes in the soil milieu are constantly and unavoidably exposed to foreign chemicals (xenobiotics). Some xenobiotics are easily tolerated and degraded, while others have inhibitory effects (Parkinson et al., 2001). Xenobiotics that are deleterious to the growth or metabolic activities of other microorganisms can be considered antibiotics, and play critical ecological roles in competitive interactions (Davelos et al., 2004; Kinkel et al., 2012; Thomashow et al., 1997). It has been posited that microorganisms and plants have adopted antibiotic production as offensive and/or defensive strategies to adjust to changing circumstances, allowing microbial colonization in the rhizosphere or persistence of plants in the environment (Lynch et al., 2004).

Compared to the surrounding soil, the rhizosphere of plants can be particularly rich in nutrients (Marschner et al., 2004). This microbial oasis stimulates competitive and antagonistic relationships among would-be colonizers. For example, phenazine production by Pseudomonads and trifolitoxin production from certain *Rhizobium* species correlate with soil survival and suppressive activity, demonstrating that antibiotic production can be integral to niche competition and microbial community structure (Mazzola et al., 1992; Robleto et al., 1998).

Antibiotic production by both plants and microbes is a remarkable strategy possibly adopted in response to their sessile nature and limited mobility, respectively (Agrawal, 2011; Grotewold, 2005). Heritable genetic alterations such as mutation, gene duplication/modification, and horizontal gene transfer have expanded the antibiotic repertoires of plants and microbes. (Soucy et al., 2015). A number of antibiotics have been detected from soil or produced by soil microbes and display *in vivo* or *in vitro* antagonistic effects, such as penicillin, trichothecene, chloromycetin, actinomycin, clavacin, griseofulvin, etc. (Kinsella et al., 2009; Stallings, 1954). Yet, antibiotics can occur in nature at sub-inhibitory concentrations, and rather than inhibiting growth, the compounds elicit transcriptional responses suggestive of a form of microbial communication (Davies, 2006; Goh et al., 2002). In addition to microbial sources, compounds with antibiotic activity are also found in plants (Bozdogan and Appelbaum, 2004; González-Lamothe et al., 2009; VanEtten et al., 1994). Maackiain is a plant-derived antibiotic extracted from red clover and alfalfa. Previous work has shown that maackiain is toxic to several genera of fungal pathogens of legume and non-legume hosts (Delserone et al., 1992; Duczek and Higgins, 1976). Maize, wheat and rye can constitutively produce benzoxazinones and benzoxazolinones, which help reduce insect damage and confer resistance to various fungal and bacterial pathogens (Couture et al., 1971; Elizabeth et al., 1977; Glenn et al., 2016).

To combat antibiosis, bacteria have developed resistance mechanisms such as efflux pumps and hydrolytic enzymes. Notorious among the latter group, β-lactamases have been thoroughly studied due to the resistance they confer to the widespread clinically used β-lactam antibiotics. Parallel to the presence in bacteria, genes encoding "β-lactamases" are also abundant across different fungal families. In contrast to bacteria, almost nothing is known about the function of these genes in fungi. Previous work is limited to two studies on the hydrolytic function of lactamase encoding genes with strong homology to metallo-β-lactamases in *Fusarium verticillioides* and *Fusarium pseudograminearum* (Glenn et al., 2016; Kettle et al., 2015b) . This evidence serves as a foundational paradigm for studying hydrolytic lactamases in fungi and prompts the hypothesis that, as in bacteria, many of these enzymes function in degradation and resistance to xenobiotic compounds. Here we will describe an initial look at the distribution of lactamase-encoding genes in fungi and speculate on their ecological roles. We will also describe current and planned approaches to decipher the roles of 46 lactamase-family genes in the *F. verticillioides* genome.

LACTAMS – THE ARCHETYPICAL CLASS OF ANTIBIOTICS

Bactericidal β-lactams

β-lactams comprise the largest group of antibiotics, and they have been extensively utilized for their antibacterial effect (Tipper, 1985). Beginning with Alexander Fleming's Nobel Prize-winning serendipitous discovery of a penicillin-producing mold (Fleming, 1929), β-lactams and their semisynthetic derivatives have been the most impactful antibiotics in medicine (Demain and Elander, 1999; Lewis, 2013). Their mode of action is well characterized and involves a four-membered cyclic amide ring (Fig. 2.1) that occupies the catalytic sites of transpeptidases, also referred to as penicillin-binding proteins. These proteins are essential for cross-linking

peptidoglycan layers of bacterial cell walls, thus β-lactam antibiotics disrupt bacterial cell wall synthesis, resulting in cell lysis (Waxman and Strominger, 1983).

Lactam production in fungi

Fungi are the original source of two foundational β-lactam antibiotics: penicillin and cephalosporin. These drugs are still industrially produced, primarily using *Penicillium chrysogenum* and *Acremonium chrysogenum* (previously *Cephalosporium*), respectively (Brakhage et al., 2009). Lactam production in fungi is frequently coordinated through the activity of gene clusters containing necessary biosynthetic enzymes and pathway-specific transcriptional regulators (Brakhage et al., 2009; Brakhage and Schroeckh, 2011; Khaldi et al., 2010; Osbourn, 2010). Fungal gene clusters are hypothesized to assist in retention of biochemical functions by reducing gene loss due to recombination in highly dynamic genomes (Osbourn, 2010). Fungal genomes provide enormous potential to produce many complex lactam-containing compounds (Fig. 2.2), including higher order lactam compounds (e.g., five-membered, γ-lactam rings). Two new hetero-spirocyclic γ-lactams, azaspirofurans A and B, were isolated from a marine sediment-derived fungus *Aspergillus sydowi* (Ren et al., 2010). A maize seed-borne endophyte *Sarocladium zeae* (formerly *Acremonium zeae*) was found to produce γ-lactam compounds, named pyrrocidine A and B (He et al., 2002). Further, the cytotoxic awajanomycin from *Acremonium* species, cytochalasins from *Rhinocladiella,* and colletotrilactams A-D from endophytic *Colletotrichum gloeosporioides* all exemplify fungal production of higher order lactams (Jang et al., 2006; Wagenaar et al., 2000; Wei et al., 2016). Such lactam production among fungi diversifies xenobiotic composition in soil and may contribute to the discovery of new valuable antibiotics.

Antifungal lactams

In addition to the fungal production of bactericidal lactams, emerging evidence indicates that certain atypical lactams can be fungistatic or fungicidal regardless of their origins (Fig. 2.3) (Brakhage et al., 2009). Novel monocyclic N-thiolated β-lactams revealed varying degrees of *in vitro* antifungal activity against seven *Candida* species (Culbreath, 2006; Perea and Patterson, 2002). The fungistatic mode of action against *Candida* was postulated to simulate what was observed against *Staphylococcus aureus*, where these lactams diffused through the cell membrane and interacted covalently with an unknown and possibly evolutionarily conserved target (Culbreath, 2006). Two synthetic azetidin-2-one compounds showed moderate antifungal activity against *Botrytis cinerea, Colletotrichum lindemuthianum* and the oomycete *Phytophthora infestans* (Arnoldi et al., 1990). Previously mentioned pyrrocidine A and B from *S. zeae* are antagonistic to kernel rotting fungi including *Aspergillus flavus* and *F. verticillioides* (Wicklow et al., 2005). Interestingly, pyrrocidine A differs from B only in that it possesses a double bond in the γ-lactam ring, and pyrrocidine A shows inhibition at a lower concentration than does B, implying the relevance of the lactam ring to antibiosis. Alternatively, structural conformation changes conveyed by the single vs. double bond could potentially play a role in the observed differential toxicity. Recent studies on synthetic bicyclic lactam analogs of natural plant derived lactones have also revealed their fungistatic effects against *B. cinerea*, *Penicillium citrinum,* and *Aspergillus glaucus* (Walczak et al., 2014). For example by replacing an oxygen atom with nitrogen in the five-membered ring during a heteroatom analysis of *cis*-3-oxabicyclo-[4.3.0]non-7-en-2-one created a novel γ-lactam compound with a significant increase in antifungal activity (Walczak et al., 2014). These discoveries should stimulate further exploration of antifungal lactams and their modes of action.

β-LACTAMASES

Lactam resistance

The spread of antibiotic resistance among bacteria is one of today's major world health concerns (Berendonk et al., 2015). In fact, many current publications in the popular press are predicting the end of the age of antibiotics in the near future (Sun and Dennis, 2016), and the World Health Organization recently held a conference on the subject entitled "The end of antibiotics?" Natural sources and clinical/agricultural overuse of antibiotics impose selection pressure for antibiotic resistance, leading to a rise in the number of resistant microbes and the spread of resistant genes regardless of their origins (Allen et al., 2010; Chang et al., 2015). Currently, three major mechanisms have been proposed to generate resistance to β-lactam antibiotics (Fig. 2.4): 1) restricted access to drug targets either by a) preventing drug entry or b) enhanced drug efflux (Li et al., 1994), 2) alteration of drug targets (Malouin and Bryan, 1986), or 3) the presence of drug-degrading enzymes (Fernandes et al., 2013). Moderate lactam resistance may be developed by intragenic recombination, where genetically distinct alleles occasionally are produced. Such events generate, for example, new alleles of mosaic transpeptidase (penicillin target protein) genes with low penicillin-binding affinities (Campos et al., 1992; Zhang et al., 1990). Horizontal gene transfer (HGT) was proposed decades ago as another means of acquisition of lactam resistance. HGT appears responsible for the spread of resistance-conferring transpeptidases and plasmid-encoded β-lactamases contributing to high-level lactam resistance and the appearance of "superbugs" with resistance to most or all current antibiotic therapies (Coffey et al., 1993; Davies et al., 2010; Dowson et al., 1990; Weldhagen, 2004).

Bacterial β-lactamases

β-lactamase enzymes are the most common mechanism of resistance to β-lactam antibiotics, hydrolyzing the lactam bond in their four-membered ring structures to abolish activity (Livermore, 1998). As these antibiotics are classically active against peptidoglycan cell wall synthesis, the corresponding hydrolytic β-lactamases result in high prevalence of resistant strains and a potential increase in virulence. The first penicillin-hydrolyzing β-lactamase identified was an AmpC cephalosporinase in *Escherichia coli* in 1940, several years before the actual introduction of penicillin into clinical practice (Abraham and Chain, 1940).

Two primary schemes of classifying bacterial β-lactamases have been proposed, based primarily on functionality or molecular characteristics (Table 2.1). The first classification scheme based on functionality divides bacterial β-lactamases into three major groups based on inhibitory specificities and the potential requirement of zinc ion for activity (Bush et al., 1995; Frère, 1995). Group 1 includes cephalosporinases that are not well inhibited by clavulanic acid. Group 2 encompasses β-lactamases that are inhibited by active site-directed β-lactamase inhibitors, such as clavulanic acid. Group 3 refers to metallo-β-lactamases (MBLs) that require zinc ions for activity. In addition to conventional hydrolases targeting β-lactams, the MBL superfamily includes lactonases that hydrolyze lactone bonds. A classic example is the N-acyl homoserine lactonases produced by various bacteria. These enzymes are able to inactivate N-acyl homoserine lactones by hydrolyzing the lactone bond, resulting in quenching of bacterial quorum-sensing signaling (Dong et al., 2001; Riaz et al., 2008). The necessity of zinc ions is suspected by the universal presence of a conserved di-nuclear zinc binding site in known lactonases and confirmed by zinc's essential role during catalytic activity and protein folding (Thomas et al., 2005). The second scheme for classification of β-lactamases utilizes nucleotide and amino acid sequences to divide them into

four molecular classes designated A-D (Bush et al., 1995). Enzymes belonging to class A, C and D act by a serine-based mechanism, often containing Pfam domain PF00144. Those in class B are zinc-based MBLs with Pfam domain PF00753, equivalent to functional Group 3. Serine-based β-lactamases (SBLs) possess conserved motifs S-X-X-K, S/Y-X-N/V, and K-T/S-G in that order, where the serine in the first motif serves as the active site targeting the β-lactam ring. Class B β-lactamases contain a primary zinc-binding motif H-X-H-X-D-H followed by conserved amino acids of Gly, Leu, His, Gly, Asn, and His at specific positions. Except for these conserved amino acids, the rest of their sequences are generally divergent, with greatly differing tertiary structures and catalytic efficiencies (Ehmann et al., 2012).

Fungal lactamases

Interestingly, genes identified with β-lactamase homology are widely distributed across major taxa. As of March 1, 2017, there were 1,096,469 manually and computationally annotated β-lactamase genes reported in the National Center for Biotechnology Information (NCBI) protein database across all kingdoms of life. As depicted in Figure 2.5, 93% of them (1,021,177 genes) lie in the domain Bacteria. Although non-bacterial lactamases share similarities with those found in bacteria, less than 1% have been functionally characterized. It is very likely that many non-bacterial "β-lactamases" are not involved in degrading classic β-lactams, so we will refer to them simply as lactamases below. Interestingly, of the roughly one million database entries with suspected β-lactamase homologues, 14,923 genes were found in fungi, which represents approximately half of the Eukaryotic total (29,804 genes). Due to ever-increasing affordability and ease of sequencing, newly identified genes encoding putative lactamases are being added at an accelerating rate to databases.

As mentioned above, a large number of fungal lactamases have been identified and annotated, frequently containing Pfam domains PF00753 or PF00144, as in bacteria. However, only a few gene products have confirmed functions. Model species, *Saccharomyces cerevisiae,* possesses a small core set of highly conserved enzymes with lactamase domains, but they tend to have specialized functions not involving lactam hydrolysis (Table 2.2). The essential gene *TRZ1* from *S. cerevisiae* encodes tRNase Z, involved in RNA processing (Chen et al., 2005; Zhelkovsky et al., 2006). The essential endonuclease YSH1 in *S. cerevisiae* contains a MBL domain and plays key roles in pre-mRNA 3' end formation, cooperating with other cleavage factors (Stumpf and Domdey, 1996). Filamentous fungi, including *Fusarium* (Table 2.2), possess YSH1 and TRZ1 orthologs in their genomes. Non-essential fungal lactamases appear to have diversified functions, not restricted to nucleases. The non-essential BDS1 in *S. cerevisiae,* presumably horizontally acquired from bacteria, possesses an MBL domain and functions as a sulfuric ester hydrolase (Hall et al., 2005). A discrete MBL type thioesterase in *Aspergillus fumigatus* was found to be required for biosynthesis of endocrocin, a simple anthraquinone commonly identified in fungal extracts (Lim et al., 2012). Asperthecin, a polyketide anthraquinone pigment, is produced by certain *Aspergillus* species (Howard and Raistrick, 1955), and disruption of the asperthecin biosynthetic gene cluster in *A. nidulans* revealed that a lactamase assisted the adjacent polyketide synthase to hydrolyze an aromatic polyketide into endocrocin-9-anthrone (Szewczyk et al., 2008). LovD, a SBL containing the PF00144 motif, in *Aspergillus terreus* was essential for lovastatin biosynthesis, and it was also later described to be involved in synthesizing simvastatin, a lipid-lowering agent, by acting on a protein-bound acyl substrate (Jiménez-Osés et al., 2014; Kennedy, 1999). Through proteomic studies on both weakly and highly aggressive *Verticillium dahliae* isolates, it was inferred that a β-lactamase family protein might act as a pathogenicity factor that is recognized by

the host plant immune system as an elicitor (El-Bebany et al., 2010). Thus, the functional diversity of fungal lactamases is evident despite limited studies.

Recent literature has shown that one fungal lactamase functions in xenobiotic hydrolysis, similar to bacterial counterparts. In fact, our interest in fungal lactamases stems from the observation that the gene FVEG_08291 in *F. verticillioides* and its ortholog in *F. pseudograminearum* (FPSE_08124) encode a lactamase designated MBL1 that is responsible for the degradation of 2-benzoxazolinone (BOA) (Glenn et al., 2016; Kettle et al., 2015). BOA is a γ-lactam phytochemical produced by graminaceous crops that is implicated in resistance to insect herbivory and microbial pathogens. The enzymatic capacity of *Fusarium* species to hydrolyze BOA is suggested to enhance colonization of the host, thus increasing the frequency and abundance of the species (Saunders et al., 2010; Saunders and Kohn, 2008). Interestingly, *MBL1* is part of a gene cluster that is up-regulated in response to BOA, and this cluster, called the *FDB1* cluster, was also observed in the other maize pathogens *Fusarium subglutinans* and *Colletotrichum graminicola* (Glenn et al., 2016). The highly conserved synteny of the *FDB1* cluster between these fungi suggests *C. graminicola* acquired the cluster from *Fusarium* by HGT, and that the maize host and its phytochemicals, notably BOA and related lactams, are driving factors influencing the evolution and genomic content of these fungi.

FUSARIUM LACTAMASES

Fusarium lactamase analysis as a paradigm?

Our analysis suggests that soil-borne fungi tend to possess more lactamase genes compared with the minimal sets from fungi predicted to live in environments of relatively low microbial diversity (Fig. 2.6). Broadly distributed in soil, *Fusarium* species are likely in competition with diverse microbes and are presumably often exposed to xenobiotic compounds. Frequent

confrontation with competing microorganisms inhabiting overlapping ecological niches is expected to hone genetic determinants of xenobiotic resistance. *Fusarium* interactions with soil competitors are complex, involving nutrient competition and chemical warfare (Kinkel et al., 2012). As noted in Fig. 2.5, the majority (84.3%) of sequenced fungal lactamase genes are from the phylum Ascomycota (12,771 genes), 11.6% of which belonged to the genus of *Fusarium* (1479 genes). There were, on average, 37 lactamase genes per *Fusarium* species, as opposed to 15 per species among non-*Fusarium* fungal genomes. The species noted with the highest number of lactamases, 88, was the soil limited root pathogen *Fusarium solani* (Fig. 2.6). Thus, we further propose that the abundance of *Fusarium* lactamases is likely integral to the success of this genus as a soil competitor. Further analysis of the global and individual roles of lactamases is important for more fully understanding *Fusarium* biology and its ecological interactions.

Detailed analysis of *Fusarium verticillioides* lactamases

To better understand molecular characteristics of *Fusarium* lactamases, we cataloged the complete set of lactamase encoding genes from three representative and pathogenically important sequenced *Fusarium* genomes, *F. verticillioides* 7600 (*Fv*), *F. oxysporum* 4287 (*Fo*) and *F. graminearum* PH-1 (*Fg*), via homology-based protein reciprocal BLAST and bacterial β-lactamase HMMER sequence logo scanning (Wheeler and Eddy, 2013). We identified 46 lactamase domain–containing genes in *Fv*, 63 in *Fo* and 38 in *Fg*, as listed in Table 2.3 by predicted enzymatic mechanisms (MBLs and SBLs). PSI-BLAST of each lactamase gene in *F. verticillioides* helped uncover distant homologs and confirm domain integrity. Interestingly, some predicted SBL gene annotations (FVEG_03300, FVEG_14143, FVEG_15166, FVEG_17257, FVEG_17258) were missing core catalytic serine motifs or possessed only part of the conventional β-lactamase folds. Thus, these five genes were further evaluated for their open reading frames

using the FGENESH program from Softberry (http://www.softberry.com) to refine gene predictions. Re-annotated sequences suggested FVEG_17257 and FVEG_17258 should be merged as one lactamase gene, while FVEG_03300, FVEG_14143, and FVEG_15166 remained unchanged, still missing the core serine and lacking canonical amino acids at the majority of conserved sites. These three were thus excluded from later syntenic and phylogenetic analysis here due to the sequencing gaps (FVEG_03300) or that these sequences might confer novel activity rather than a hydrolytic function (FVEG_14143, FVEG_15166). PSI-BLAST of MBLs in *F. verticillioides* also predicted several members could be involved in metabolizing RNA (FVEG_05485, FVEG_11466, FVEG_14723), degrading lipids (FVEG_11923, FVEG_03849), repairing DNA (FVEG_00815, FVEG_04252), and hydrolyzing hydroxylacylglutathione (FVEG_08018, FVEG_16907), which also require zinc ions for appropriate functions.

Fusarium verticillioides-oriented syntenic studies were performed such that corresponding orthologs and adjacent genes in *Fg* and *Fo* were examined. In terms of species phylogeny, *Fv* is more closely related to *Fo* than *Fg*. Thus, we naturally expect more orthologs identified in *Fo*. Except for those *Fv* lactamase genes with no orthologs in the other two species, the rest of the genes generally retained syntenic clusters in the *Fg* and/or *Fo* genome (Fig. 2.7). Phylogenetic evaluation of 41 *Fv* genes having the core lactamase motifs revealed a high consistency with species evolution (Fig. 2.8), where 37 genes fall into position A, clustering with orthologs in *Fusarium fujikuroi* in the respective phylograms. This suggests that *Fv* lactamases are most similar to those annotated in closely related species compared with other relatively distant species. Lactamase genes in *Fusarium* species generally form a clade distinct from other Sordariomycetes. Interestingly, only 29% of the *Fv* MBLs had evidence of paralogy (Fig. 2.7), whereas 63% of the *Fv* SBLs appeared to have paralogs. This suggests the two types of lactamases may have different

evolutionary pressures impacting duplication and diversification. Only six *Fv* lactamase genes lack possible orthologs in both *Fo* and *Fg* (Fig. 2.7). Collectively the data indicate that some lactamase genes originated before the divergence of *Fusarium* species, resulting in greater sequence diversity accompanying species divergence. Interestingly, FVEG_12347 was the only gene in the phylogenetic position B (Fig. 2.8), suggesting that it is similar to *Fg* ortholog FGSG_04727 and lacks an ortholog in *Fo* (Fig. 2.7). FVEG_08291, FVEG_09433, and FVEG_12457 notably exhibited more similarities to orthologs in other Sodariomycetes rather than in closely related *Fusarium* species. These fall into phylogenetic position C and are thus good candidates for HGT derivation. The FVEG_08291 protein sequence possessed 85% identity to an ortholog in *C. graminicola* (NCBI Reference Sequence: XP_008099767.1), another Sodariomycete pathogen of maize, surpassing homology to other related genes in *Fusarium* species. This is the *MBL1* gene above noted as part of the *FDB1* cluster conferring resistance to BOA. A similar case was observed for FVEG_09433, where it was more closely related to orthologs in *C. graminicola* and other genera than to those of most other *Fusarium* species, even though there are apparent orthologs in *F. mangiferae* (GenBank ID: CVL02248.1) and *F. fujikuroi* (GenBank ID: CCT69225.1). One possible explanation is that FVEG_09433 was introduced to *Fusarium* species within the *Gibberella fujikuroi* species complex prior to the divergence of these three species, but its orthologs among other species of the complex were somehow lost. The serine-based lactamase FVEG_12457 was most similar to its orthologs in *Aspergillus terreus* (NCBI Reference ID: XP_001217058.1) and *Penicillium roqueforti* (GenBank ID: CDM29397.1) with a sequence identity of over 70%, exceeding the 60% average identity among related *Fusarium* genes.

Multiple Alignment using Fast Fourier Transform (MAFFT) analysis of presumed hydrolysis-related lactamase protein sequences was performed separately for MBLs and SBLs, presenting

two distinctive patterns of conserved motifs (Figs. 2.9, 2.10). Although these *Fv* lactamases exhibited considerable sequence diversity, conserved motifs were still observed. As to MBLs, the conserved motif His-X-His-X-Asp-His-X-Gly resembled that in classic bacterial MBLs (Fig. 2.9). However, compared to typical cases in bacteria, the overall conserved motif pattern is different in *Fv* MBLs, and additional motifs were identified, including Pro-X-Gly-His in Motif 3, Gly-Asp in Motif 4, and Pro-Gly in Motif 5 (Fig. 2.9). A retrospective scrutiny of conserved motifs of bacterial PSI-BLAST hits revealed that these sites in *Fv* lactamases are also present in certain bacterial β-lactamases (data not shown) (Kelley et al., 2015). *Fv* SBLs demonstrate an interesting molecular pattern that is not present in bacteria (Fig. 2.10). A total of nine motifs were identified in all intact *Fv* SBLs that are predicted to be hydrolysis-associated. Besides the catalytic core motif shared with bacteria (Ser-X-X-Lys as Motif 1), *Fv* lactamases contain conserved amino acids Leu-X-X-X-Gly in Motif 2, Pro-Glu-Leu in Motif 3, Leu-X-X-His-X-X-Gly in Motif 4, Pro-X-X-X-X-X-X-Tyr in Motif 5, Glu-X-X-X-Gly in Motif 6, a single conserved amino acid Pro in Motif 7, the Asp in Motif 8, and the Leu in Motif 9. However, none of these motifs (Motif 2-9) are represented in bacterial species.

Phyre2 predictions of tertiary structures reflected an interesting discovery that the majority of *Fv* MBLs were similar to bacterial β-lactamases, presenting a α-β/β-α sandwich structure composed of two β sheets at the core and α helices on the external surfaces. Those conserved residues are generally located at flexible loops connecting different secondary structures. It can be inferred that the spatial adjacency of histidines would facilitate the coordination of zinc ions and that the aspartic acid residues participate in the hydrolysis reaction. As exemplified in Figure 2.11, FVEG_08291 was predicted to have the signature sandwich conformation with a flap structure (the flexible mobile loop), which is situated at the bottom of a wide shallow groove between two

β-sheets (Fig. 2.11A). This structure has proven to be critical in substrate binding in bacteria (Materon and Palzkill, 2001). Superimposition of protein structures revealed that FVEG_08291 resembles a quorum-quenching lactonase (AiiB) from *Agrobacterium tumerfaciens* (Fig. 2.11B). The conserved zinc-coordinated residues on the flexible loop as well as the easily accessible groove placement suggest the potential to accommodate various lactam or lactone molecules (Fig. 2.11C and 2.11D). Other conserved amino acids not directly predicted to be associated with catalytic reactions may be involved in structure maintenance or substrate recognition, and overall the catalytic mechanisms of fungal lactamases require further exploration.

CONCLUSION AND FUTURE DIRECTION

The complexity of soil environments, particularly those with nutrient-driven competition in the rhizosphere, has led to diverse organisms capable of antimicrobial activity (Gottlieb, 1977). Plants also contribute to rhizospheric antimicrobial content, either proactively (phytoanticipins), or reactive to pathogen contact (phytoalexins) (Kato-Noguchi et al., 2008; Morrissey and Osbourn, 1999). Thus, the soil environment contains high antibiotic diversity including β-lactams, tetracyclines, sulfonamides, aminoglycosides, imidazoles, etc. (Thiele-Bruhn, 2003). Competitive relationships among soil microflora exert selective pressure on genes for antibiotic production and resistance, which in turn shape microbial populations and diversity, largely through development of antibiotic resistance mechanisms, such as the enzymatic degradation of β-lactam-containing compounds. Xenobiotic degradation in soil is propelled by enzymatic processes such as hydrolysis, oxidative decarboxylation, and hydroxylation (Al-Ahmad et al., 1999; Chen et al., 1997; Halling-Sørensen, 2000; Mcgrath et al., 1998; Thiele-Bruhn, 2003). Interestingly, functional metagenomics have revealed that, as the major resistance source against β-lactams, β-lactamase

encoding genes were abundant even in undisturbed soil absent of anthropogenic selective pressure, contributing to a massive reservoir for genetic exchange among soil microflora (Allen et al., 2009).

Given our examination of fungal hydrolytic lactamases, we propose an ecological model (Fig. 2.12) centering on the production and function of both lactams and lactamases produced by plants, bacteria, and fungi. We expand the conventional focus beyond that of solely bacterial β-lactamases and instead propose a more generic ecological model linking lactam production with hydrolytic functions of organismal lactamases. Lactam antibiotics presumably benefit their producers by securing ecological niches, whereas numerous lactam producers have also developed hydrolytic lactamases postulated to combat antibiosis. For example, soil-associated fungi typically possess more lactamase encoding genes than those from environments with lower microbial diversity since soil environments contain significant antibiotic diversity. Analysis of *Fusarium* species provides the foundation for our hypothesis that soil fungi frequently utilize lactamases in detoxification of xenobiotics, especially given *Fusarium* species' wide soil distribution, lactamase-rich genomes, and recent functional characterization of lactamase genes. The general abundance and persistence of lactamase genes in fungal genomes suggests a significant role for these enzymes in the soil environment, presumably in protection from many as yet unknown xenobiotics. We have generated a large set of lactamase mutants in *F. verticillioides* and are conducting transcriptional and phenotypic analyses upon exposure to various lactam compounds in order to more thoroughly evaluate the role and activity of these lactamases, thus broadening our appreciation of both the lactam compounds and corresponding lactamases in terms of their diversity and impact on both bacterial and fungal communities. This work also has the potential to broaden our appreciation of environmental sources of antimicrobial resistance to include both bacteria and fungi, especially with regard to use of antibiotics in agriculture.

REFERENCES

Abraham, E. P., and Chain, E. (1940). An enzyme from bacteria able to destroy penicillin. 1940. *Rev. Infect. Dis.* 10, 677–678. doi:10.1038/146837a0.

Agrawal, A. A. (2011). Current trends in the evolutionary ecology of plant defence. *Funct. Ecol.* 25, 420–432. doi:10.1111/j.1365-2435.2010.01796.x.

Al-Ahmad, a., Daschner, F. D., and Kümmerer, K. (1999). Biodegradability of cefotiam, ciprofloxacin, meropenem, penicillin G, and sulfamethoxazole and inhibition of waste water bacteria. *Arch. Environ. Contam. Toxicol.* 37, 158–163. doi:10.1007/s002449900501.

Allen, H. K., Donato, J., Wang, H. H., Cloud-Hansen, K. A., Davies, J., and Handelsman, J. (2010). Call of the wild: antibiotic resistance genes in natural environments. *Nat. Rev. Microbiol.* 8, 251–259. doi:10.1038/nrmicro2312.

Allen, H. K., Moe, L. A., Rodbumrer, J., Gaarder, A., and Handelsman, J. (2009). Functional metagenomics reveals diverse beta-lactamases in a remote Alaskan soil. *ISME J* 3, 243–251. doi:10.1038/ismej.2008.86.

Arnoldi, A., Cabrini, M. R., Farina, G., and Merlini, L. (1990). Activity of a series of beta-lactams against some phytopathogenic fungi. *J. Agric. Food Chem.* 38, 2197–2199. doi:10.1021/jf00102a019.

Berendonk, T. U., Manaia, C. M., Merlin, C., Fatta-Kassinos, D., Cytryn, E., Walsh, F., et al. (2015). Tackling antibiotic resistance: the environmental framework. *Nat. Rev. Microbiol.* 1, 1. doi:10.1038/nrmicro3439.

Bozdogan, B., and Appelbaum, P. C. (2004). Oxazolidinones: activity, mode of action, and mechanism of resistance. *Int. J. Antimicrob. Agents* 23, 113–9. doi:10.1016/j.ijantimicag.2003.11.003.

Brakhage, A. A., and Schroeckh, V. (2011). Fungal secondary metabolites - strategies to activate silent gene clusters. *Fungal Genet. Biol.* 48, 15–22. doi:10.1016/j.fgb.2010.04.004.

Brakhage, A. A., Thön, M., Spröte, P., Scharf, D. H., Al-Abdallah, Q., Wolke, S. M., et al. (2009). Aspects on evolution of fungal β-lactam biosynthesis gene clusters and recruitment of trans-acting factors. *Phytochemistry* 70, 1801–11. doi:10.1016/j.phytochem.2009.09.011.

Bush, K., Jacoby, G. A., and Medeiros, A. A. (1995). A functional classification scheme for beta-lactamases and its correlation with molecular structure. *Antimicrob. Agents Chemother.* 39, 1211–1233.

Campos, J., Carmen Fusté, M., Trujillo, G., Sáez-Nieto, J., Vázquez, J., Lorén, J. G., et al. (1992). Genetic diversity of penicillin-resistant *Neisseria meningitidis*. *J. Infect. Dis.* 166, 173–177. doi:10.1093/infdis/166.1.173.

Chang, Q., Wang, W., Regev-Yochay, G., Lipsitch, M., and Hanage, W. P. (2015). Antibiotics in agriculture and the risk to human health: how worried should we be? *Evol. Appl.* 8, 240–7. doi:10.1111/eva.12185.

Chen, Y., Beck, A., Davenport, C., Chen, Y., Shattuck, D., and Tavtigian, S. V (2005). Characterization of TRZ1, a yeast homolog of the human candidate prostate cancer susceptibility gene ELAC2 encoding tRNase Z. *BMC Mol. Biol.* 6, 12. doi:10.1186/1471-2199-6-12.

Chen, Y., Rosazza, J. P. N., Reese, C. P., Chang, H. Y., Nowakowski, M. A., Kiplinger, J. P., et al. (1997). Microbial models of soil metabolism: biotransformations of danofloxacin. *J. Ind. Microbiol. Biotechnol.* 19, 378–384. doi:10.1038/sj.jim.2900409.

Coffey, T. J., Dowson, C. G., Daniels, M., and Spratt, B. G. (1993). Horizontal spread of an

altered penicillin-binding protein 2B gene between *Streptococcus pneumoniae* and *Streptococcus oralis*. *FEMS Microbiol Lett* 110, 335–339. doi:10.1016/0378-1097(93)90125-L.

Couture, R. M., Routley, D. G., and Dunn, G. M. (1971). Role of cyclic hydroxamic acids in monogenic resistance of maize to *Helminthosporium turcicum*. *Physiol. Plant Pathol.* 1, 515–521. doi:10.1016/0048-4059(71)90013-0.

Culbreath, M. (2006). An investigation into the antifungal activities of N-thiolated beta-lactams against selected *Candida* species. Available at: http://scholarcommons.usf.edu/etd/3763 [Accessed January 13, 2015].

Davelos, A. L., Kinkel, L. L., and Samac, D. A. (2004). Spatial variation in frequency and intensity of antibiotic interactions among Streptomycetes from prairie soil. *Appl. Environ. Microbiol.* 70, 1051–8. doi:10.1128/AEM.70.2.1051-1058.2004.

Davies, J. (2006). Are antibiotics naturally antibiotics? *J. Ind. Microbiol. Biotechnol.* 33, 496–9. doi:10.1007/s10295-006-0112-5.

Davies, J., Davies, D., and Davies, J, & Davies, D. (2010). Origins and evolution of antibiotic resistance. *Microbiol. Mol. Biol. Rev.* 74, 417–433. doi:10.1128/MMBR.00016.

Delserone, L. M., Matthews, D. E., and VanEtten, H. D. (1992). Differential toxicity of enantiomers of maackiain and pisatin to phytopathogenic fungi. *Phytochemistry* 31, 3813–3819. doi:10.1016/S0031-9422(00)97534-4.

Demain, A. L., and Elander, R. P. (1999). The beta-lactam antibiotics: past, present, and future. *Antonie Van Leeuwenhoek* 75, 5–19.

Dong, Y. H., Wang, L. H., Xu, J. L., Zhang, H. B., Zhang, X. F., and Zhang, L. H. (2001). Quenching quorum-sensing-dependent bacterial infection by an N-acyl homoserine lactonase. *Nature* 411, 813–817. doi:10.1038/35081101.

Dowson, C. G., Hutchison, A., Woodford, N., Johnson, a P., George, R. C., and Spratt, B. G. (1990). Penicillin-resistant *Viridans streptococci* have obtained altered penicillin-binding protein genes from penicillin-resistant strains of *Streptococcus pneumoniae*. *Proc. Natl. Acad. Sci. U. S. A.* 87, 5858–5862. doi:10.1073/pnas.87.15.5858.

Duczek, L. J., and Higgins, V. J. (1976). Effect of treatment with the phytoalexins medicarpin and maackiain on fungal growth *in vitro* and *in vivo*. *Can. J. Bot.* 54, 2620–2629. doi:10.1139/b76-282.

Ehmann, D. E., Jahić, H., Ross, P. L., Gu, R.-F., Hu, J., Kern, G., et al. (2012). Avibactam is a covalent, reversible, non–β-lactam β-lactamase inhibitor. *Proc. Natl. Acad. Sci.* 109, 11663–11668. doi:10.1073/pnas.1205073109.

El-Bebany, A. F., Rampitsch, C., and Daayf, F. (2010). Proteomic analysis of the phytopathogenic soilborne fungus *Verticillium dahliae* reveals differential protein expression in isolates that differ in aggressiveness. *Proteomics* 10, 289–303. doi:10.1002/pmic.200900426.

Elizabeth, B. Y., Er, A. B. A. X., and Smith, I. M. (1977). Antifungal compounds in winter wheat resistant and susceptible to Septoria nodorum. 67–73.

Fernandes, R., Amador, P., and Prudêncio, C. (2013). β-Lactams: chemical structure, mode of action and mechanisms of resistance. *Rev. Med. Microbiol.* 24. doi:10.1097/MRM.0b013e3283587727.

Fleming, A. (1929). On the antibacterial action of cultures of a *Penicillium*, with special reference to their use in the isolation of *B. influenzae*. *Br. J. Exp. Pathol.* 10, 226–236. doi:10.1038/146837a0.

Frère, J. M. (1995). Beta-lactamases and bacterial resistance to antibiotics. *Mol. Microbiol.* 16, 385–395. doi:10.1111/j.1365-2958.1995.tb02404.x.

Gans, J. (2006). Response to comment by Bunge et al. on "Computational improvements reveal great bacterial diversity and high metal toxicity in soil." *Science (80-.).* 313, 918d–918d. doi:10.1126/science.1126853.

Glenn, A. E., and Bacon, C. W. (2009). *FDB2* encodes a member of the arylamine N-acetyltransferase family and is necessary for biotransformation of benzoxazolinones by *Fusarium verticillioides*. *J. Appl. Microbiol.* 107, 657–671. doi:10.1111/j.1365-2672.2009.04246.x.

Glenn, A. E., Davis, C. B., Gao, M., Gold, S. E., Mitchell, T. R., Proctor, R. H., et al. (2016). Two horizontally transferred xenobiotic resistance gene clusters associated with detoxification of benzoxazolinones by *Fusarium* species. *PLoS One* 11, e0147486. doi:10.1371/journal.pone.0147486.

Goh, E.-B., Yim, G., Tsui, W., McClure, J., Surette, M. G., and Davies, J. (2002). Transcriptional modulation of bacterial gene expression by subinhibitory concentrations of antibiotics. *Proc. Natl. Acad. Sci. U. S. A.* 99, 17025–17030. doi:10.1073/pnas.252607699.

González-Lamothe, R., Mitchell, G., Gattuso, M., Diarra, M. S., Malouin, F., and Bouarab, K. (2009). Plant antimicrobial agents and their effects on plant and human pathogens. *Int. J. Mol. Sci.* 10, 3400–19. doi:10.3390/ijms10083400.

Gottlieb, D. (1977). Production and role of uteroglobulin. *Res. Reprod.* 9, 4.

Grotewold, E. (2005). Plant metabolic diversity: A regulatory perspective. *Trends Plant Sci.* 10, 57–62. doi:10.1016/j.tplants.2004.12.009.

Hall, C., Brachat, S., and Dietrich, F. S. (2005). Contribution of horizontal gene transfer to the evolution of *Saccharomyces cerevisiae*. *Eukaryot. Cell* 4, 1102–1115. doi:10.1128/EC.4.6.1102-1115.2005.

Halling-Sørensen, B. (2000). Algal toxicity of antibacterial agents used in intensive farming. *Chemosphere* 40, 731–739. doi:10.1016/S0045-6535(99)00445-2.

He, H., Yang, H. Y., Bigelis, R., Solum, E. H., Greenstein, M., and Carter, G. T. (2002). Pyrrocidines A and B, new antibiotics produced by a filamentous fungus. *Tetrahedron Lett.* 43, 1633–1636. doi:10.1016/S0040-4039(02)00099-0.

Howard, B. H., and Raistrick, H. (1955). Studies in the biochemistry of micro-organisms. 94. The colouring matters of species in the *Aspergillus nidulans* group. I. Asperthecin, a crystalline colouring matter of *Aspergillus quadrilineatus* Thom & Raper. *Biochem.J.* 59, 475–484. Available at: https://www.ncbi.nlm.nih.gov/pmc/articles/PMC1216271/ [Accessed February 10, 2017].

Jang, J. H., Kanoh, K., Adachi, K., and Shizuri, Y. (2006). Awajanomycin, a cytotoxic gamma-lactone-delta-lactam metabolite from marine-derived *Acremonium* sp. AWA16-1. *J. Nat. Prod.* 69, 1358–1360. doi:10.1021/np060170a.

Jiménez-Osés, G., Osuna, S., Gao, X., Sawaya, M. R., Gilson, L., Collier, S. J., et al. (2014). The role of distant mutations and allosteric regulation on LovD active site dynamics. *Nat. Chem. Biol.* 10, 431–6. doi:10.1038/nchembio.1503.

Kato-Noguchi, H., Ino, T., and Ota, K. (2008). Secretion of momilactone A from rice roots to the rhizosphere. *J. Plant Physiol.* 165, 691–6. doi:10.1016/j.jplph.2007.07.018.

Kelley, L. A., Mezulis, S., Yates, C. M., Wass, M. N., and Sternberg, M. J. E. (2015). The Phyre2 web portal for protein modeling, prediction and analysis. *Nat. Protoc.* 10, 845–858. doi:10.1038/nprot.2015.053.

Kennedy, J. (1999). Modulation of polyketide synthase activity by accessory proteins during lovastatin biosynthesis. *Science (80-.).* 284, 1368–1372. doi:10.1126/science.284.5418.1368.

Kettle, A. J., Batley, J., Benfield, A. H., Manners, J. M., Kazan, K., and Gardiner, D. M. (2015a). Degradation of the benzoxazolinone class of phytoalexins is important for virulence of *Fusarium pseudograminearum* towards wheat. *Mol. Plant Pathol.* 16, 946–962. doi:10.1111/mpp.12250.

Kettle, A. J., Carere, J., Batley, J., Benfield, A. H., Manners, J. M., Kazan, K., et al. (2015b). A γ-lactamase from cereal infecting *Fusarium* spp. catalyses the first step in the degradation of the benzoxazolinone class of phytoalexins. *Fungal Genet. Biol.* 83, 1–9. doi:10.1016/j.fgb.2015.08.005.

Khaldi, N., Seifuddin, F. T., Turner, G., Haft, D., Nierman, W. C., Wolfe, K. H., et al. (2010). SMURF: Genomic mapping of fungal secondary metabolite clusters. *Fungal Genet. Biol.* 47, 736–741. doi:Doi 10.1016/J.Fgb.2010.06.003.

Kinkel, L. L., Schlatter, D. C., Bakker, M. G., and Arenz, B. E. (2012). Streptomyces competition and co-evolution in relation to plant disease suppression. *Res. Microbiol.* 163, 490–499. doi:10.1016/j.resmic.2012.07.005.

Kinsella, K., Schulthess, C. P., Morris, T. F., and Stuart, J. D. (2009). Rapid quantification of *Bacillus subtilis* antibiotics in the rhizosphere. *Soil Biol. Biochem.* 41, 374–379. doi:10.1016/j.soilbio.2008.11.019.

Lewis, K. (2013). Platforms for antibiotic discovery. *Nat. Rev. Drug Discov.* 12, 371–87. doi:10.1038/nrd3975.

Li, X. Z., Ma, D., Livermore, D. M., and Nikaido, H. (1994). Role of efflux pump(s) in intrinsic resistance of *Pseudomonas aeruginosa*: Active efflux as a contributing factor to beta-lactam resistance. *Antimicrob. Agents Chemother.* 38, 1742–1752. doi:10.1128/AAC.38.8.1742.Updated.

Lim, F. Y., Hou, Y., Chen, Y., Oh, J. H., Lee, I., Bugni, T. S., et al. (2012). Genome-based cluster deletion reveals an endocrocin biosynthetic pathway in *Aspergillus fumigatus*. *Appl. Environ. Microbiol.* 78, 4117–4125. doi:10.1128/AEM.07710-11.

Livermore, D. M. (1998). Beta-lactamase-mediated resistance and opportunities for its control. *J. Antimicrob. Chemother.* 41, 25–41. doi:10.1093/jac/41.suppl_4.25.

Lynch, J. M., Benedetti, a., Insam, H., Nuti, M. P., Smalla, K., Torsvik, V., et al. (2004). Microbial diversity in soil: Ecological theories, the contribution of molecular techniques and the impact of transgenic plants and transgenic microorganisms. *Biol. Fertil. Soils* 40, 363–385. doi:10.1007/s00374-004-0784-9.

Malouin, F., and Bryan, L. E. (1986). Modification of penicillin-binding proteins as mechanisms of beta-lactam resistance. *Antimicrob. Agents Chemother.* 30, 1–5. doi:10.1128/AAC.30.1.1.Updated.

Marschner, P., Crowley, D., and Yang, C. H. (2004). Development of specific rhizosphere bacterial communities in relation to plant species, nutrition and soil type. *Plant Soil* 261, 199–208. doi:10.1023/B:PLSO.0000035569.80747.c5.

Materon, I. C., and Palzkill, T. (2001). Identification of residues critical for metallo-beta-lactamase function by codon randomization and selection. *Protein Sci.* 10, 2556–2565. doi:10.1110/ps.40884.

Mazzola, M., Cook, R. J., Thomashow, L. S., Weller, D. M., and Pierson, L. S. (1992). Contribution of phenazine antibiotic biosynthesis to the ecological competence of

fluorescent pseudomonads in soil habitats. *Appl. Environ. Microbiol.* 58, 2616–2624. Available at: http://aem.asm.org/content/58/8/2616.short [Accessed April 20, 2015].
Mcgrath, J. W., Hammerschmidt, F., and Quinn, J. P. (1998). Biodegradation of phosphonomycin by *Rhizobium huakuii* PMY1. *Appl. Environ. Microbiol.* 64, 356–358. Available at: http://www.pubmedcentral.nih.gov/articlerender.fcgi?artid=124718&tool=pmcentrez&rendertype=abstract.
Morrissey, J. P., and Osbourn, A. E. (1999). Fungal resistance to plant antibiotics as a mechanism of pathogenesis. *Microbiol. Mol. Biol. Rev.* 63, 708–24. Available at: https://www.ncbi.nlm.nih.gov/pubmed/10477313.
Osbourn, A. (2010). Secondary metabolic gene clusters: evolutionary toolkits for chemical innovation. *Trends Genet* 26, 449–457. doi:10.1016/j.tig.2010.07.001.
Parkinson, A., Klaasen, C. D., and Watkins, J. B. (2001). "Biotransformation of xenobiotics," in *Casarett & Doull's Essentials of Toxicology*, 133–144. doi:10.1036/0071470514.
Perea, S., and Patterson, T. F. (2002). Antifungal resistance in pathogenic fungi. *Clin. Infect. Dis.* 35, 1073–1080. doi:10.1086/344058.
Petersen, T. N., Brunak, S., von Heijne, G., and Nielsen, H. (2011). SignalP 4.0: discriminating signal peptides from transmembrane regions. *Nat. Methods* 8, 785–786. doi:10.1038/nmeth.1701.
Ren, H., Liu, R., Chen, L., Zhu, T., Zhu, W. M., and Gu, Q. Q. (2010). Two new hetero-spirocyclic γ-lactam derivatives from marine sediment-derived fungus *Aspergillus sydowi* D2-6. *Arch. Pharm. Res.* 33, 499–502. doi:10.1007/s12272-010-0401-4.
Riaz, K., Elmerich, C., Moreira, D., Raffoux, A., Dessaux, Y., and Faure, D. (2008). A metagenomic analysis of soil bacteria extends the diversity of quorum-quenching lactonases. *Environ. Microbiol.* 10, 560–570. doi:10.1111/j.1462-2920.2007.01475.x.
Robleto, E. A., Borneman, J., and Triplett, E. W. (1998). Effects of bacterial antibiotic production on rhizosphere microbial communities from a culture-independent perspective. *Appl. Environ. Microbiol.* 64, 5020–5022. Available at: http://aem.asm.org/content/64/12/5020.short [Accessed April 20, 2015].
Saunders, M., Glenn, A. E., and Kohn, L. M. (2010). Exploring the evolutionary ecology of fungal endophytes in agricultural systems: using functional traits to reveal mechanisms in community processes. *Evol. Appl.* 3, 525–537. doi:10.1111/j.1752-4571.2010.00141.x.
Saunders, M., and Kohn, L. M. (2008). Host-synthesized secondary compounds influence the *in vitro* interactions between fungal endophytes of maize. *Appl Env. Microbiol* 74, 136–142. doi:10.1128/AEM.01538-07.
Soucy, S. M., Huang, J., and Gogarten, J. P. (2015). Horizontal gene transfer: building the web of life. *Nat. Rev. Genet.* 16, 472–482. doi:10.1038/nrg3962.
Stallings, J. H. (1954). Soil produced antibiotics—plant disease and insect control. *Bacteriol. Rev.* 18, 131. Available at: http://www.ncbi.nlm.nih.gov/pmc/articles/PMC180792/.
Stumpf, G., and Domdey, H. (1996). Dependence of yeast pre-mRNA 3'-end processing on CFT1: A sequence homolog of the mammalian AAUAAA binding factor. *Science (80-.).* 274, 1517–1520. doi:10.1126/science.274.5292.1517.
Sun, L. H., and Dennis, B. (2016). The superbug that doctors have been dreading just reached the U.S. *Washington Post*. Available at: https://www.washingtonpost.com/news/to-your-health/wp/2016/05/26/the-superbug-that-doctors-have-been-dreading-just-reached-the-u-s/?utm_term=.d47b14742fcb [Accessed January 1, 2017].

Szewczyk, E., Chiang, Y. M., Oakley, C. E., Davidson, A. D., Wang, C. C. C., and Oakley, B. R. (2008). Identification and characterization of the asperthecin gene cluster of *Aspergillus nidulans*. *Appl. Environ. Microbiol.* 74, 7607–7612. doi:10.1128/AEM.01743-08.

Taylor, D. L., Hollingsworth, T. N., McFarland, J. W., Lennon, N. J., Nusbaum, C., and Ruess, R. W. (2014). A first comprehensive census of fungi in soil reveals both hyperdiversity and fine-scale niche partitioning. *Ecol. Monogr.* 84, 3–20. doi:10.1890/12-1693.1.

Thiele-Bruhn, S. (2003). Pharmaceutical antibiotic compounds in soils - A review. *J. Plant Nutr. Soil Sci.* 166, 145–167. doi:10.1002/jpln.200390023.

Thomas, P. W., Stone, E. M., Costello, A. L., Tierney, D. L., and Fast, W. (2005). The quorum-quenching lactonase from *Bacillus thuringiensis* is a metalloprotein. *Biochemistry* 44, 7559–7569. doi:10.1021/bi050050m.

Thomashow, L. S., Bonsall, R. F., and Weller, D. M. (1997). Antibiotic production by soil and rhizosphere microbes *in situ*. *Man. Environ. Microbiol.*, 1–24. Available at: http://www.wsu.edu/~mavrodi/Documents/Paper.pdf [Accessed April 20, 2015].

Tipper, D. J. (1985). Mode of action of beta-lactam antibiotics. *Pharmacol. Ther.* 27, 1–35. doi:0163-7258/85.

VanEtten, H. D., Mansfield, J. W., Bailey, J. A., and Farmer, E. E. (1994). Two classes of plant antibiotics: Phytoalexins versus Phytoanticipins. *Plant Cell* 6, 1191–1192. doi:10.1105/tpc.6.9.1191.

Wagenaar, M. M., Corwin, J., Strobel, G., and Clardy, J. (2000). Three new cytochalasins produced by an endophytic fungus in the genus *Rhinocladiella*. *J. Nat. Prod.* 63, 1692–1695. doi:10.1021/np0002942.

Walczak, P., Pannek, J., Boratyński, F., Janik-Polanowicz, A., and Olejniczak, T. (2014). Synthesis and fungistatic activity of bicyclic lactones and lactams against *Botrytis cinerea*, *Penicillium citrinum*, and *Aspergillus glaucus*. *J. Agric. Food Chem.* 62, 8571–8578. doi:10.1021/jf502148h.

Waxman, D. J., and Strominger, J. L. (1983). Penicillin-binding proteins and the mechanism of action of beta-lactam antibiotics. *Annu. Rev. Biochem.* 52, 825–869. doi:10.1146/annurev.bi.52.070183.004141.

Wei, B., Yang, Z. D., Chen, X. wei, Zhou, S. Y., Yu, H. T., Sun, J. Y., et al. (2016). Colletotrilactam A–D, novel lactams from *Colletotrichum gloeosporioides* GT-7, a fungal endophyte of *Uncaria rhynchophylla*. *Fitoterapia* 113, 158–163. doi:10.1016/j.fitote.2016.08.005.

Weldhagen, G. F. (2004). Integrons and beta-lactamases - A novel perspective on resistance. *Int. J. Antimicrob. Agents* 23, 556–562. doi:10.1016/j.ijantimicag.2004.03.007.

Wheeler, T. J., and Eddy, S. R. (2013). Nhmmer: DNA homology search with profile HMMs. *Bioinformatics* 29, 2487–2489. doi:10.1093/bioinformatics/btt403.

Wicklow, D. T., Roth, S., Deyrup, S. T., and Gloer, J. B. (2005). A protective endophyte of maize: *Acremonium zeae* antibiotics inhibitory to *Aspergillus flavus* and *Fusarium verticillioides*. *Mycol. Res.* 109, 610–618. doi:10.1017/S0953756205002820.

Zhang, Q. Y., Jones, D. M., Saez Nieto, J. A., Perez Trallero, E., and Spratt, B. G. (1990). Genetic diversity of penicillin-binding protein 2 genes of penicillin-resistant strains of *Neisseria meningitidis* revealed by fingerprinting of amplified DNA. *Antimicrob. Agents Chemother.* 34, 1523–1528. doi:10.1128/AAC.34.8.1523.

Zhelkovsky, A., Tacahashi, Y., Nasser, T., He, X., Sterzer, U., Jensen, T. H., et al. (2006). The role of the Brr5/Ysh1 C-terminal domain and its homolog Syc1 in mRNA 3'-end processing

in *Saccharomyces cerevisiae*. *RNA* 12, 435–45. doi:10.1261/rna.2267606.

Table 2.1. Classification of bacterial β-lactamase genes

Functional Classification	Molecular Classification	Inhibition by Clavulanic Acid	Zinc Requirement	Function
Group 1	Class C	No	No	Cephalosporinase
Group 2				
2a	Class A	Yes	No	Penicillinases
2be	Class A	Yes	No	Extended-spectrum β-lactamases
2br	Class A	Yes	No	Inhibitor-resistant TEM-derivative enzymes
2c	Class A	Yes	No	Carbenicillinase
2d	Class A/D	Yes	No	Cloxacilanase
2e	Class A	Yes	No	Cephalosporinase
2f	Class A	Yes	No	Carbapenemase
Group 3	Class B	No	Yes	Metalloenzyme

Table 2.2. *Saccharomyces cerevisiae* lactamase orthologs in three *Fusarium* species

Saccharomyces cerevisiae* Lactamase Genes			***Fuasrium* Orthologs****		
Systematic Name	**Standard Name**	**Function**	**Fv FVEG_**	**Fo FOXG_**	**Fg FGSG_**
YDR272W	GLO2	Hydroxyacylglutathione hydrolase GLO2	08018/ 16907	01652/ 12249	13072
YKR079C	TRZ1	tRNase Z	05485	02309	06635
YLR277C	YSH1	Cleavage polyadenylation factor subunit YSH1	14723	17946	00819
YMR137C	PSO2	Pso2p nuclease	00815	00696	00361
YOL164W	BDS1	Sulfuric ester hydrolase	N/I***	N/I	N/I
YOR040W	GLO4	Hydroxyacylglutathione hydrolase GLO4	08018/ 16907	01652/ 12249	13072
YPL103C	FMP30	N-acetylphosphatidylethanolamine-hydrolyzing phospholipase D	03849	05981	09261

**Saccharomyces cerevisiae* has 7 lactamase genes, two of which (TRZ1 and YSH1) are essential.
** Fv = *F. verticillioides*; Fo = *F. oxysporum*; Fg = *F. graminearum*.
*** N/I represents no orthologs identifed in these three *Fusarium* species.

Table 2.3. β-lactamase domain-containing genes in three *Fusarium* genomes

Species	Accession Number									
	MBL* (FVEG_)					**SBL* (FVEG_)**				
***F. verticillioides* 7600**	00815	03849	04252	05261	05485	01581	01641	**01651**	03303	05963
	05734	05854	08018	08291	09433	09854	09904	12457	12760	13172
	11466	11838	11923	12159	12288	05685	**04555**	**03457**	10996	**01795**
	12347	**12526**	12637	13253	13366	03300	14143	10753	**10740**	09057
	13675	14723	14874	16907		15166	17257			
	MBL (FOXG_)					**SBL (FOXG_)**				
***F. oxysporum* f.sp. *lycopersici* 4287**	00696	01652	02309	02559	03706	02097	02670	02810	02811	02821
	03847	03877	04928	06402	06970	03275	03924	**05576**	05981	**07628**
	07119	08819	08964	12116	12249	08711	10409	10814	10816	10887
	12727	12984	13156	13240	13402	10911	10955	**12166**	12179	**13106**
	14524	15197	15260	15319	15773	13918	**14363**	15115	**15119**	15429
	15776	16562	17598	17946	18400	17393	**18438**	18914	21695	22119
	20403					22149	22249			
	MBL (FGSG_)					**SBL (FGSG_)**				
***F. graminearum* PH-1**	00079	00361	00819	03085	04727	00024	02452	02875	**03050**	03364
	05331	06635	07959	10497	10653	**04656**	04809	04813	05706	07314
	10795	11082	11291	11553	13072	07538	07702	**07996**	08136	08476
	13173					09143	09261	**10287**	10497	11664
						13212	13439			

* MBL and SBL are abbreviated for metallo-β-lactamases and serine-based β-lactamases, respectively. Bolded accession numbers are those with signal peptides idenfied by SignalP 4.1 Server, suggesting likely secretion (Petersen et al., 2011).

.

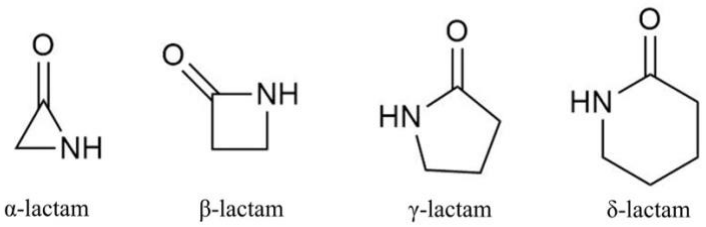

Figure 2.1. Basic lactam structures with differing ring sizes.

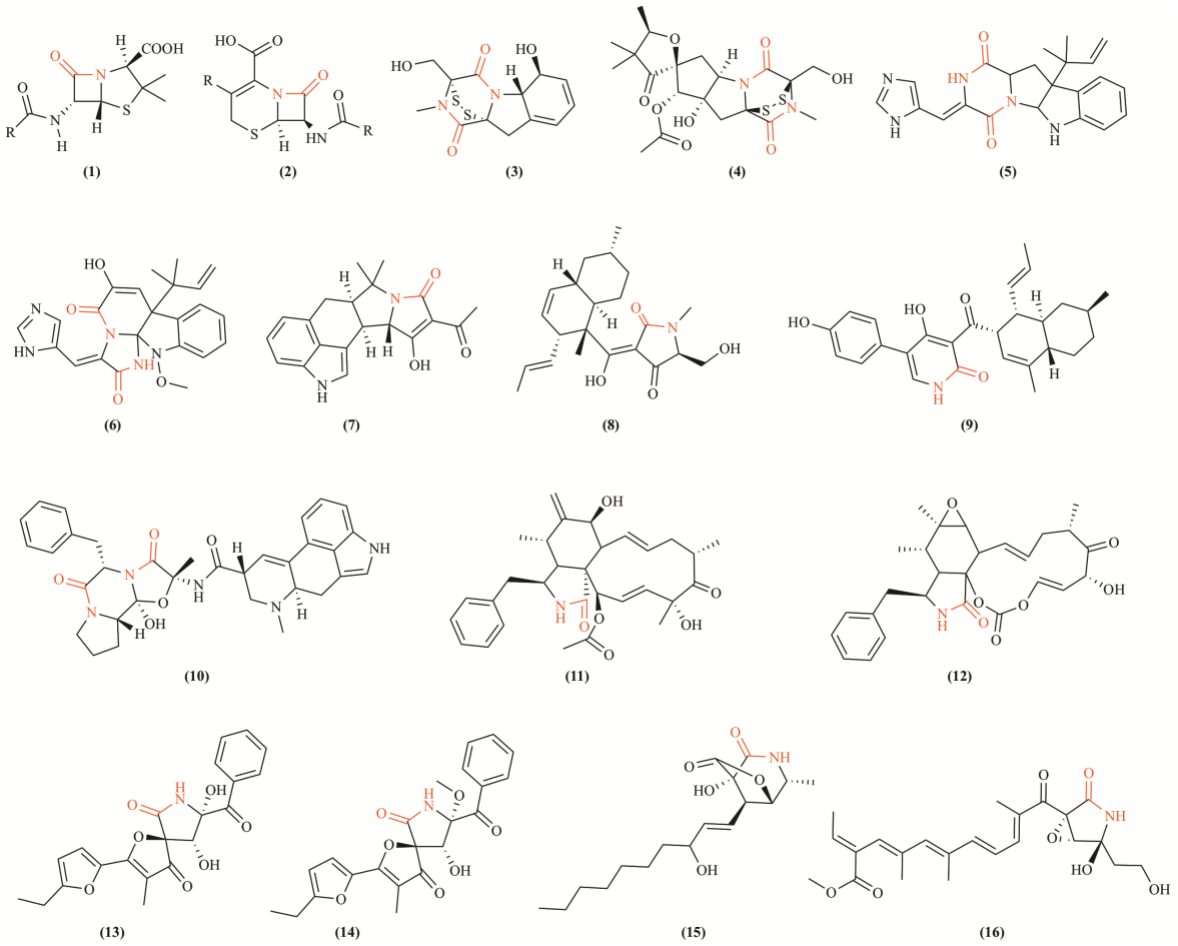

Figure 2.2. Examples of lactam-containing fungal compounds. Lactam bonds are highlighted in red. (1) Penicillin, the historically significant fungal lactam produced by *Penicillium chrysogenum* (Fleming, 1929); (2) Cephalosporins, a group of bactericidal β-lactams from *Acremonium chrysogenum* (Harrison and Bratcher, 2008); (3) Gliotoxin, a mycotoxin produced by *Aspergillus fumigatus* and several other species (Forseth et al., 2011); (4) Sirodesmin PL, a phytotoxin produced by the fungus *Leptosphaeria maculans* causing blackleg disease of canola (Gardiner et al., 2004); (5) Roquefortine C, a mycotoxin produced by *Penicillium* species (Kokkonen et al., 2005); (6) Meleagrin, a bioactive alkaloid produced by deep ocean *Penicillium* (Nozawa and Nakajima, 1979); (7) Cyclopiazonic acid, a toxic fungal secondary metabolite originally isolated from *Penicillium cyclopium* (Holzapfel, 1968); (8) Equisetin, a *Fusarium equiseti* metabolite (Hazuda et al., 1999); (9) Ilicicolin H is an NRPS-polyketide hybrid product discovered from *Cylindrocladium iliciola* MFC-870 and is a potent antifungal agent (Singh et al., 2011); (10) Ergotamine, an ergopeptine and part of the ergot family of alkaloids from *Claviceps purpurea* (Schiff, 2006); (11) Cytochalasin D, a cytostatically active metabolite isolated from *Tubercularia* species (Wang et al., 2003); (12) Fusarin C, a mycotoxin produced by several *Fusarium* species (Wiebe and Bjeldanes, 1981); (13) Azaspirofuran A and (14) Azaspirofuran B produced by *Aspergillus sydowi* (Ren et al., 2010); (15) Awajanomycin produced by *Acremonium* species (Jang et al., 2006); (16) Cytochalasin from *Rhinocladiella* species (Wagenaar et al., 2000)

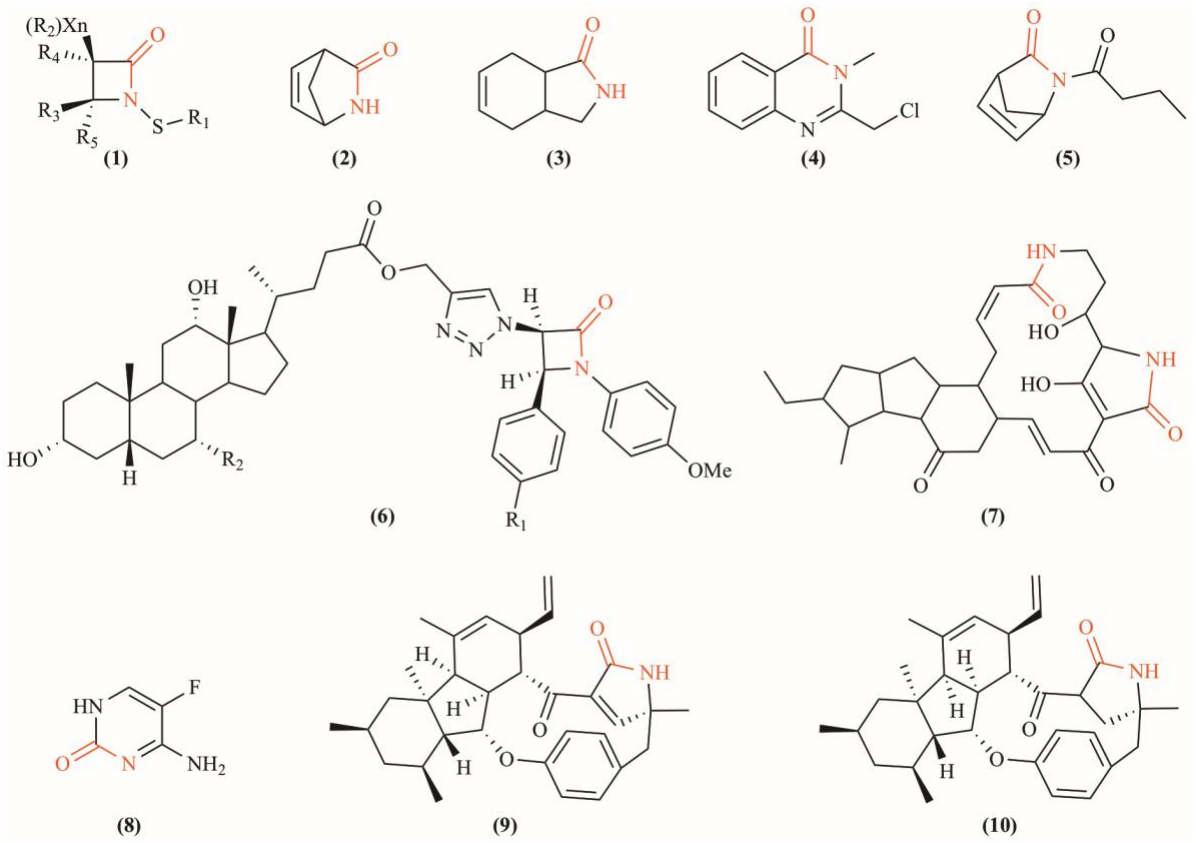

Figure 2.3. Fungicidal or fungistatic lactams. (1) N-thiolated β-lactams, artificial compounds that possess antifungal activity against *Candida* and other fungi by exerting powerful cytostatic effects that disrupt the structural integrity of cytoplasmic membranes (O'Driscoll et al., 2008); (2) Vince lactam, a versatile artificial chemical intermediate used in organic and medicinal chemistry that shows fungistatic effects against *Botrytis cinerea*, *Penicillium citrium*, and *Aspergillus glaucus* (Walczak et al., 2014); (3) (±)-*cis*-3-azabicyclo[4.3.0]non-7-en-2-one, an artificially synthesized compound that is also fungistatic to the same three species as vince lactam (Walczak et al., 2014); (4) 2-Chloromethyl-3-methyl-4 (3H)-quinazolinone, exhibiting antifungal activity against *Fusarium oxysporum* and *Macrophomina sorgina* (Reddy et al., 2010); (5) (±)-2-butyl-2-azabicyclo[2.2.1]hept-5-en-3-one, an artificially synthesized compound that moderately inhibits the growth of *A. glaucus*; (6) 1,2,3-triazole-linked β-lactam-bile acid conjugates (R_1=H or Cl, R_2=H or OH), a group of artificially synthesized compounds that inhibit the growth of *F. oxysporum, Candida albincans, Cryptococcus neoformans, Benjaminiella poitrasii, Yarrowia lipolytica* (Vatmurge et al., 2008); (7) Maltophilin, produced by a ubiquitous free-living bacterium *Stenotromonas maltophilia*, which demonstrates inhibitory effects against several Ascomycetes, such as *Aspergillus terreus, B. cinerea, C. albicans, Fusarium solani*, etc. (Jakobi et al., 1996); (8) Flucytosine, an effective antifungal compound indicated for the treatment of serious infections caused by susceptible strains of *Candida* or *Cryptococcus neoformans* (Cuenca-Estrella et al., 2001); (9), (10) Pyrrocidine A and B, respectively, broad spectrum antibiotics produced by *Sarocladium zeae* (He et al., 2002).

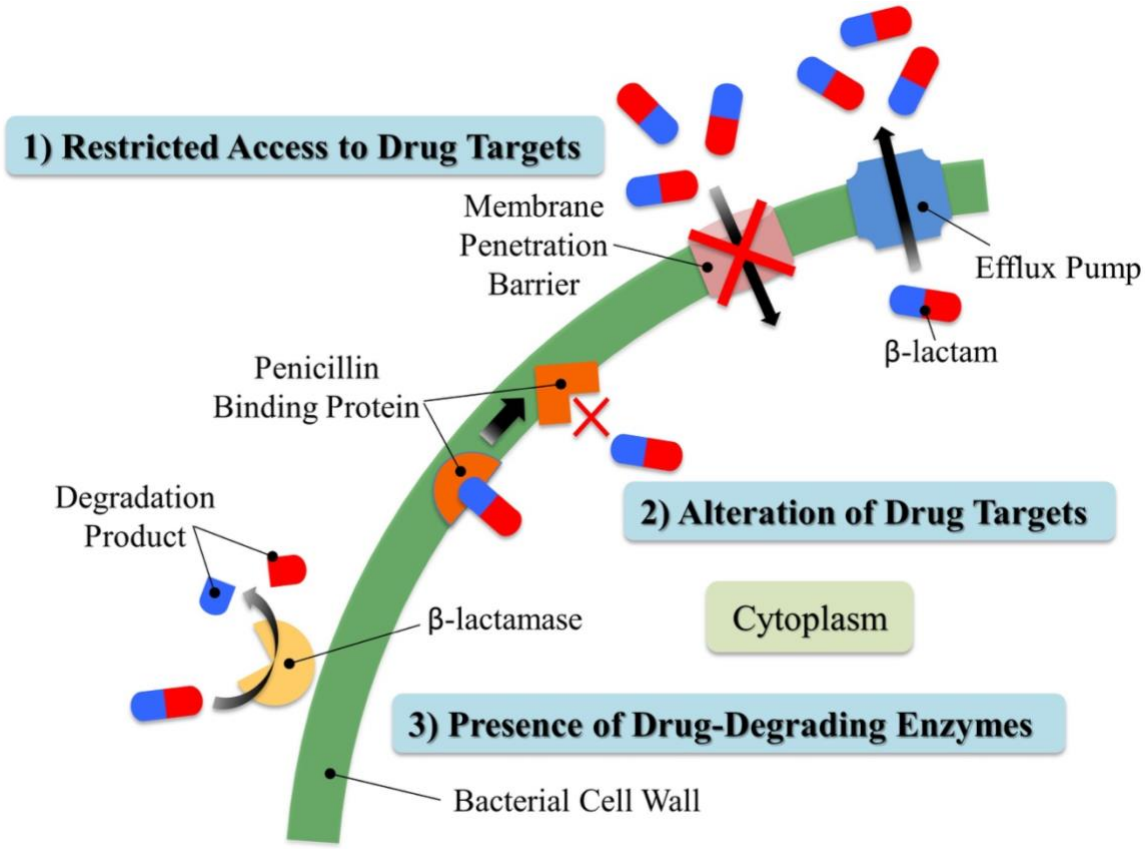

Figure 2.4. Three major resistant mechanisms present in bacteria against β-lactam antibiotics. The three mechanisms are indicated in the drawing. Generally speaking, Gram-negative bacteria retain β-lactamases in the periplasmic space between inner and outer membranes. In contrast, Gram-positive bacteria do not possess an outer membrane, and they usually release β-lactamases to the extracellular environment. Fine details of the bacterial membranes and peptidoglycan layer are not shown in this simplified drawing.

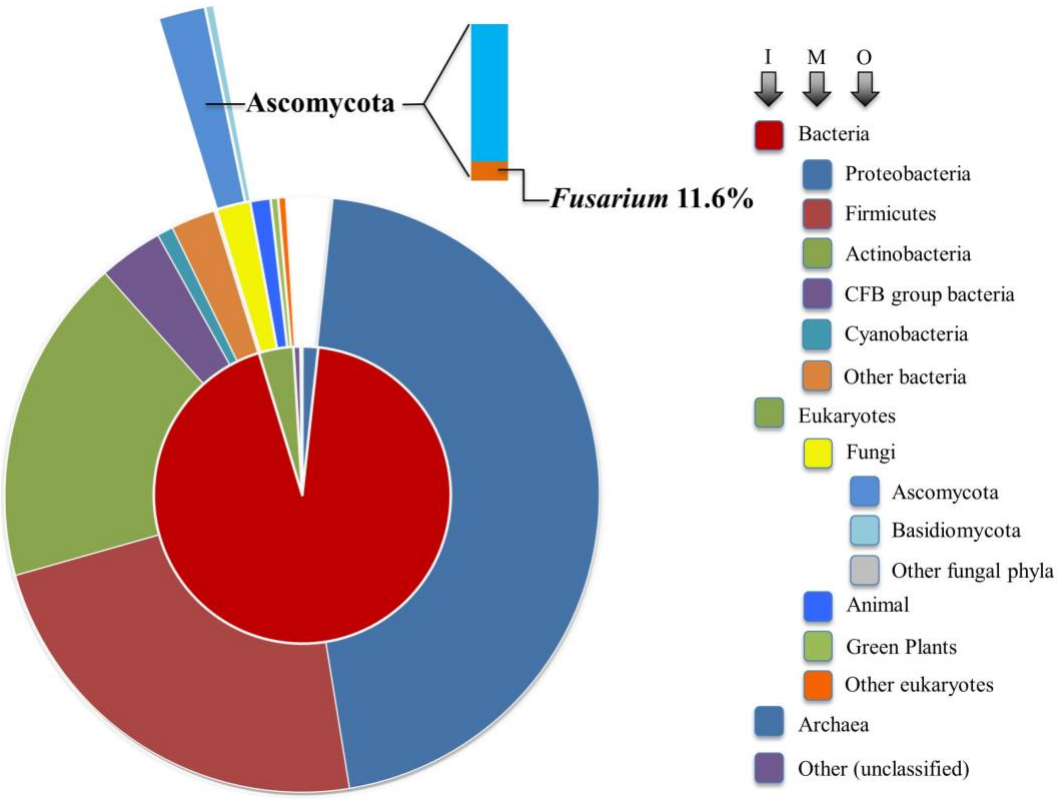

Figure 2.5 Sunburst visualization of β-lactamase gene distribution by major taxon. Each node of the taxonomic hierarchy is represented as a separate arc, arranged radially with the domains at the center and the phyla arrayed around the outermost ring. The area of each arc is proportional to the number of β-lactamases reported in the NCBI protein database. I, M, and O refer to inner, middle and outer arcs. The frequency of *Fusarium* lactamases among the Ascomycota is denoted in bar chart form.

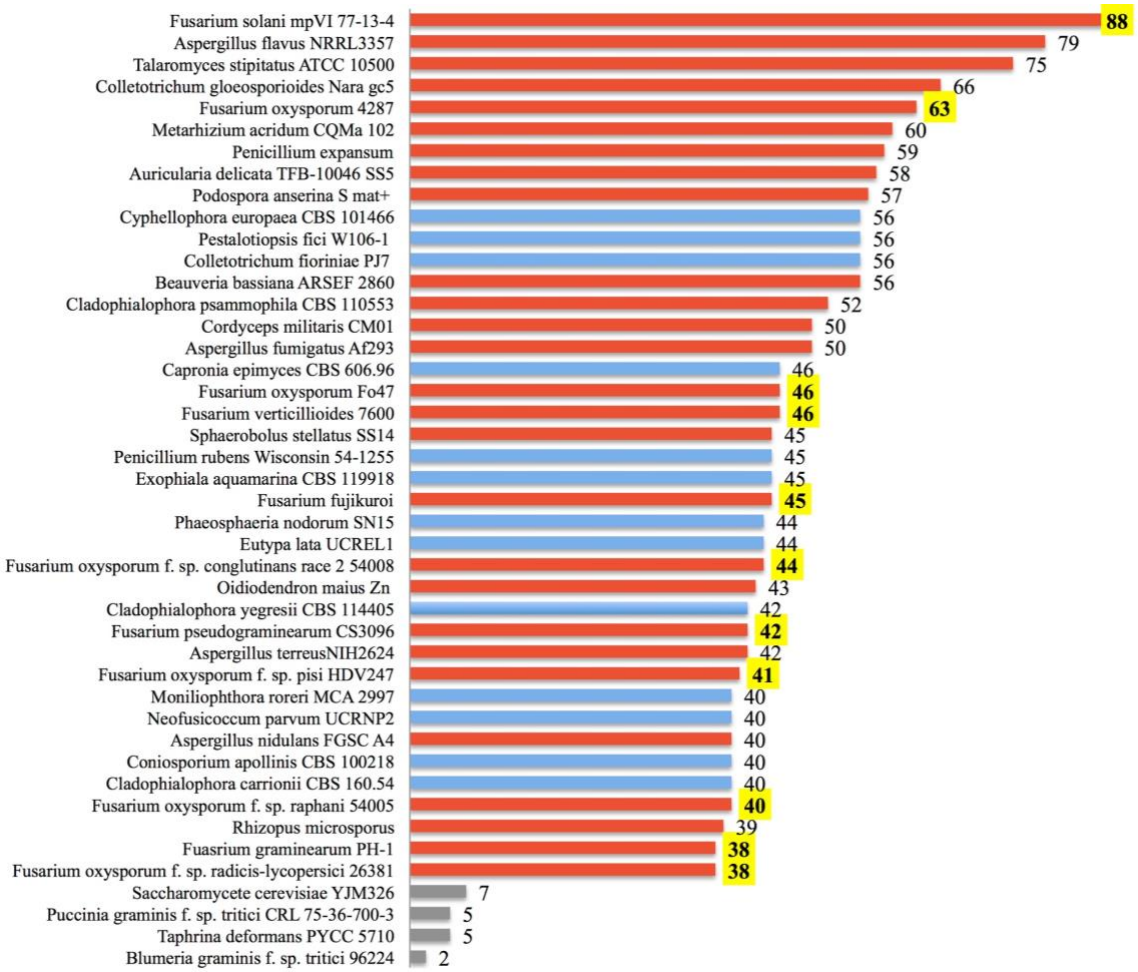

Figure 2.6 Lactamase genes are abundant within some fungi. The number of annotated ORFs possessing a lactamase domain is shown for the top forty fungi among all annotated fungal species identified from the NCBI Protein Database. Species are ranked by the abundance of lactamases. Fungi known to be soil-borne are displayed with red bars, those not clearly cited in literature as soil-borne fungi are in blue, and yeast along with selected obligate plant pathogens are in gray. Numbers of *Fusarium* lactamases are highlighted in yellow.

(A)

FG	FV	FO
	FVEG_05734	FOXG_02559
FGSG_04727	FVEG_12347	
FGSG_16057	FVEG_05854	FOXG_08819
	FVEG_08291	
FGSG_00079	FVEG_12637	FOXG_15319
FGSG_13072	FVEG_08018	FOXG_01652
	FVEG_16907	FOXG_12249
	FVEG_09433	
	FVEG_13366	FOXG_14524
FGSG_00361	FVEG_00815	FOXG_00696
FGSG_09261	FVEG_03849	FOXG_05981
FGSG_05331	FVEG_04252	FOXG_06402
FGSG_07314	FVEG_05261	FOXG_02097
FGSG_06635	FVEG_05485	FOXG_02309
FGSG_10795	FVEG_11466	FOXG_12727
FGSG_11291	FVEG_11838	FOXG_13402
	FVEG_11923	
FGSG_07959	FVEG_12159	FOXG_03706
	FVEG_12288	FOXG_13240
	FVEG_12526	
	FVEG_13253	FOXG_15776
FGSG_16268	FVEG_13675	FOXG_16562
FGSG_00819	FVEG_14723	FOXG_17946
	FVEG_14874	

(B)

FG	FV	FO
	FVEG_01581	
	FVEG_03303	FOXG_04843
	FVEG_01641	FOXG_02811
FGSG_08136	FVEG_01651	FOXG_02821
	FVEG_01795	FOXG_02939
FGSG_04656	FVEG_03457	FOXG_05576
	FVEG_04555	FOXG_07628
FGSG_09143	FVEG_05685	FOXG_02494
	FVEG_17257*	FOXG_13108
FGSG_07702	FVEG_09904	FOXG_10887
	FVEG_12457	
FGSG_02875	FVEG_13172	FOXG_15708
FGSG_05706	FVEG_05963	FOXG_08711
FGSG_02452	FVEG_09057	FOXG_10409
FGSG_00024	FVEG_09854	FOXG_10955
FGSG_03050	FVEG_10740	FOXG_12166
	FVEG_10753	FOXG_12179
FGSG_07996	FVEG_10996	FOXG_17393
FGSG_07538	FVEG_12760	FOXG_15429

(C)

Figure 2.7 Orthological and syntenic analysis of *Fusarium verticillioides*, *F. graminearum*, and *F. oxysporum* lactamase genes. Each column lists predicted β-lactamase orthologs in the three *Fusarium* species. Those sharing synteny of the adjacent 20kb regions are shaded (10kb upstream and 10kb downstream). Amino acid sequences of *Fv* β-lactamases sharing more than 40% sequence identity are considered as paralogs and grouped in outlined boxes. (A) MBLs synteny. (B) SBLs synteny. The modified nucleotide sequence merging FVEG_17257 and FVEG_17258 based on FGENESH prediction was renamed FVEG_17257* here and used for syntenic studies. (C) Demonstration of synteny of genes flanking β-lactamases exemplified by FVEG_12637, which represents part of the *FDB2* gene cluster essential for the biotransformation of 2-benzoxazolinone (Glenn et al., 2016; Glenn and Bacon, 2009). Orthologs are shown in the same color with accession numbers above, and direction of arrows represents the orientation of genes.

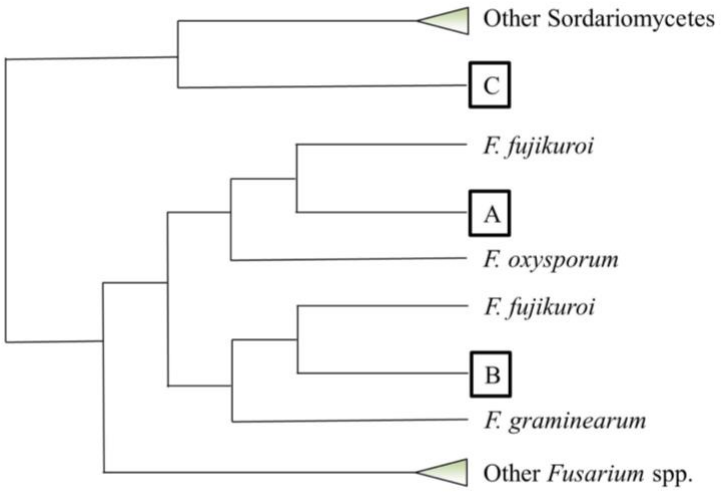

Figure 2.8 Phylogenetic placement of predicted *Fusarium verticillioides* lactamase genes based on amino acid sequence alignment. This cartoon summarizes the phylogenetic pattern of lactamase genes with intact core motifs in *F. verticillioides*. Each query lactamase amino acid sequence was searched for its top 50 homologs using BLASTP in NCBI. Neighbor-joining trees using the Jukes-Cantor genetic distance model were constructed by Geneious Tree Builder (Ver. 8.1) for each individual homology search. All tree topographies complied with the configuration such that each *F. verticillioides* lactamase fell into one of three positions marked as A, B and C. Collapsed clades are shown as triangles.

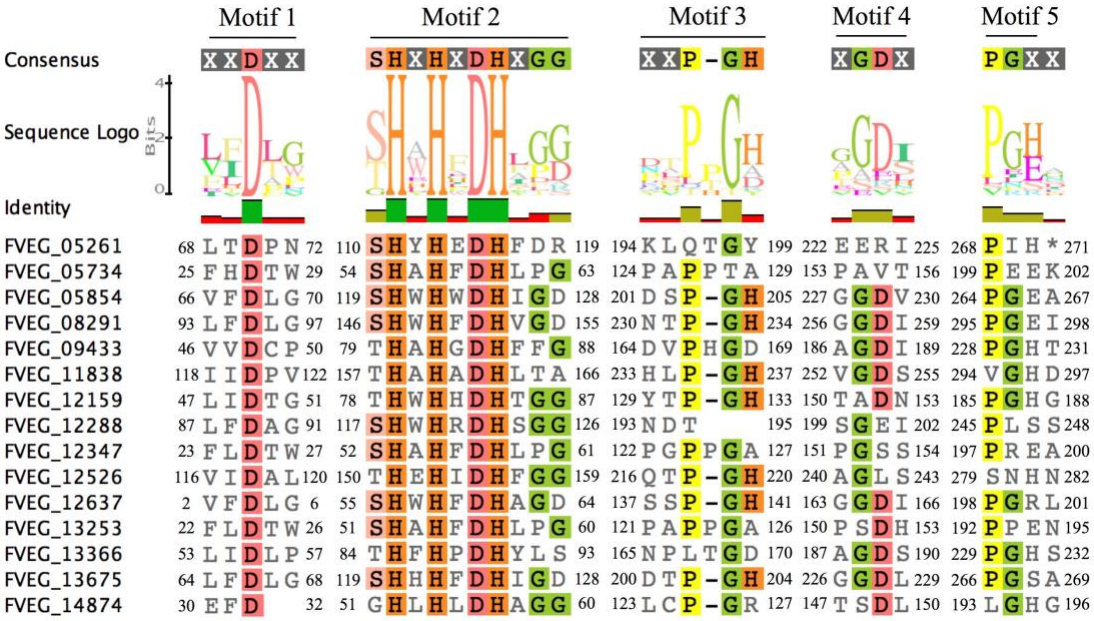

Figure 2.9 Sequence alignment of motifs within *Fusarium verticillioides* metallo-based β-lactamase proteins that are presumably associated with lactam hydrolysis. Amino acids matching at least 50% of all sequences are highlighted.

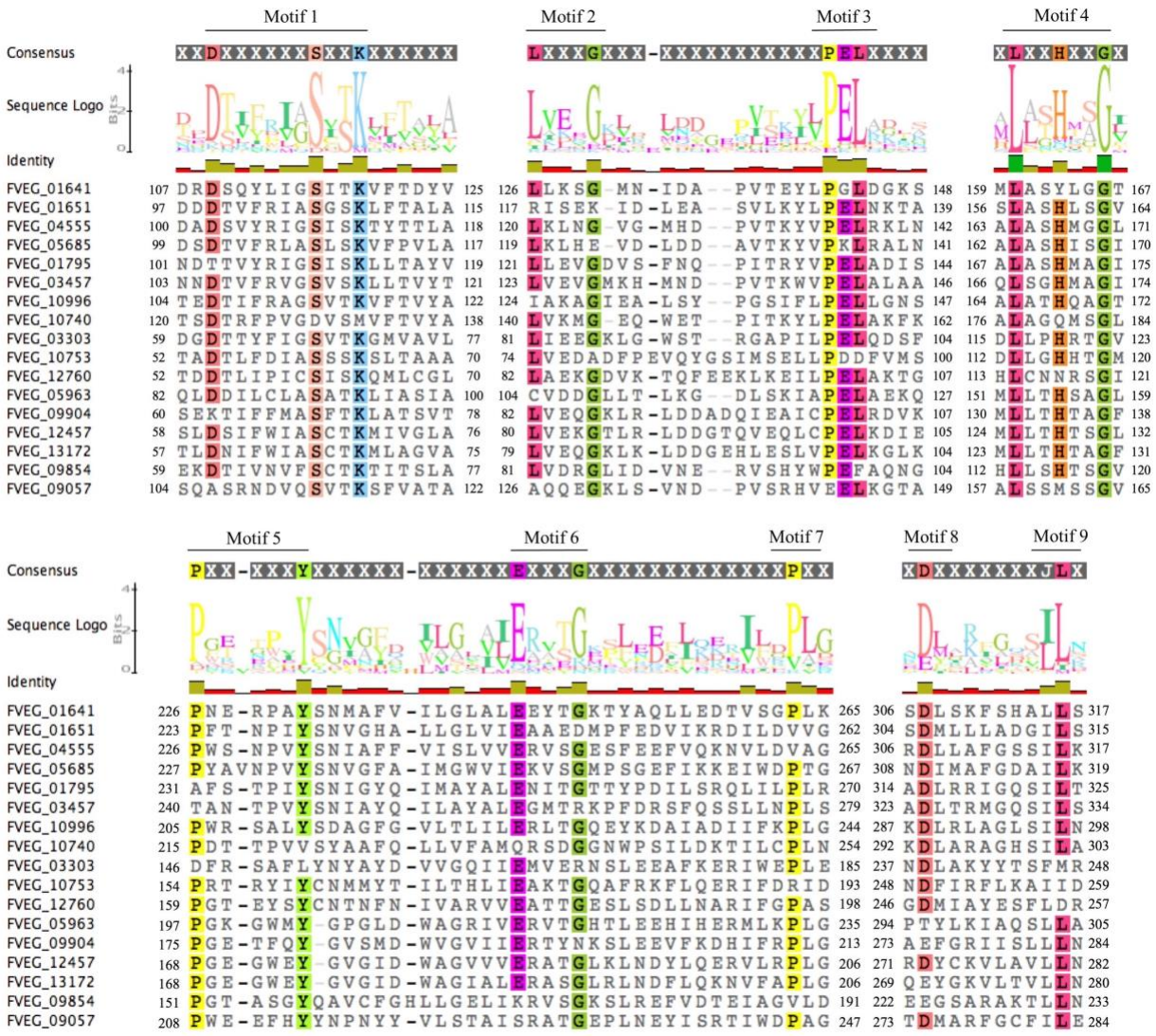

Figure 2.10 Sequence alignment of motifs within *Fusarium verticillioides* serine-based β-lactamases proteins that are presumably associated with lactam hydrolysis. Amino acids matching at least 75% of all sequences included were highlighted.

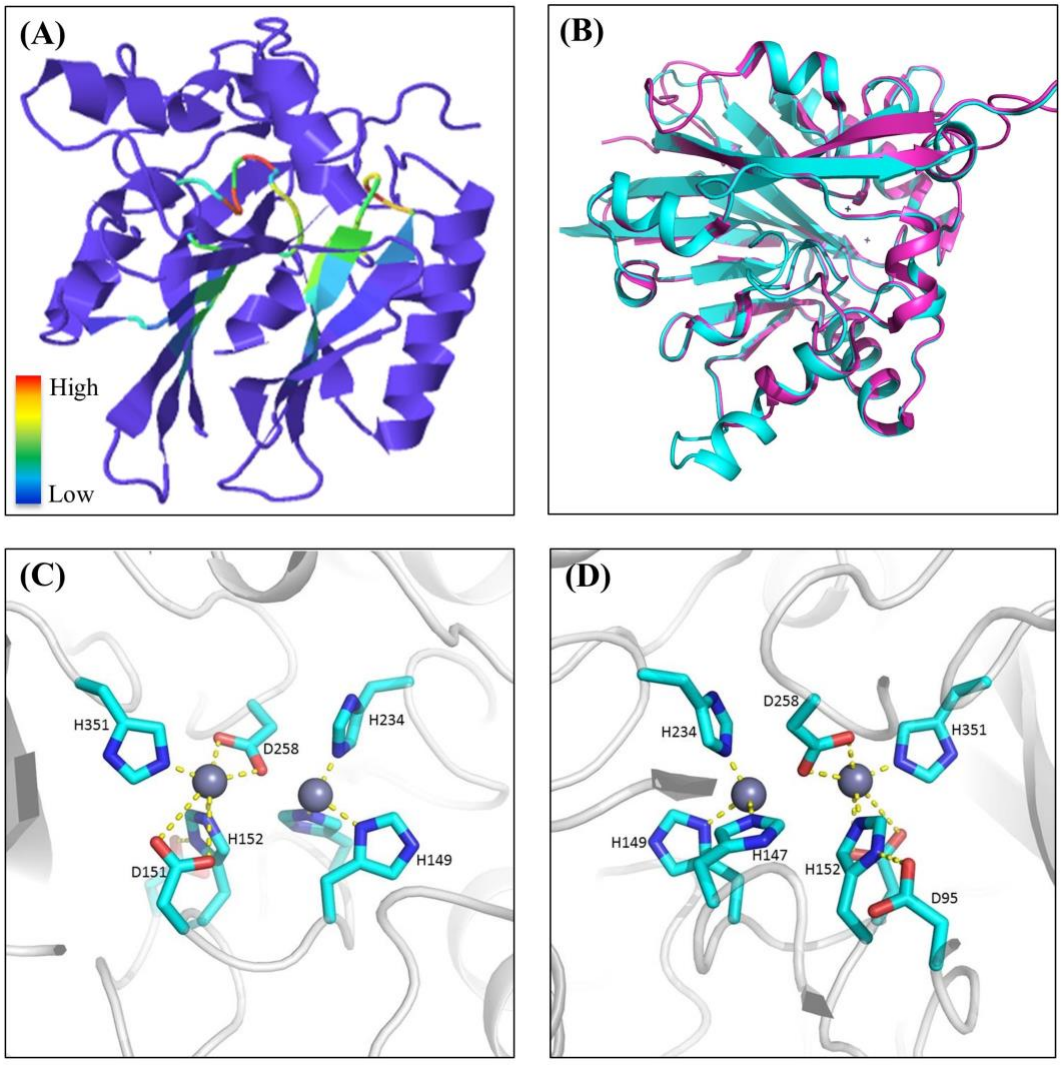

Figure 2.11 Example of metallo-β-lactamase tertiary structures. (A) Predicted protein structure of FVEG_08291 exemplifying a general tertiary structure of metallo-β-lactamases. Motifs are color-coded according to relative conservation as shown in the scale bar. (B) Protein superimposition of FVEG_08291 and 2R2D chain C in Protein Data Bank (http://www.ebi.ac.uk/pdbe/), where cyan represents FVEG_08291 and magenta represents 2R2D chain C. Front (C) and rear (D) view of proposed interactions between zinc ions and conserved MBL amino acids in FVEG_08291.

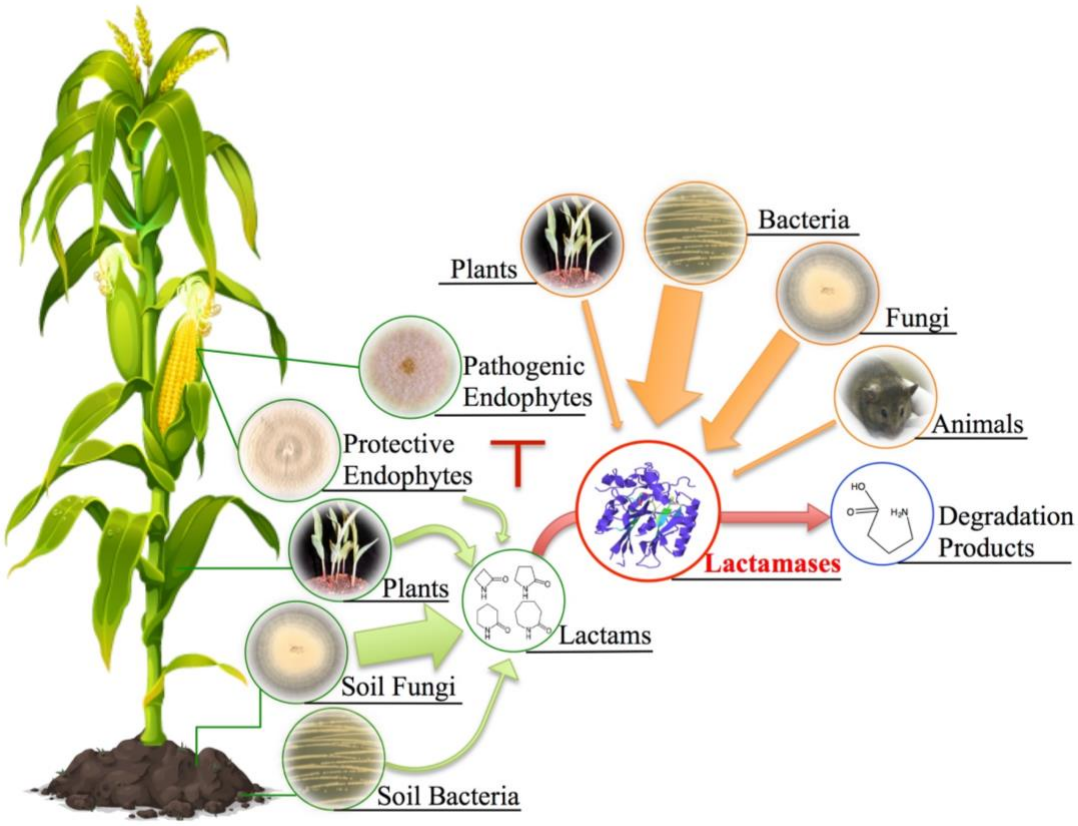

Figure 2.12 Potential ecological sources of lactam compounds and lactamases. Soil fungi, bacteria, plants, and protective endophytes (e.g. *S. zeae*) have all been documented to produce lactam-containing compounds. The antibiotic characteristic of these lactams has been implied to be associated with ecological niche competition. Plants, bacteria, fungi, and even animals have developed corresponding hydrolytic lactamases to combat antibiosis. To expand the conventional examples of bacterial β-lactamases, we propose a more generic ecological model linking lactam production with possible hydrolytic functions of organismal lactamases given their universal presence across different kingdoms. Note that arrow width depicts predicted relative abundance based on genomic frequencies.

CHAPTER 3

ENDO-FIGHT: TRANSCRIPTIONAL AND FUNCTIONAL ANALYSIS OF PYRROCIDINE-MEDIATED ANTAGONISM OF *FUSARIUM VERTICILLIOIDES* BY *SAROCLADIUM ZEAE*, TWO MAIZE SEED ENDOPHYTES

Gao, M., Glenn, A. E., Gu, X., Mitchell, T. R., Duke, M. V., Scheffler, B. E., & Gold, S. E. For submission to PLOS PATHOGENS

ABSTRACT

As the causal agent of maize ear rot, the fungus *Fusarium verticillioides* poses a great threat to food safety due to its production of the fumonisin mycotoxins. *F. verticillioides* is seed borne and shares the maize kernel habitat with another endophyte, *Sarocladium zeae*. Although frequently coinhabiting single seeds, the fungi are generally segregated in separate seed tissues. *S. zeae* produces pyrrocidines A and B that inhibit the growth of *F. verticillioides* and may limit its spread within the seed to locations lacking *S. zeae*. To understand *F. verticillioides'* physiological response to pyrrocidines and to potentially identify its tolerance mechanism(s), we carried out RNA sequencing of the *F. verticillioides* transcriptome upon exposure to purified pyrrocidine A or B at sub-inhibitory concentrations. Functional analysis by deletion was carried out for 10 genes strongly induced by both pyrrocidine A and B, and their impact on resistance to pyrrocidine B was assessed. The gene *FvABC3* (FVEG_11089), encoding a pleiotropic-drug resistance (PDR)-type ABC transporter, dramatically contributed to tolerance of pyrrocidine B. Transcriptional induction of *FvABC3* was independent of an adjacent similarly induced transcription factor, *FvZEAR* (FVEG_11090). Also amongst the ten analyzed genes was *FvZBD1* (FVEG_00314), a gene encoding a zinc-binding dehydrogenase and positioned immediately adjacent to the fumonisin biosynthetic gene cluster. Interestingly, deletion of *FvZBD1* appeared to strongly derepress the production of fumonisins and significantly enhanced the mutant's virulence towards Silver Queen® maize seedlings. The strong induction of *FvZBD1* combined with its genomic location and impact on fumonisin biosynthesis suggested a link between pyrrocidine exposure and suppression of fumonisin production by *F. verticillioides* and provides additional support for *S. zeae* as a potential biological control agent against *F. verticillioides* and fumonisin contamination of maize.

INTRODUCTION

As one of the most notorious mycotoxigenic pathogens, *Fusarium verticillioides* poses a serious worldwide threat to the health of maize as well as livestock and humans. *F. verticillioides* can elicit severe kernel rot symptoms, which are often coupled with high levels of mycotoxin contamination (Blacutt et al., 2018). Production of *F. verticillioides* mycotoxins, predominantly the fumonisins, are associated with animal toxicoses, such as leukoencephalomalacia in horses and pulmonary edema in swine (Marasas et al., 1988; Ross et al., 1990). Further, its endophytic life style increases difficulties of disease management, as the infected kernels often remain visually symptomless (Blacutt et al., 2018).

Along with *F. verticillioides* inhabiting the same ecological niche is another kernel endophyte, *Sarocladium zeae* (formerly known as *Acremonium zeae*) (King, 1981; Munkvold et al., 1997). Earlier histopathological studies on "sound-appearing" maize kernels revealed that *F. verticillioides* primarily colonizes the pedicel and abscission layers of the developing maize seed, while *S. zeae* was often detected in the embryo and endosperm (Sumner, 1967). These observations describe an interesting phenomenon in which these two endophytes may sympatrically co-inhabit the same seed but retain structure or tissue specificity.

Sarocladium zeae produces the pyrrocidines, first described in 2002 for their antibacterial properties (He et al., 2002). These lactam compounds, pyrrocidine A and B, also demonstrated *in vitro* inhibitory activity against *Candida albicans*, *Aspergillus flavus*, and *F. verticillioides*, which might impact the partitioning of *F. verticillioides* and *S. zeae* to different tissues within maize kernels (Wicklow et al., 2005; Wicklow and Poling, 2009). Pyrrocidine A and B differ by presence or absence of a double bond in the lactam ring, resulting in a higher toxicity of pyrrocidine A than B against a number of fungal and bacterial species (Wicklow et al., 2005;

Wicklow and Poling, 2009). The crucial role of this double bond in determining apoptosis inducing cytotoxicity against human acute promyelocytic leukemia HL60 cells was also addressed (Uesugi et al., 2016). Pyrrocidine A and B can both be detected in *S. zeae*-infested kernels through liquid chromatography-mass spectrometry (LC-MS), but the concentration of pyrrocidines during natural occurrence in maize seeds has not been described (Wicklow et al., 2005; Wicklow and Poling, 2009). *S. zeae* is not reported to synthesize secondary metabolites harmful to plants, nor does it cause any ear or stem rot symptoms (White, 1998). Collectively, these studies support a role of *S. zeae* as a "protective" endophyte and bring attention to its potential as a biological control agent (Wicklow et al., 2005).

The hypothesis that *S. zeae* employs pyrrocidines as metabolic weapons to exclude *F. verticillioides* from *S. zeae*-colonized seed structures is fascinating, but how *F. verticillioides* genetically or biochemically responds to pyrrocidine exposure is unknown, as is whether such responses contribute to coexistence of the two endophytes in the plant. For example, since pyrrocidines contain lactam rings, do any of the *F. verticillioides* genes induced by the compounds encode lactamases? We recently reported a thorough inventory of fungal lactamases and their potential functions in the environment (Gao et al., 2017). In order to speculate on the possible defensive mechanisms by which *F. verticillioides* survives in the presence of pyrrocidines, we explored the transcriptional responses via RNA sequencing in *F. verticillioides* upon exposure to purified pyrrocidine A or B at sub-inhibitory concentrations. Pyrrocidine A and B treatments shared 395 up-regulated and 130 down-regulated genes. Ten of the up-regulated genes were selected for functional characterization, and three of the genes proved to be particularly informative. Mutants in one of these genes, encoding a pleiotropic-drug resistance (PDR)-type ATP-binding cassette (ABC) transporter (FVEG_11089), showed dramatically

increased sensitivity to pyrrocidine B. A co-upregulated adjacent gene encoding a putative transcription factor (FVEG_11090) was found to be dispensable to the induction of FVEG_11089. Lastly, a gene encoding a zinc-binding dehydrogenase (FVEG_00314), appeared to repress production of fumonisins. Interestingly, FVEG_00314 is located directly adjacent to the *FUM21* gene encoding the *cis*-regulatory transcription factor for the fumonisin biosynthetic gene cluster. Thus, a link between exposure to *S. zeae* pyrrocidines and fumonisin production by *F. verticillioides* is proposed.

RESULTS

1. Pyrrocidine A and B elicited differential gene responses in *Fusarium verticillioides.*

To explore the transcriptional responses of *F. verticillioides* upon exposure to pyrrocidine A or pyrrocidine B, the transcriptome of wild-type *F. verticillioides* induced by either compound was sequenced and compared to that of a DMSO-treated control. The raw RNA-seq reads of each biological replicate ranged from 14.2 to 21.9 million, of which 13.9 – 21.5 million reads were mapped to the reference genome of *F. verticillioides* (Supplemental Table 3.1) (Ma et al., 2010). When applying two thresholds (first a false discovery rate-adjusted p-value < 0.05, and second a $\log_2$ fold change > 1 for up-regulated genes or < -1 for down-regulated genes), we identified 770 and 4290 differentially expressed genes upon exposure to pyrrocidine A and B, respectively, when compared to the DMSO only treated control. Similar levels of regulation were observed among the biological replicates (Fig. 3.1A). Pyrrocidine A and B treatments shared 395 up-regulated genes and 130 down-regulated genes. Only 25 genes were identified as up-regulated in one treatment and down-regulated in the other (Fig. 3.1B). Considering the high similarity between the two chemical structures, we focused on genes co-upregulated by both compounds for subsequent functional analyses.

2. Pyrrocidine-responsive genes were primarily enriched in metabolism, cellular transport, and cell rescue functions.

To better understand the functional potential of genes responsive to both pyrrocidines A and B, the 395 up-regulated and 130 down-regulated genes were categorized using the MIPS Functional Catalogue (http://mips.helmholtz-muenchen.de/funcatDB/) (Ruepp et al., 2004), and enriched categories with p-value < 0.05 are shown in Figure 3.2. We identified 196 genes significantly enriched in the following functional categories with corresponding catalog numbers in parentheses: metabolism (01), cellular transport (20), cellular communication/signal transduction mechanism (30), cell rescue, defense and virulence (32), and interaction with the environment (34). The vast majority of the enriched genes (158/196) were associated with metabolism and cellular transport, while only nine genes were exclusively enriched in cell rescue, defense, and virulence (Fig. 3.2). There were also nine genes demonstrating significant enrichment in the four functional categories of (01), (20), (32), and (34). Among these was an ABC transporter-encoding gene (*FvABC3*, FVEG_11089) highly induced under both pyrrocidine A and B treatments (Table 3.1). Directly upstream of *FvABC3* is the co-induced *FvZEAR* (FVEG_11090), which encodes a putative transcription factor.

3. Deletion of ten select genes

To explore the molecular relevance to pyrrocidine resistance, 10 *F. verticillioides* genes of interest spanning different MIPS categories were targeted for functional characterization. These 10 genes demonstrated strong and statistically significant induction by pyrrocidines (log_2 fold change > 1 in pyrrocidine A treatment and > 6 in pyrrocidine B treatment, plus a false discovery rate-adjusted p-value < 0.01), low or nominal FPKM (Fragments Per Kilobase of transcript per Million mapped reads) values (< 100) in the control treatment, and high expression

levels in the pyrrocidine B treatment (FPKM > 950) (Table 3.1). These targets were weighted towards pyrrocidine B induction due to a relatively adequate amount of pyrrocidine B available for functional analyses. Our availability of pyrrocidine A was very limited.

F. verticillioides deletion mutants were generated with the OSCAR protocol (Gold et al., 2017; Paz et al., 2011) for each of the 10 target genes and validated by specific PCR assays for each gene and deletion construct and by quantitative PCR (qPCR) to determine copy number for the hygromycin resistance cassette to ensure the mutants had only single insertions (Supplemental Figure 3.1 and 3.2). Subsequent growth curve analyses were carried out by challenging the collection of mutants with pyrrocidine B at 20 μg/mL, the same concentration employed in RNA-seq experiments. Initial screening of the deletion mutants in liquid PDB revealed that Δ*FvABC3* mutants exhibited almost no growth, and that Δ*FvZBD1* mutants appeared slightly more sensitive, while gene deletion strains for the other eight genes demonstrated no significantly enhanced sensitivity compared to the wild-type M3125 (data not shown).

4. *FvABC3* significantly impacted the resistance to pyrrocidine B, whereas the adjacent transcription factor *FvZEAR* did not.

To investigate the significant role of this ABC transporter gene, a qRT-PCR assay was conducted to confirm the pyrrocidine B-induced expression levels of *FvABC3* and its adjacent transcription factor gene, *FvZEAR*. The *Fusarium graminearum* orthologs of both of these genes were previously characterized (Ammar et al., 2013; Lee et al., 2010). Both genes were highly induced in M3125 PDB liquid cultures when exposed to pyrrocidine B at 20 μg/mL for 1 hour. The induction level of *FvABC3* remained comparably high when challenging the Δ*FvZEAR* mutant under the same conditions (Fig. 3.3A and 3.3B). This suggested that pyrrocidine-induced

FvABC3 expression is independent of its neighboring transcription factor, which was consistent with the phenotype of no enhanced sensitivity to pyrrocidine B in Δ*FvZEAR* mutants (data not shown), while *FvABC3* mutants showed extreme sensitivity (Fig. 3.4). Evaluation of Δ*FvABC3* mutant strains revealed that the elevated sensitivity to pyrrocidine B was maintained even at 10 μg/mL, half the concentration utilized for transcriptional induction. Inhibition could be visualized in the honeycomb plates after the 100-hour incubation with continuous shaking (Fig. 3.4). The increased pyrrocidine B sensitivity of Δ*FvABC3* mutants was complemented to a level similar to wild type by reintroducing the *FvABC3* gene into Δ*FvABC3* mutants by protoplast transformation.

5. Deletion of *FvABC3* did not alter fungal virulence on maize seedlings nor fumonisin production in GYAM medium.

All the fungal strains tested in this experiment, including wild-type FRC M3125, Δ*FvABC3* mutants, and the complemented strains, reduced maize seedling height by approximately 60% compared to uninoculated water control seedlings. Necrotic leaf lesions and other typical disease symptoms were observed across all fungal strains, and no change in virulence was observed between M3125 and Δ*FvABC3* mutants (Supplemental Figure 3.3).

Since the Silver Queen® maize cultivar used in the seedling assay is known to be sensitive to the phytotoxic effects of fumonisins, symptomology typically reflects the level of fumonisin production by the *F. verticillioides* strains tested (Baldwin et al., 2014; Glenn et al., 2008). To support previous seedling observations, fumonisin production capability of the Δ*FvABC3* mutants was assessed and compared to their wild-type progenitor in GYAM liquid cultures, a medium conducive to fumonisin production (Brown et al., 2007). The fumonisin concentrations were normalized to the weight of vacuum-desiccated fungal tissue from the

cultures. The individual gene deletion mutants did not exhibit significant differences in fumonisin B1 (FB1), B2 (FB2), or B3 (FB3) production. FRC M3125 produced FB1 at an average concentration of 375 μg/mL/g, while two Δ*FvABC3* mutants, Δ*FvABC3*-1 and Δ*FvABC3*-2, produced 349 and 345 μg/mL/g, respectively (Supplemental Figure 3.4). As is typical, compared to FB1 production, all strains produced consistently lower concentrations of FB2 (69 – 75 μg/mL/g) and FB3 (152 – 172 μg/mL/g).

6. Deletion of *FvZBD1* caused a minor delay in growth under pyrrocidine B exposure.

FvZBD1 (FVEG_00314) was the most highly induced gene from both the pyrrocidine A and pyrrocidine B exposure treatments with a log2 induction value of 12 for each, which is approximately a 4100-fold change in expression (Table 3.1). We validated the induction of *FvZBD1* in M3125 through qRT-PCR (Fig. 3.3C). Interestingly, *FvZBD1* is directly adjacent to the fumonisin biosynthetic cluster (Supplemental Figure 3.5). Due to the distinctive genomic location of *FvZBD1*, we further characterized phenotypic changes as a consequence of its deletion. When Δ*FvZBD1* mutants were challenged with 10 μg/mL pyrrocidine B, we observed a significant and repeatable delay in growth, compared to the wild type (Supplemental Figure 3.6). The phenotype of increased sensitivity was not observed in complemented strains.

7. Deletion of *FvZBD1* significantly enhanced fungal virulence on maize seedlings.

As expected, all the fungal treatments exhibited stunted growth of Silver Queen® maize seedlings, compared to the uninoculated water control. However, Δ*FvZBD1* mutant-treated plants displayed the earliest onset of disease symptoms (on day 4 post planting, compared to day 6 for M3125), increased disease severity with reduced growth, and higher frequency of necrotic lesions and other severe symptoms, compared to the wild-type treatment (Fig. 3.5A, 3.5B). The mean heights of seedlings treated with Δ*FvZBD1*-1 and Δ*FvZBD1*-2 were 6.5 cm and 8.2 cm,

respectively, whereas the mean heights of M3125, ectopic, and complemented-strain treatments ranged from 12.5 cm to 13.5 cm. Two-tailed Mann Whitney Wilcoxon tests revealed significant differences in mean seedling heights between Δ*FvZBD1* mutant treatments and wild-type treatments, while there were no statistical distinctions between seedlings inoculated with wild type, ectopic, or complemented strains (Fig. 3.5A). Uninoculated control plants showed the highest germination percentage and mean seedling height. Δ*FvZBD1* treatments showed the most stunted growth and the lowest germination percentage, while M3125, ectopic, and complemented strain treatments exhibited better growth and greater germination (Fig. 3.5B, 3.5C).

8. Enhanced seedling virulence of Δ*FvZBD1* mutants was likely due to increased fumonisin production.

The enhanced seedling virulence of Δ*FvZBD1* mutants and the proximity of *FvZBD1* to the fumonisin biosynthetic cluster led us to evaluate fumonisin production by Δ*FvZBD1* mutants. Interestingly, deletion of *FvZBD1* elicited a remarkable increase in FB1, FB2, and FB3 production. The two Δ*FvZBD1* mutants produced over 9 mg/mL FB1 per gram of fungal tissue in GYAM liquid cultures, a > 30-fold increase compared to the 284.4 µg/mL/g for M3125. The mean FB2 production of Δ*FvZBD1*-1 and Δ*FvZBD1*-2 mutants was 2581.3 and 2439.4 µg/mL/g, respectively, which is approximately a 40-fold increase over the 58.4 µg/mL/g in wild type. A prominent increase in FB3 production was also seen in Δ*FvZBD1* mutants. Δ*FvZBD1*-1 and Δ*FvZBD1*-2 mutants produced, on average, 2054.1 and 2200.7 µg/mL/g FB3, respectively, compared with wild-type M3125 which produced an average of 260.1 µg/mL/g FB3 in GYAM liquid cultures. All *F. verticillioides* strains in this assay produced more FB1 than FB2 or FB3. M3125 and complemented strains typically produced more FB3 than FB2, while Δ*FvZBD1* mutants exhibited an inverse trend by generating more FB2 than FB3 (Fig. 3.6).

9. Δ*FvZBD1* mutants exhibited a more uniform growth morphology on GYAM plates compared to wild type.

After 7-day incubation on GYAM plates, Δ*FvZBD1* mutants exhibited more radial growth with smooth colony margins, while M3125, an ectopic transformant, and complemented strains showed slightly slower growth with irregular, undulating colony edges and some sectoring (Fig. 3.7A). Δ*FvZBD1* colonies appeared to be flat with enhanced orange pigmentation of the fungal mycelia, while M3125 and complemented strains appeared less pigmented (Fig. 3.7B). Rough colony margins were observed from three days after inoculation and became progressively more evident as colonies aged.

10. Pyrrocidines elicited the differential expression of lactamase-encoding genes

Pyrrocidine A displays higher toxicity than pyrrocidine B (Wicklow and Poling, 2009). The only difference between these xenobiotic compounds is a double bond present in the lactam ring of pyrrocidine A, which implies the relevance of the lactam ring to antibiosis (Wicklow et al., 2005; Wicklow and Poling, 2009). Inspired by our previous research on the molecular and functional characterization of fungal lactamases (Gao et al., 2017; Glenn et al., 2016), we further investigated the transcriptional regulation of the 46 lactamase genes in the *F. verticillioides* genome. Four lactamase genes in *F. verticillioides* were up- or down-regulated by both pyrrocidine A and B treatments, four lactamase genes were exclusively induced by pyrrocidine A, and nine were exclusively regulated by pyrrocidine B (Table 3.2). Although FVEG_05734, FVEG_12457, and FVEG_13675, and exhibited over 16-fold changes in gene expression, the average FPKM values remained low after induction at 23, 18, and 74, respectively, indicating their transcripts were not highly abundant despite the induction.

DISCUSSION

F. verticillioides and *S. zeae* frequently co-inhabit maize kernels, yet they partition their colonization to separate kernel tissues. The potential role of pyrrocidines in such partitioning and spatially limiting seed colonization by *F. verticillioides* inspired us to pursue the impact of these secondary metabolites on the *F. verticillioides* transcriptome. We aimed to gain insights into the survival mechanisms of *F. verticillioides* in the presence of inhibitory pyrrocidines by examining transcriptional responses to pyrrocidine exposure. RNA sequencing of the transcriptome revealed 770 and 4290 genes differentially responsive to pyrrocidine A and B, respectively. Of the 395 up-regulated genes shared by both treatments, we selected 10 gene targets for functional analyses based on expression levels and significant fold changes. Preliminary screening of the single gene deletion mutants indicated that two genes, an ABC transporter gene (*FvABC3*) and a zinc-binding dehydrogenase gene (*FvZBD1*), proved to be particular interesting and were characterized in greater detail. *FvABC3* was shown to have a crucial role in tolerating pyrrocidine B. Further, *FvZBD1*'s proximity to the well-characterized fumonisin biosynthetic gene cluster led us to assess the impact of *FvZBD1* on fumonisin production and virulence. To our surprise, deletion of *FvZBD1* significantly enhanced the fungal virulence on maize seedlings, which was correlated with the remarkable increase in fumonisin production by the mutants.

We targeted ten genes to generate individual deletion mutants for functional analyses. During the initial screening with 20 μg/mL pyrrocidine B, only *FvABC3* exhibited significantly elevated sensitivity compared to wild type. Among the ten targeted genes, FVEG_17422 is another ABC transporter-encoding gene with differential induction upon exposure to both pyrrocidine A and B, with the level of induction being much higher in pyrrocidine B exposure than A (Table 3.1). However, deletion of FVEG_17422 did not result in a noticeable change in

pyrrocidine B sensitivity in the initial screening with 20 μg/mL pyrrocidine B (data not shown). Hence, FVEG_17422 may potentially be involved in transporting intermediate secondary metabolites generated during the degradation of pyrrocidine B, which in turn suggests the functional specificity of *FvABC3* in pyrrocidine B exposure. Along with FVEG_11089 and FVEG_17422, FVEG_02410 and FVEG_16559 are another two ABC transporter encoding genes also exhibiting high induction levels ($\log_2$ fold change = 9.6 and 6.1, respectively) upon exposure to pyrrocidine B, and it would be interesting to pursue their impact on pyrrocidine B tolerance.

ABC transporters have been characterized in all extant phyla from prokaryotes to humans for their critical roles in drug resistance, which is also how some of them were first identified (Lodish, 2008). As the name indicates, ABC transporters mediate intake of the nutrients (importers; in prokaryotes only) or extrusion of toxins/drugs (exporters; in all phyla) across cellular membranes, which are energized by ATP binding and hydrolysis. A common characteristic of ABC transporters is that they possess nucleotide-binding domains (NBDs) and transmembrane domains (TMDs), responsible for substrate recognition and conformational changes (Ambudkar et al., 1992).

As noted above, we targeted two genes (FVEG_11089 and FVEG_17422) encoding ABC transporters for genomic deletion and tested the mutants for increased sensitivity to pyrrocidine B. Of these, only deletion of *FvABC3* (FVEG_11089) resulted in increased sensitivity. *FvABC3* putatively encodes a protein of 1488 amino acids, and it shares high protein sequence identities (> 85%) with clear orthologs in other *Fusarium* pathogens including *Fusarium fujikuoi*, *Fusarium proliferatum*, *F. graminearum*, *F. oxysporum*, and others (data not shown). Similar to other fungal ABC transporters, FvABC3 topology contains two modules, each with a nucleotide-

binding domain (NBD) and a transmembrane domain (TMD), reminiscent of its extensively studied *Saccharomyces cerevisiae* ortholog, PDR5 (Supplemental Figure 3.7). Similar to PDR5, the first NBD of FvABC3 is present at the N-terminus followed by a TMD with five transmembrane segments (TMSs) followed by another NBD and a TMD with 6 TMSs (Supplemental Figure 3.7A and 3.7B). A close examination of the tertiary structures revealed conventional α-helical structures in the TMDs regions, while the NBDs possess two signature catalytic Walker A motifs or P-loops (GXXGXGKS/T) inferred by psi-blast. The majority of conserved amino acids are predicted in the NBDs (data not shown) (Kelley et al., 2015). This conformation of FvABC3 resembles the crystal structure of a characterized multidrug resistance transporter (Protein Data Bank ID: 4F4C) in *Caenorhabditis elegans*, which is supportive of its role as a pyrrocidine extruder (Jin et al., 2012; Kelley et al., 2015).

FvABC3 is critical for resistance to pyrrocidine B. As a consequence of *FvABC3* deletion, mutant strains could not grow under exposure to pyrrocidine B at half the sub-inhibitory concentration used in RNA-seq experimental treatments (Fig. 3.4). Its ortholog in *F. graminearum*, *FgABC3* (FGSG_04580) was previously characterized for its role in azole fungicide tolerance (Ammar et al., 2013), and deletion of *FgABC3* resulted in significantly reduced tolerance in the triazoles tebuconazole, prothioconazole, epoxyconazole, and fenarimol. Treatment of prothioconazole and fenarimol also elicited aberrant hyphal morphology in Δ*FgABC3* mutants. Interestingly, when we measured the growth rate of Δ*FvABC3* and ΔFVEG_17422 mutants as well as wild type in PDA plates amended with gradient concentrations of tebuconazole, no growth differences were observed. In contrast, exposing Δ*FvABC3* mutants to 10 μg/mL pyrrocidine B resulted in abnormal hyphal morphology with no conidiation (data not shown), suggestive of unfavorable growth conditions (Fig. 3.4). This

differential response to two structurally distinct xenobiotics suggests *FvABC3* may have substrate specificity for pyrrocidines and no utility for tolerance toward fungicides such as tebuconazole.

Reported microarray analysis identified a zearalenone (ZEA) responsive gene, *ZEAR*, in *F. graminearum* with a 50-fold induction in expression upon exposure to zearalenone for one hour (Lee et al., 2010). Its orthologous transcription factor encoding genes, *FvZEAR* (FVEG_11090) in *F. verticillioides* and *FoZEAR* in *F. oxysporum*, were also shown to be induced by ZEA exposure (Lee et al., 2010). In our study, *FvZEAR* exhibited more than 39- and 174-fold induction upon exposure to pyrrocidine A and B, respectively. It's interesting to observe that *FvZEAR* is responsive to pyrrocidines and ZEA, despite their unrelated chemical structures. Deletion of *FvZEAR* did not impact the expression of its adjacent *FvABC3*, nor did it alter the sensitivity of *F. verticillioides* to pyrrocidine B. This implies the dispensable role of *FvZEAR* in tolerating pyrrocidine B. It is worth noting that FVEG_10488, encoding a putative transcription factor sharing 62% amino acid sequence identity with *FvZEAR* (FVEG_11090), was also significantly induced with $\log_2$ fold changes of 5.8 and 8.7 and FPKM values of 16 and 127 after pyrrocidine A and B exposure, respectively. Although the high fold changes were largely due to no expression of FVEG_10488 in the control treatment, it's still interesting to observe this transcription factor being induced during pyrrocidine exposure. The amino acid similarity of FVEG_10488 to FVEG_11090, particularly the 80% identity over the first two-thirds of their alignment where the GAL4-like Zn2Cys6 binuclear cluster DNA-binding domain is located, may indicate possible functional redundancy regarding transcriptional regulation of genes such as *FvABC3*.

Fumonisins are polyketide-based mycotoxins produced by several closely related *Fusarium* species, and these metabolites, especially FB1, cause severe species-specific animal health problems (Howard et al., 2001; Sadler et al., 2002). Among the fumonisin producers, *F. verticillioides* has received worldwide attention due to its pathogenicity, toxicity, and wide occurrence on maize, a major economically important crop. Four different types of fumonisins are produced by *F. verticillioides* (FB1, FB2, FB3, and FB4), among which FB1 is the most abundant and toxic in naturally infected maize kernels (Musser and Plattner, 1997). Brown et al. (2012) described the co-regulated expression pattern of fumonisin biosynthetic (*FUM*) cluster genes with accession numbers ranging from FVEG_14633 (formerly FVEG_00315) to FVEG_00329. Interestingly, while the *FUM* genes displayed very low expression levels after pyrrocidine exposure (FPKM<30), the zinc-binding dehydrogenase *FvZBD1* (FVEG_00314) immediately adjacent to the identified *FUM* cluster was induced to a high level (FPKM>3400) in both pyrrocidine A and B treatments. In fact, *FvZBD1* was the most highly induced gene in these treatments.

Inspired by its unique genomic position, we explored the impact of *FvZBD1* on fumonisin biosynthesis. Surprisingly, Δ*FvZBD1* strains showed dramatic elevation in productions of fumonisins. Deletion of *FvZBD1* appeared to unleash the potential of fumonisin production in *F. verticillioides*, leading to more than 30-fold increase in FB1 production, >40-fold increase in FB2, and >8 fold increase in FB3, compared to wild type. FB3 is a precursor to FB1 in the fumonisin biosynthetic pathway (Alexander et al., 2009), and we observed a comparable amount of FB1 and FB3 production in M3125 after 7-day incubation. Interestingly, deletion of *FvZBD1* favors the production of FB1 by more than four-fold over the FB3 under the same growing conditions (Fig. 3.6). The link between *FvZBD1* and the *FUM* cluster was not

reflected in the previously published microarray data, where the expression profile of *FvZBD1* seemed unrelated to the production of fumonisins under normal growth conditions in GYAM medium (Brown et al., 2012). Based on the premise of co-regulation, the *FvZBD1* gene does not appear to be a member of the *FUM* biosynthetic gene cluster, but since its deletion dramatically boosts fumonisin production, it may be that *FvZBD1* represents a noncanonical *FUM* cluster gene possibly involved in regulating production of the mycotoxin.

Along with the elevated production of fumonisins, we also observed enhanced virulence on maize seedlings, since the Silver Queen® maize cultivar employed in this study is known to be highly sensitive to fumonisin phytotoxic effects (Baldwin et al., 2014; Glenn et al., 2008). Compared to wild-type and complemented-strain treatments, Δ*FvZBD1*-infected plants exhibited earlier appearance of disease symptoms, including poor germination rate, increased stunting and more severe lesion development leading to near whole-plant necrosis (Fig. 3.5). The enhanced virulence of Δ*FvZBD1* mutants in the seedling assay reflects their elevated production of fumonisin, and to our knowledge, this is the first case of *F. verticillioides* eliciting maize hypervirulence, or for that matter hyperproduction of a secondary metabolite, due to a single-gene deletion. Such changes in physiology and pathology may be expected with the loss of a transcription factor (Cho et al., 2012), yet FvZBD1 has a conserved protein domain indicating its relationship to zinc-dependent alcohol dehydrogenases and quinone oxidoreductases, suggesting the encoded protein may impact metabolic activity and fumonisin production in a manner not yet understood but perhaps involving energy production or conversion.

As another example of enhanced activity, Δ*FvZBD1* mutants exhibited a more uniform and slightly faster growth morphology on fumonisin-conducive GYAM media (Fig. 3.7). On the contrary, the wild-type, ectopic, and *FvZBD1* complemented strains showed irregular and

undulating colony edges, a type of morphology commonly observed when fungi are exposed to compounds that adversely affect growth, and thus, perhaps their growth morphology reflects reduced fitness in the presence of secondary metabolites being produced by the strains as a result of growth on GYAM. However, these strains did not demonstrate undulating growth morphology in regular PDA plates, a fumonisin non-conducive medium. Considering the greatly enhanced fumonisin production in GYAM by Δ*FvZBD1* mutants and their healthier culture morphology, we may conclude that deletion of Δ*FvZBD1* not only unleashes the potential of fumonisin production in *F. verticillioides*, but there may also be enhanced fitness and tolerance to fumonisin and other metabolites in the GYAM environment. Future studies will attempt to address the underlying genetic mechanisms conferring these enhanced phenotypes.

Despite the importance of the lactam moiety in the pyrrocidines for toxicity, the *F. verticillioides* lactamase genes did not exhibit strong expression levels before and after pyrrocidine exposure (Table 3.2). This may be an artifact of the experimental design of the exposure treatments. The RNA-seq experiments were conducted with a one-hour induction by pyrrocidines A or B, and thus genes typically involved in early responses (e.g. transporters or metabolic genes) were among the most highly induced. In contrast, genes encoding lactamases and other hydrolytic enzymes may be involved at later time points. We did observe the degradation of pyrrocidine B after two-day incubation with wild-type *F. verticillioides* in PDB liquid cultures (data not shown). Therefore, transcriptional analysis of later time points may help identify hydrolytic lactamase-encoding genes involved in pyrrocidine B degradation.

In summary, we functionally analyzed 10 pyrrocidine up-regulated genes for their role in conferring resistance to pyrrocidine B. Detailed analyses were carried out for an ABC transporter encoding gene required for wild type resistance to pyrrocidines, *FvABC3*, and a zinc-binding

dehydrogenase encoding gene, *FvZBD1*. We hypothesize that *FvABC3* facilitates persistence of *F. verticillioides* in maize seeds when encountering pyrrocidines, while the *S. zeae* pyrrocidines induced the expression of *FvZBD1* in *F. verticillioides*, a gene putatively having a negative impact on the production of fumonisins and virulence toward fumonisin sensitive maize seedlings (Fig. 3.8). *FvZBD1* was the most highly induced gene in both pyrrocidine A and B treatments, and its impact on fumonisin production provides evidence for chemical warfare. We also propose to incorporate *FvZBD1* as a non-canonical part of the fumonisin biosynthetic cluster, since its deletion dramatically boosts the fumonisin production. The strong induction of *FvZBD1* coupled with its genomic location and impact on fumonisin biosynthesis suggested a link between pyrrocidine exposure and suppression of fumonisin production by *F. verticillioides* and provides additional support for *S. zeae* as a potential biological control agent against *F. verticillioides* and fumonisin contamination of maize. Future experiments will test if *i*) exposure to pyrrocidines represses fumonisin production in conducive conditions through induction of *FvZBD1*, and *ii*) *FvZBD1* deletion is able to produce fumonisin in non-conducive conditions.

MATERIALS AND METHODS

Fungal and bacterial strains, media and growth conditions

Strains of *F. verticillioides* used in this study are listed in Table 3.3. Wild-type strain FRC M-3125 was utilized for genetic characterization and modification. Fungal strains were routinely grown in a dark incubator at 27 °C on potato dextrose agar (PDA; Neogen Food Safety, Lansing, MI, USA) or in potato dextrose broth (PDB; Neogen Food Safety, Lansing, MI, USA) at 250 rpm for 4 days. Transformed strains were screened on PDA plates amended with 150 μg/mL hygromycin B (Invitrogen, Carlsbad, CA, USA) or 300 μg/mL geneticin (Life

Technologies, Carlsbad, CA, USA). Water agar (3%) plates were used for single conidial germling isolation (Choi et al., 1999).

To construct fungal gene deletion mutants, *Escherichia coli* (One Shot® MAX Efficiency® DH5αTM-T1R, Invitrogen, Carlsbad, CA, USA) was used as the recipient of OSCAR deletion constructs (see below) and was cultured in/on low sodium (0.5 g/L) Luria-Bertani (LB) medium amended with 100 µg/mL spectinomycin (Thermo Fisher Scientific, Waltham, MA, USA) at 37 °C overnight. The fungal transformation was mediated by OSCAR deletion plasmid containing-*Agrobacterium tumefaciens* AGL-1 strains cultured on low sodium LB medium amended with 100 µg/mL spectinomycin at 27 °C for 24 hours (Gold et al., 2017; Paz et al., 2011).

Growth curve analysis was performed initially with one confirmed deletion mutant per gene of interest with a Bioscreen C automated system (Growth Curves USA, Piscataway, NJ, USA). Fungal strains were inoculated in PDB (2×10^3 conidia per 200 µL PDB per well) using the Bioscreen honeycomb microtiter plates (Growth Curves Ab Ltd. Helsinki, Finland). The wells were amended with 10 µg/mL pyrrocidine B dissolved in dimethyl sulfoxide (DMSO; Thermo Fisher Scientific, Waltham, MA, USA), and 5 replicates were prepared for each treatment. All treatments, including the controls, contained 0.5% DMSO. The microtiter plates were incubated 100 hours at 28 °C with continuous shaking, and OD_{600} measurements were recorded every 30 min. For the presentation of the growth curves, only 2h incremental time points were plotted. The experiment was conducted three times. For genes FVEG_11089 and FVEG_00314 that showed growth defects in the presence of pyrrocidine B, additional Bioscreen experiments were carried out with at least two independently generated mutants and their complemented strains.

Isolation and purification of pyrrocidine B

Pyrrocidine A was kindly gifted by the USDA, ARS, Mycotoxin Prevention and Applied Microbiology Research Unit (Peoria, IL, USA). Pyrrocidine B purification was conducted as previously described with minor modifications (He et al., 2002; Wicklow et al., 2005; Wicklow and Poling, 2009). In brief, the ethyl acetate (E) extract from 12 lyophilized 15-day-old rice cultures (50 g of Kroger long grain white rice, 50 mL deionized water) of *S. zeae* NRRL 13540 at 25°C in the dark was separated by flash chromatography packed with silica powder (Sigma-Aldrich, St. Louis, MO, USA). The silica column was preconditioned with 100mL hexane (H) and eluted with 200 mL of 100%H, 80%H/20%E, 60%H/40%E, 40%H/60%E, 20%H/80%E, 100%E, 50%E/50%methanol (M), and 100%M. Each fraction was analyzed by LC-MS. Pyrrocidine B was detected in 40%H/60%E, 20%H/80%E, and 100%E fractions.

Fractions with pyrrocidines were combined, evaporated, re-dissolved in 200 mL hexane, and further purified using a 10g-Silica Sep-Pak cartridge (Waters Corporation, Milford, MA, USA). The Silica Sep-Pak cartridge was preconditioned with 100 mL H. Fractions were applied to the column and eluted with 100 mL of 100%H, 4 × 50 mL of 70%H/30%E, 2 × 50 mL of 60%H/40%E, 2 × 50 mL of 50%H/50%E, 100 mL of 30%H/70%E, 100mL 100%E, and 100 mL 100%M. Each fraction was analyzed by LC-MS. Pyrrocidine B was detected in the two 50%H/50%E fractions.

Fractions with pyrrocidines were combined, evaporated, and re-dissolved in 50 mL acetonitrile (A). Subsequently, 50 mL double distilled water (ddH_2O) was added to obtain 100 mL volume. 10g-tC18 Sep-Pak cartridges (Waters Corporation) were used to further purify pyrrocidine B. The cartridge was conditioned with 200 mL of 100% methanol followed by 50%ddH_2O/50%A. Samples were applied and eluted with 100 mL of 50%A/50%ddH_2O, 2×50

mL of 60%A/40%ddH_2O, 2×50 mL of 70%A/30%ddH_2O, 2 × 50 mL of 80%A/20%ddH_2O, 100 mL A, and 100mL E. Each fraction was analyzed by LC-MS. Pyrrocidine B was detected in 60%A/40%ddH_2O and 70%A/30%ddH_2O fractions. The following steps remain the same as previously described (He et al., 2002; Wicklow et al., 2005; Wicklow and Poling, 2009). The extraction process yielded 53.5 mg pyrrocidine B in the form of a fine light yellow powder.

RNA-seq experiment and data analyses

Two milliliter PDB cultures in sterile snap-cap tubes, with caps loose, were inoculated with 10^4 FRC M3125 *F. verticillioides* conidia and grown at 27 °C, 250 rpm for 47 hours, at which time 5 μL DMSO containing 10 μg or 40 μg (final concentrations of 5 μg/mL and 20 μg/mL) of pyrrocidine A and B, respectively, was added to the respective treatments. Five microliters of DMSO was added to negative control samples. All culture tubes were incubated for a final one-hour induction. Three biological replicates were prepared for each pyrrocidine A, pyrrocidine B, and negative control treatments. After 48 hours, 1 mL liquid culture from each tube was pelleted by centrifugation at 8000 g for 5 min at 4 °C, resuspended in 1 mL lysis buffer, and transferred to lysing matrix D tubes (MP Biomedicals, LLC, Santa Ana, CA, USA). The samples were homogenized with a FastPrep-24™ 5G instrument (MP Biomedicals) at 6 m/s with 2 pulses of 30 s and a 1 min intervening pause at room temperature. Total RNA of each sample was isolated with a PureLink® RNA Mini Kit (Thermo Fisher Scientific Inc., MA, USA) following the manufacturer's protocol, and RNA quality was determined with an Agilent 2100 Bioanalyzer (Agilent Technologies, Palo Alto, CA, USA). Sequencing libraries were constructed with an Illumina Truseq DNA LT sample prep kit (Illumina Inc., San Diego, CA, USA) following the manufacturer's protocol. Illumina library size validation was performed using the Agilent Tapestation 2200 High Sensitivity D1000 Assay (Part No. 5067-5584, Agilent

Technologies, Santa Clara, CA, USA). Prior to equimolar library pool preparation, individual libraries were assayed for concentration by an Illumina library quantification kit (Product number KK4854, Kapa Biosystems, Inc, Wilmington, MA, USA) on a qPCR instrument (LightCycler 96, Roche Applied Science, Indianapolis, IN, USA). Each pool was clustered onboard an Illumina HiSeq2500 DNA sequencer with SR Rapid v2 flowcell clustering kits (Product number GD-402-4002, Illumina, San Diego, CA, USA). Single-end 50 bp sequencing was carried out with Rapid SBS v2 (Product number FC-402-4022, Illumina) reagents, and approximately 15 million reads were collected for each sample library. Sequencing reads were processed by Cutadapt 1.9.dev1 (Martin, 2011), Trimmomatic 0.32 (Bolger et al., 2014) and custom scripts to remove adapters, low-quality reads, rRNA and organellar sequences, which were obtained from National Center for Biotechnology Information (NCBI) Gene Database (https://www.ncbi.nlm.nih.gov/). Reads were mapped to *F. verticillioides* 7600 genome by Tophat 2.0.13 (Kim et al., 2013; Ma et al., 2010), alignment sorted by Samtools 1.2 (Li et al., 2009), and read count and expression estimation obtained by HTseq 0.6.1p1 (Anders et al., 2015) and DESeq2 (Love et al., 2014).

Quantitative PCR confirmation of pyrrocidine B responsive genes

FRC M3125 PDB liquid culture preparation, pyrrocidine B challenge, and RNA extraction were conducted in the same way as described in RNA-seq experiments. Three biological replicates were prepared for treatment groups and the control. For qRT-PCR, RNA samples were digested with DNase (Turbo DNA-freeTM Kit, Thermo Fisher Scientific) following the manufacturer's protocol and analyzed with an Agilent 2100 Bioanalyzer (Agilent Technologies) to control quality (RNA-integrity number > 8). Conventional PCR (primers P1/50 and P1/51) targeting the β-tubulin reference gene (FVEG_04081) was performed with digested

RNA templates, and PCR products were electrophoresed to ensure no DNA residues remained. qPCR reactions were carried out using a one-step qRT-PCR Kit (SuperScript III Platinum SYBR Green One-Step qRT-PCR Kit, Thermo Fisher Scientific) with 3 technical replicates for each biological replicate following the manufacturer's protocol. The data were normalized to the expression level of the β-tubulin gene (primers P1/50 and P1/51) by subtracting the β-tubulin Ct values from the Ct values of the genes of interest. The real-time primers used in this study are shown in Table 3.4.

Gene deletion and complementation

Ten select up-regulated genes identified from the RNA-seq experiment were targeted to generate single deletion mutants. Plasmids pMG00314_OSCAR, pMG01675_OSCAR, pMG07235_OSCAR, pMG09038_OSCAR, pMG11089_OSCAR, pMG11090_OSCAR, pMG13271_OSCAR, pMG13322_OSCAR, pMG17422_OSCAR, and pMG17625_OSCAR were created as the gene deletion constructs for FVEG_00314 (*FvZBD1*), FVEG_01675, FVEG_07235, FVEG_09038, FVEG_11089 (*FvABC3*), FVEG_11090 (*FvZEAR*), FVEG_13271, FVEG_13322, FVEG_17422, and FVEG_17625, respectively, using the OSCAR method (Gold et al., 2017; Paz et al., 2011). Primers used in this study are summarized in Table 3.4 and Supplemental Table 3.2. Detailed steps are described below for *FvABC3*, *FvZEAR*, and *FvZBD1*. Two sets of primers were synthesized to amplify 1kb of the 5' flank sequence (primers HP1/1 and HP1/2 for *FvABC3*; HP1/11 and HP1/12 for *FvZEAR*; HP1/21 and HP1/22 for *FvZBD1*) and the 3' flank sequence (primers HP1/3 and HP1/4 for *FvABC3*; HP1/13 and HP1/14 for *FvZEAR*; HP1/23 and HP1/24 for *FvZBD1*) of the target open reading frames (ORFs). the gene of interest surrounding flanks but excluding the ORF. Each gene-encoding region was deleted in FRC M3125 through *Agrobacterium tumefaciens*-mediated transformation and double crossover

homologous recombination. Hygromycin-resistant transformants were screened for the presence of the HRC (primer P1/46 and P1/47) and absence of the corresponding ORFs (primer pairs: HP1/5 and HP1/6 for *FvABC3*; HP1/15 and HP1/16 for *FvZEAR*; HP1/25 and HP1/26 for *FvZBD1*). Transformant candidates were single-spore isolated and confirmed by PCR screening subjected to the following criteria: 1) presence of the HRC; 2) absence of corresponding ORFs; 3) homologous recombination at the 5' flank and 4) homologous recombination at the 3' flank of the target gene with expected sizes (*FvABC3* 5' flank, HP1/7 and P1/4; *FvABC3* 3' flank HP1/8 and P1/3; *FvZEAR* 5' flank, HP1/17 and P1/3; *FvZEAR* 3' flank, HP1/18 and P1/4; *FvZBD1* 5' flank, HP1/27 and P1/3; *FvZBD1* 3' flank, HP1/28 and P1/4). The copy number of HRC was characterized by qPCR (see below). Similar gene deletion methods were also applied to the other seven targeted genes, and corresponding primers are summarized in Supplemental Table 3.2.

The wild-type *FvABC3*, *FvZEAR*, and *FvZBD1* genes were amplified with primer pairs HP1/1+HP1/4, HP1/11+HP1/14, and HP1/21+HP1/24, respectively, to encompass the ORF regions plus 5' and 3' flanks, each of 1kb in length. The reactions were prepared with TaKaRa high fidelity Taq (TaKaRa Bio, Kyoto, Japan) following the manufacturer's protocol. The amplicons were purified (QIAquick PCR purification kit, Qiagen, Inc., Valencia, CA, USA) and combined with undigested pGEN-NotI (1 μg) for PEG-mediated co-transformation of protoplasts (Glenn and Bacon, 2009) generated from the Δ*FvABC3*, Δ*FvZEAR*, Δ*FvZBD1* deletion strains. Transformants were selected on geneticin (300 μg/mL; Sigma-Aldrich) and screened by ORF primer pairs HP1/5+HP1/6, HP1/15+HP1/16, and HP1/25+HP1/26 to confirm complementation fragment integration of *FvABC3*, *FvZEAR*, and *FvZBD1* respectively. PCR reactions were carried out with NEB Taq 2X Master Mix (New England Biolabs, Ipswich, Massachusetts, USA) following the manufacturer's protocol.

Copy number determination

To ensure only one copy of HRC was introduced into the deletion mutant genomes, we further determined the copy number of HRC in deletion mutants. Genomic DNA was extracted from each 4-day old 50 mL PDB culture using the DNeasy Plant Mini Kit (Qiagen, Inc.) following the manufacturer's protocol. FRC M3125 served as the negative control, and strain ΔFv_08294 (known single HRC copy) served as the positive control. Quantitative PCR was performed using Platinum Taq DNA Polymerase (Thermo Fisher Scientific) and SYBR® Green I dye (Thermo Fisher Scientific) following the manufacturer's protocol, using the DNeasy extracted genomic DNA. The relative copy number of target genes was normalized to the single copy reference β-tubulin (FVEG_04081) gene (Primers P1/50 and P1/51), and calculated via the $2^{-\Delta\Delta Ct}$ method (Livak and Schmittgen, 2001).

MIPS functional enrichment analysis

Functional enrichment analysis was conducted with MIPS functional catalog web server (http://mips.helmholtz-muenchen.de/funcatDB/) with *Fusarium verticillioides* 7600 – p3_p15553_Fus_verti_v31 serving as the reference species database (Ruepp et al., 2004). A p-value of 0.05 was applied to filter the enrichment results.

Maize seedling assay

Seeds of sweet corn variety Silver Queen® (W. Atlee Burpee & Co., Warminster, PA, USA) were treated as previously described to eliminate pre-existent endophytes and surface microbes (Glenn et al., 2008). Approximately 50 seeds were placed in a 100-mm Petri dish and immersed in 10 mL sterile deionized water (SDW) containing 10^5 conidia. Ten milliliters of SDW was added to the uninoculated control. After 16-hour incubation in the dark at 27 °C, 10 seeds were planted in one 4-in azalea pot filled with twice-autoclaved moist Fafard 2 potting mix

(Agawam, MA, USA). Three pots per treatment were prepared, situated on sterile plastic saucers in plastic trays, and watered from below by filling the saucers on days 0, 2, 4, and 6. Subsequent watering was performed as needed and also added from below. Plants were incubated for 14 days in a growth room alternating with 16 hours day-light (approximately 320 μmol/m^2/s) at 30 °C and 8 hours in dark at 20 °C. On day 14, plants were harvested by cutting at the first node at the soil surface, and corresponding heights were measured for each seedling. Disease symptoms were visually inspected, and the experiment was repeated two times.

Fumonisin production assay

Fumonisin production assays were conducted in GYAM medium, containing 0.05% yeast extract, 0.24 M glucose, 8 mM L-asparagine, 1.7 mM NaCl, 4.4 mM K_2HPO_4, 2 mM $MgSO_4$, 8.8 mM $CaCl_2$, and 5.0 mM malic acid (Proctor et al., 1999). Two milliliters of GYAM medium in sterile 15 mL snap-cap culture tubes, with caps loose, were inoculated with 10^5 spores and cultured in the dark at 27 °C, 250 rpm for 7 days. Upon harvesting, 2 mL of acetonitrile + 5% formic acid was added to each culture tube, which stood at room temperature for 3 hours after mixing thoroughly. The mixtures were vacuum-filtered through sterile 25 mm, 5-micron pore size MAGNA nylon filters (N50SP2500, MSI, Westboro, MA), which were previously desiccated under vacuum at room temperature for >24 hours prior to obtaining the tare weight. The mycelial mass collected on the filter was desiccated under vacuum for > 24 hours before weighing. The filtered extract (roughly 3 mL) was diluted (1:1) by adding 3 mL ddH_2O. The diluted samples were analyzed as previously described using LC-MS (Williams et al., 2007).

GYAM plate assay

F. verticillioides strains were inoculated and grown for 7 days at 27 °C on 20 mL GYAM 1.5% agar plates (Proctor et al., 1999). A peri-marginal 6-mm diameter agar plug of each strain

was transferred to the center of fresh 20 mL GYAM plates and allowed to grow in the dark at 27 °C. Growth phenotypes were visually inspected daily until 9 days post-inoculation. Three biological replicates were prepared for each strain.

Public availability of data

RNA-seq data were deposited in NCBI's Gene Expression Omnibus (GEO) and are accessible through GEO Series accession GSE116351 (http://www.ncbi.nlm.nih.gov/geo/). The reference genome *Fusarium verticillioides* 7600 (ASM14955V1) was obtained from NCBI genome database (https://www.ncbi.nlm.nih.gov/genome/) (Ma et al., 2010).

REFERENCES

Alexander, N. J., Proctor, R. H., and McCormick, S. P. (2009). Genes, gene clusters, and biosynthesis of trichothecenes and fumonisins in *Fusarium*. *Toxin Rev.* 28, 198–215. doi:10.1080/15569540903092142.

Ambudkar, S. V, Lelong, I. H., Zhang, J., Cardarelli, C. O., Gottesman, M. M., and Pastan, I. (1992). Partial purification and reconstitution of the human multidrug-resistance pump: characterization of the drug-stimulatable ATP hydrolysis. *Proc. Natl. Acad. Sci. U. S. A.* 89, 8472–6. Available at: http://www.ncbi.nlm.nih.gov/pubmed/1356264 [Accessed February 12, 2018].

Ammar, G. A., Tryono, R., Doll, K., Karlovsky, P., Deising, H. B., and Wirsel, S. G. R. (2013). Identification of ABC transporter genes of *Fusarium graminearum* with roles in azole tolerance and/or virulence. *PLoS One* 8, e79042. doi:10.1371/journal.pone.0079042.

Anders, S., Pyl, P. T., and Huber, W. (2015). HTSeq-A Python framework to work with high-throughput sequencing data. *Bioinformatics* 31, 166–169. doi:10.1093/bioinformatics/btu638.

Baldwin, T. T., Zitomer, N. C., Mitchell, T. R., Zimeri, A. M., Bacon, C. W., Riley, R. T., et al. (2014). Maize seedling blight induced by *Fusarium verticillioides*: Accumulation of fumonisin B1 in leaves without colonization of the leaves. *J. Agric. Food Chem.* 62, 2118–2125. doi:10.1021/jf5001106.

Blacutt, A. A., Gold, S., Voss, K. A., Gao, M., and Glenn, A. E. (2018). *Fusarium verticillioides* : Advancements in understanding the toxicity, virulence, and niche adaptations of a model mycotoxigenic pathogen of maize. *Phytopathology*, PHYTO-06-17-0203-RVW. doi:10.1094/PHYTO-06-17-0203-RVW.

Bolger, A. M., Lohse, M., and Usadel, B. (2014). Trimmomatic: A flexible trimmer for Illumina sequence data. *Bioinformatics* 30, 2114–2120. doi:10.1093/bioinformatics/btu170.

Brown, D. W., Butchko, R. A. E., Busman, M., and Proctor, R. H. (2007). The *Fusarium verticillioides* FUM gene cluster encodes a Zn(II)2Cys6 protein that affects FUM gene expression and fumonisin production. *Eukaryot. Cell* 6, 1210–1218. doi:10.1128/EC.00400-06.

Brown, D. W., Butchko, R. A. E., Busman, M., and Proctor, R. H. (2012). Identification of gene clusters associated with fusaric acid, fusarin, and perithecial pigment production in *Fusarium verticillioides*. *Fungal Genet. Biol.* 49, 521–532. doi:DOI 10.1016/j.fgb.2012.05.010.

Choi, Y., Hyde, K. D., and Ho, W. W. H. (1999). Single spore isolation of fungi. *Fungal Divers.*

Gao, M., Glenn, A. E., Blacutt, A. A., and Gold, S. E. (2017). Fungal lactamases: Their occurrence and function. *Front. Microbiol.* 8, 1775. doi:10.3389/fmicb.2017.01775.

Glenn, A. E., and Bacon, C. W. (2009). *FDB2* encodes a member of the arylamine N-acetyltransferase family and is necessary for biotransformation of benzoxazolinones by *Fusarium verticillioides*. *J. Appl. Microbiol.* 107, 657–671. doi:10.1111/j.1365-2672.2009.04246.x.

Glenn, A. E., Davis, C. B., Gao, M., Gold, S. E., Mitchell, T. R., Proctor, R. H., et al. (2016). Two horizontally transferred xenobiotic resistance gene clusters associated with detoxification of benzoxazolinones by *Fusarium* species. *PLoS One* 11, e0147486. doi:10.1371/journal.pone.0147486.

Glenn, A. E., Zitomer, N. C., Zimeri, A. M., Williams, L. D., Riley, R. T., and Proctor, R. H. (2008). Transformation-mediated complementation of a FUM gene cluster deletion in *Fusarium verticillioides* restores both fumonisin production and pathogenicity on maize seedlings. *Mol. Plant-Microbe Interact.* 21, 87–97. doi:10.1094/MPMI-21-1-0087.

Gold, S. E., Paz, Z., García-Pedrajas, M. D., and Glenn, A. E. (2017). Rapid deletion production in fungi via *Agrobacterium* mediated transformation of OSCAR deletion constructs. *J. Vis. Exp.* doi:10.3791/55239.

He, H., Yang, H. Y., Bigelis, R., Solum, E. H., Greenstein, M., and Carter, G. T. (2002). Pyrrocidines A and B, new antibiotics produced by a filamentous fungus. *Tetrahedron Lett.* 43, 1633–1636. doi:10.1016/S0040-4039(02)00099-0.

Howard, P. C., Eppley, R. M., Stack, M. E., Warbritton, A., Voss, K. A., Lorentzen, R. J., et al. (2001). Fumonisin B1 carcinogenicity in a two-year feeding study using F344 rats and B6C3F1 mice. *Environ. Health Perspect.* 109 Suppl, 277–82. doi:sc271_5_1835 [pii].

Jin, M. S., Oldham, M. L., Zhang, Q., and Chen, J. (2012). Crystal structure of the multidrug transporter P-glycoprotein from Caenorhabditis elegans. *Nature* 490, 566–9. doi:10.1038/nature11448.

Kelley, L. A., Mezulis, S., Yates, C. M., Wass, M. N., and Sternberg, M. J. E. (2015). The Phyre2 web portal for protein modeling, prediction and analysis. *Nat. Protoc.* 10, 845–858. doi:10.1038/nprot.2015.053.

Kim, D., Pertea, G., Trapnell, C., Pimentel, H., Kelley, R., and Salzberg, S. L. (2013). TopHat2: Accurate alignment of transcriptomes in the presence of insertions, deletions and gene fusions. *Genome Biol.* 14. doi:10.1186/gb-2013-14-4-r36.

King, S. B. (1981). Time of infection of maize kernels by *Fusarium moniliforme* and *Cephalosporium acremonium*. *Phytopathology* 71, 796. doi:10.1094/Phyto-71-796.

Lee, J., Son, H., Lee, S., Park, A. R., and Lee, Y. W. (2010). Development of a conditional gene expression system using a zearalenone-inducible promoter for the ascomycete fungus gibberella zeae. *Appl. Environ. Microbiol.* doi:10.1128/AEM.02999-09.

Li, H., Handsaker, B., Wysoker, A., Fennell, T., Ruan, J., Homer, N., et al. (2009). The Sequence Alignment/Map format and SAMtools. *Bioinformatics* 25, 2078–2079. doi:10.1093/bioinformatics/btp352.

Livak, K. J., and Schmittgen, T. D. (2001). Analysis of relative gene expression data using real-

time quantitative PCR and the 2-ΔΔCT method. *Methods* 25, 402–408. doi:10.1006/meth.2001.1262.
Lodish, H. F. (2008). *Molecular cell biology*. W.H. Freeman.
Love, M. I., Huber, W., and Anders, S. (2014). Moderated estimation of fold change and dispersion for RNA-seq data with DESeq2. *Genome Biol.* 15. doi:10.1186/s13059-014-0550-8.
Ma, L. J., Van Der Does, H. C., Borkovich, K. A., Coleman, J. J., Daboussi, M. J., Di Pietro, A., et al. (2010). Comparative genomics reveals mobile pathogenicity chromosomes in *Fusarium*. *Nature* 464, 367–373. doi:10.1038/nature08850.
Marasas, W. F., Kellerman, T. S., Gelderblom, W. C., Coetzer, J. a, Thiel, P. G., and van der Lugt, J. J. (1988). Leukoencephalomalacia in a horse induced by fumonisin B1 isolated from *Fusarium moniliforme*. *Onderstepoort J. Vet. Res.* 55, 197–203.
Martin, M. (2011). Cutadapt removes adapter sequences from high-throughput sequencing reads. *EMBnet.journal* 17, 10. doi:10.14806/ej.17.1.200.
Munkvold, G. P., McGee, D. C., and Carlton, W. M. (1997). Importance of different pathways for maize kernel infection by *Fusarium moniliforme*. *Phytopathology* 87, 209–217. doi:10.1094/PHYTO.1997.87.2.209.
Musser, S. M., and Plattner, R. D. (1997). Fumonisin composition in cultures of *Fusarium moniliforme*, *Fusarium proliferatum*, and *Fusarium nygami*. *J. Agric. Food Chem.* 45, 1169–1173. doi:10.1021/jf960663t.
Neumann, S., Hartmann, H., Martin-Galiano, A. J., Fuchs, A., and Frishman, D. (2012). Camps 2.0: Exploring the sequence and structure space of prokaryotic, eukaryotic, and viral membrane proteins. *Proteins Struct. Funct. Bioinforma.* 80, 839–857. doi:10.1002/prot.23242.
Paz, Z., García-Pedrajas, M. D., Andrews, D. L., Klosterman, S. J., Baeza-Montañez, L., and Gold, S. E. (2011). One Step Construction of *Agrobacterium*-Recombination-ready-plasmids (OSCAR), an efficient and robust tool for ATMT based gene deletion construction in fungi. *Fungal Genet. Biol.* 48, 677–684. doi:10.1016/j.fgb.2011.02.003.
Proctor, R. H., Desjardins, A. E., Plattner, R. D., and Hohn, T. M. (1999). A polyketide synthase gene required for biosynthesis of fumonisin mycotoxins in *Gibberella fujikuroi* mating population A. *Fungal Genet. Biol.* 27, 100–112. doi:10.1006/fgbi.1999.1141.
Ross, P. F., Nelson, P. E., Richard, J. L., Osweiler, G. D., Rice, L. G., Plattner, R. D., et al. (1990). Production of fumonisins by *Fusarium moniliforme* and *Fusarium proliferatum* isolates associated with equine leukoencephalomalacia and a pulmonary-edema syndrome in swine. *Appl. Environ. Microbiol.* 56, 3225–3226.
Ruepp, A., Zollner, A., Maier, D., Albermann, K., Hani, J., Mokrejs, M., et al. (2004). The FunCat, a functional annotation scheme for systematic classification of proteins from whole genomes. *Nucleic Acids Res.* 32, 5539–5545. doi:10.1093/nar/gkh894.
Sadler, T. W., Merrill, A. H., Stevens, V. L., Sullards, M. C., Wang, E., and Wang, P. (2002). Prevention of fumonisin B1-induced neural tube defects by folic acid. *Teratology* 66, 169–176. doi:10.1002/tera.10089.
Sumner, D. R. (1967). Ecology of corn stalk rot in Nebraska. *Phytopathology* 58, 755–760. Available at: http://digitalcommons.unl.edu/dissertations/AAI6710681%250 [Accessed July 23, 2018].
Uesugi, S., Fujisawa, N., Yoshida, J., Watanabe, M., Dan, S., Yamori, T., et al. (2016). Pyrrocidine A, a metabolite of endophytic fungi, has a potent apoptosis-inducing activity

against HL60 cells through caspase activation via the Michael addition. *J Antibiot* 69, 133–140. doi:10.1038/ja.2015.103.

White, D. G. (1998). *Compendium of corn diseases*.

Wicklow, D. T., and Poling, S. M. (2009). Antimicrobial activity of pyrrocidines from *Acremonium zeae* against endophytes and pathogens of maize. *Phytopathology* 99, 109–115. doi:10.1094/PHYTO-99-1-0109.

Wicklow, D. T., Roth, S., Deyrup, S. T., and Gloer, J. B. (2005). A protective endophyte of maize: *Acremonium zeae* antibiotics inhibitory to *Aspergillus flavus* and *Fusarium verticillioides*. *Mycol. Res.* 109, 610–618. doi:10.1017/S0953756205002820.

Williams, L. D., Glenn, A. E., Zimeri, A. M., Bacon, C. W., Smith, M. A., and Riley, R. T. (2007). Fumonisin disruption of ceramide biosynthesis in maize roots and the effects on plant development and *Fusarium verticillioides*-induced seedling disease. *J. Agric. Food Chem.* 55, 2937–2946. doi:10.1021/jf0635614.

Table 3.1 Genes targeted for functional characterization

Gene#	Annotation	Pyrrocidine A Exposure		Pyrrocidine B Exposure	
		p-value[a]	Log_2 FC[b]	p-value	Log_2 FC
FVEG_00314 (***FvZBD1***)	Alcohol dehydrogenase	1.57E-224	12.02	8.48E-228	12.08
FVEG_01675	Dioxygenase	7.18E-210	7.86	1.85E-217	7.98
FVEG_07235	NADH(P)-binding	2.49E-78	9.60	1.47E-63	8.57
FVEG_09038	Cytochrome P450	3.31E-48	7.48	9.67E-103	10.86
FVEG_11089 (***FvABC3***)	ABC transporter	0	5.63	0	8.88
FVEG_11090 (***FvZEAR***)	Zn(2)-Cys(6) transcription factor	9.02E-158	5.29	0	7.44
FVEG_13271	Short chain dehydrogenase	1.34E-111	10.36	3.52E-124	10.88
FVEG_13322	Short chain dehydrogenase	0.00313	1.52	2.68E-155	11.49
FVEG_17422	ABC transporter	1.90E-18	1.18	0	6.23
FVEG_17625	C2H2-type zinc finger	3.54E-80	2.93	0	8.30

[a] p-value, false discovery rate-adjusted p-value
[b] FC, fold change

Table 3.2 Lactamases differentially expressed in *Fusarium verticillioides* upon exposure to pyrrocidine A and/or B

Gene#	Signal peptides	Pyrrocidine A Exposure		Pyrrocidine B Exposure	
		p-value[a]	Log_2 FC[b]	p-value	Log_2 FC
FVEG_03849	N	5.41E-67	1.52	0	3.77
FVEG_05734	N	1.55E+00	1.55	1.37E-57	4.05
FVEG_09854	N	2.42E-14	1.31	7.49E-15	1.30
FVEG_12637	N	2.44E-03	-2.08	4.89E-03	-1.78
FVEG_05685	N	1.50E-02	1.74	NS[c]	
FVEG_09433	N	3.90E-04	2.53	NS	
FVEG_12347	N	3.93E-04	1.45	NS	
FVEG_13172	N	3.56E-08	1.61	NS	
FVEG_05854	N	NS		3.60E-25	-3.15
FVEG_09904	N	NS		2.26E-14	-2.51
FVEG_10996	N	NS		2.27E-10	1.28
FVEG_12159	N	NS		2.09E-90	2.23
FVEG_12457	N	NS		1.88E-39	4.91
FVEG_12526	Y	NS		3.35E-02	1.37
FVEG_13253	N	NS		1.84E-03	-1.62
FVEG_13675	N	NS		4.47E-135	4.07
FVEG_16907	N	NS		1.14E-39	-2.97

[a] p-value, false discovery rate-adjusted p-value
[b] FC, fold change
[c] NS, not significant

Table 3.3 Fungal strains used in this study.

Index	Strain	Description and Source
HF1/1	FRC M-3125[a]	Wild-type strain used for mutant generation, also known as 7600 (Ma et al., 2010)
HF1/2	Δ*FvABC3*-1	FVEG_11089 deletion mutant in FRC M3125
HF1/3	Δ*FvABC3*-2	FVEG_11089 deletion mutant in FRC M3125
HF1/4	Δ*FvABC3*-2::C1	Δ*FvABC3*-2 deletion mutant complemented with FVEG_11089
HF1/5	Δ*FvABC3*-2::C2	Δ*FvABC3*-2 deletion mutant complemented with FVEG_11089
HF1/6	Δ*FvZEAR*-1	FVEG_11090 deletion mutant in FRC M3125
HF1/8	Δ*FvZBD1*-1	FVEG_00314 deletion mutant in FRC M3125
HF1/9	Δ*FvZBD1*-2	FVEG_00314 deletion mutant in FRC M3125
HF1/10	Δ*FvZBD1*-1::C1	Δ*FvZBD1*-1 deletion mutant complemented with FVEG_00314
HF1/11	Δ*FvZBD1*-1::C2	Δ*FvZBD1*-1 deletion mutant complemented with FVEG_00314
HF1/12	Δ*FvZBD1*-2::C1	Δ*FvZBD1*-2 deletion mutant complemented with FVEG_00314
HF1/13	FvZBD-Ect	An ectopic strain containing HRC[b] and intact ORF of FVEG_00314
HF1/14	ΔFv_08294	A transcription factor mutant with one known HRC genomic copy
HF1/15	ΔFv_01675	FVEG_01675 deletion mutant in FRC M3125
HF1/16	ΔFv_07235	FVEG_07235 deletion mutant in FRC M3125
HF1/17	ΔFv_09038	FVEG_09038 deletion mutant in FRC M3125
HF1/18	ΔFv_13271	FVEG_13271 deletion mutant in FRC M3125
HF1/19	ΔFv_13322	FVEG_13322 deletion mutant in FRC M3125
HF1/20	ΔFv_17422	FVEG_17422 deletion mutant in FRC M3125
HF1/21	ΔFv_17625	FVEG_17625 deletion mutant in FRC M3125

[a] FRC, Fusarium Research Center, Pennsylvania State University

[b] HRC, hygromycin resistance cassette

Table 3.4 Primers used in this study.

Index	Primer Name	Primer Sequence (5' to 3')	Description
HP1/1	FVEG_11089_O1	GGGGACAGCTTTCTTGTACAAAGTGGAA AATCTTGAGCTGAGAGATCATAC	Amplification of 5' flank of *FvABC3*
HP1/2	FVEG_11089_O2	GGGGACTGCTTTTTTGTACAAACTTGT GTACCTGGTTAACTCTGTAAACT	Amplification of 5' flank of *FvABC3*
HP1/3	FVEG 11089 O3	GGGGACAACTTTGTATAGAAAAGTTGTT GAGAAGTACTATAGACTGGTTTGG	Amplification of 3' flank of *FvABC3*
HP1/4	FVEG 11089 O4	GGGGACAACTTTGTATAATAAAGTTGT GTCATGAAGATGGCTAAGATTTG	Amplification of 3' flank of *FvABC3*
HP1/5	FVEG 11089 ORF F	CTTGGTTGATATGCCGTATAAGA	Confirmation of *FvABC3* ORF
HP1/6	FVEG 11089 ORF R	GAATACTACCTACAGTGGAACAAG	Confirmation of *FvABC3* ORF
HP1/7	FVEG 11089 5' out	CGGAGTTTCAAAAGATTGCTAATC	Confirmation of the integrity of outer sequences flanking the 5' flank of *FvABC3*
HP1/8	FVEG_11089_3'_out	GAGAGTTTATCGGTTGTGTATTGG	Confirmation of the integrity of outer sequences flanking the 3' flank of *FvABC3*
HP1/9	FVEG_11089_RT_F	ATCTTGCCTCAGCCATTCTATC	Amplification of *FvABC3* ORF for qPCR and qRT PCR
HP1/10	FVEG 11089 RT R	CAGGTTGTGCCGTTGAGA	Amplification of *FvABC3* ORF for qPCR and qRT PCR
HP1/11	FVEG 11090 O1	GGGGACAGCTTTCTTGTACAAAGTGGAAGACCAAAGAGTTCAGACTGTAAG	Amplification of 5' flank of *FvZEAR*
HP1/12	FVEG 11090 O2	GGGGACTGCTTTTTTGTACAAACTTGTCGAATCGAAATGCAGAGAATAATAG	Amplification of 5' flank of *FvZEAR*
HP1/13	FVEG 11090 O3	GGGGACAACTTTGTATAGAAAAGTTGTTGGCATATAGCTGTGAATCACTAA	Amplification of 3' flank of *FvZEAR*
HP1/14	FVEG 11090 O4	GGGGACAACTTTGTATAATAAAGTTGTTAGTACAAGGGATGAAGAGAAATG	Amplification of 3' flank of *FvZEAR*
HP1/15	FVEG_11090_ORF_F	GAAGAAATGTGACAGAAAAAGTCC	Confirmation of *FvZEAR* ORF
HP1/16	FVEG_11090_ORF_R	ATCCATTCAGTTTTACTCATACCG	Confirmation of *FvZEAR* ORF
HP1/17	FVEG_11090_5'_out	TAGAGACTCTTGTAGGTCTCAATC	Confirmation of the integrity of outer sequences flanking the 5' flank of *FvZEAR*
HP1/18	FVEG 11090 3' out	CGATGTAGGCGTTACTAGTTTTAG	Confirmation of the integrity of outer sequences flanking the 3' flank of *FvZEAR*
HP1/19	FVEG 11090 RT F	TATCCCGAGTACACCTGCT	Amplification of *FvZEAR* ORF for qPCR and qRT PCR
HP1/20	FVEG 11090 RT R	CTCTTCACACCTCTCCAATCTC	Amplification of *FvZEAR* ORF for qPCR and qRT PCR
HP1/21	FVEG 00314 O1	GGGGACAGCTTTCTTGTACAAAGTGGAAGAAGAAACCGAAAGTCACAAATG	Amplification of 5' flank of *FvZBD1*
HP1/22	FVEG_00314_O2	GGGGACTGCTTTTTTGTACAAACTTGTGGTATATGTCAGTCAACCAGAAG	Amplification of 5' flank of *FvZBD1*
HP1/23	FVEG_00314_O3	GGGGACAACTTTGTATAGAAAAGTTGTTACTTCAGAAGCGTAGGATTATAG	Amplification of 3' flank of *FvZBD1*
HP1/24	FVEG_00314_O4	GGGGACAACTTTGTATAATAAAGTTGTCGTCGAAACATTGAGAGATAAAC	Amplification of 3' flank of *FvZBD1*
HP1/25	FVEG 00314 ORF F	GAGTTTGAGAAACCTCATCTCTC	Confirmation of *FvZBD1* ORF
HP1/26	FVEG 00314 ORF R	TACCAGATCTGCAAGAAATCAAG	Confirmation of *FvZBD1* ORF
HP1/27	FVEG 00314 5' out	CATTTTCCATCTTTCACAAACCTC	Confirmation of the integrity of outer sequences flanking the 5' flank of *FvZBD1*
HP1/28	FVEG 00314 3' out	CTCTCCAATAATACTCGAACACTG	Confirmation of the integrity of outer sequences flanking the 3' flank of *FvZBD1*
P1/3	Hyg_For_out	AGAGCTTGGTTGACGGCAATTTCG	Confirmation of the integrity of outer sequences flanking the 3' flank of target gene
P1/4	Hyg_Rev_out	GCCGATGCAAAGTGCCGATAAACA	Confirmation of the integrity of outer sequences flanking the 5' flank of target gene
P1/46	HygMarker_F	GACAGGAACGAGGACATTATTA	Confirmation of HRC ORF
P1/47	HygMarker R	GCTCTGATAGAGTTGGTCAAG	Confirmation of HRC ORF
P1/52	qPCR Hyg for	TCGATGAGCTGATGCTTTG	Amplification of HRC ORF for qPCR and qRT PCR
P1/53	qPCR Hyg rev	GTTGGCGACCTCGTATTG	Amplification of HRC ORF for qPCR and qRT PCR
P1/50	TUB2-F	CAGCGTTCCTGAGTTGACCCAACAG	Amplification of β-tubulin ORF for qPCR and qRT PCR
P1/51	TUB2-R	CTGGACGTTGCGCATCTGATCCTCG	Amplification of β-tubulin ORF for qPCR and qRT PCR

Supplemental Table 3.1 Summary of RNA-seq mapping results

Sample treatment*	Number of raw reads	Number of mapped reads	Mapping rates
Control-1	16342483	15943588	97.6%
Control-2	14185251	13921851	98.1%
Control-3	19119430	18873749	98.7%
PA5-1	17239023	17042978	98.9%
PA5-2	17788944	17377585	97.7%
PA5-3	15630242	15186301	97.2%
PB20-1	15083542	14906800	98.8%
PB20-2	21877419	21492342	98.2%
PB20-3	21183781	20818211	98.3%

* Three biological replicates were prepared for 3 treatments including 1) DMSO control, 2) PA5, pyrrocidine A at 5 μg/mL, and 3) PB20, pyrrocidine B at 20 μg/mL.

Supplemental Table 3.2 Additional primers in this study

Index	Primer Name	Primer Sequence
HP1/29	FVEG_01675_OSC1	GGGGACAGCTTTCTTGTACAAAGTGGAACCGACGAATTAATGACTCTATCT
HP1/30	FVEG_01675_OSC2	GGGGACTGCTTTTTTGTACAAACTTGTGAACCAGTTATGGTAGGAGTTAAT
HP1/31	FVEG_01675_OSC3	GGGGACAACTTTGTATAGAAAAGTTGTTCATGGATATTACAATAAGCCAAGAG
HP1/32	FVEG_01675_OSC4	GGGGACAACTTTGTATAATAAAGTTGTCAATTAATCGAGCATCAACTCAC
HP1/33	FVEG_01675_Orf_F	GGCATATTTGGGATGAAAGTAGTA
HP1/34	FVEG_01675_Orf_R	CTTTCAAAGCTGTTCGGAATTATC
HP1/35	FVEG_07235_OSC1	GGGGACAGCTTTCTTGTACAAAGTGGAAGCAGGATTTGAGTTGTAGTATTTAG
HP1/36	FVEG_07235_OSC2	GGGGACTGCTTTTTTGTACAAACTTGTGAGTTGAGCATAAATGAGGAAAC
HP1/37	FVEG_07235_OSC3	GGGGACAACTTTGTATAGAAAAGTTGTTCGTTGTAGTAAATTCCAAGCTCTA
HP1/38	FVEG_07235_OSC4	GGGGACAACTTTGTATAATAAAGTTGTTGATTTCCTCAAACATGTCTCTC
HP1/39	FVEG_07235_Orf_F	CCTGAGTATTACATGGCTTCTAC
HP1/40	FVEG_07235_Orf_R	CTACCTCAAAGTAGTCGAATGAG
HP1/41	FVEG_09038_OSC1	GGGGACAGCTTTCTTGTACAAAGTGGAACCCGATCTATCAGTGGAGTATTA
HP1/42	FVEG_09038_OSC2	GGGGACTGCTTTTTTGTACAAACTTGTAGAGAATATTGCTGAACTCTTGG
HP1/43	FVEG_09038_OSC3	GGGGACAACTTTGTATAGAAAAGTTGTTACTCATCCTAATGAATAGAGAACG
HP1/44	FVEG_09038_OSC4	GGGGACAACTTTGTATAATAAAGTTGTTTCACTTAGCATCTCAACAACTC
HP1/45	FVEG_09038_Orf_F	CGTGTAACTCAGGACTTCATTAT
HP1/46	FVEG_09038_Orf_R	TTAGTCTCTATTTGACCCTGAAAG
HP1/47	FVEG_13271_OSC1	GGGGACAGCTTTCTTGTACAAAGTGGAAGGATATACAGTCAAGGTCGAATAC
HP1/48	FVEG_13271_OSC2	GGGGACTGCTTTTTTGTACAAACTTGTGATGTCAGGTAGTACAAAGGAAG
HP1/49	FVEG_13271_OSC3	GGGGACAACTTTGTATAGAAAAGTTGTTGTGTAGGGTGATGATTGGTAATA
HP1/50	FVEG_13271_OSC4	GGGGACAACTTTGTATAATAAAGTTGTTGTCTCCTTTCTCTTGTCTTATAG
HP1/51	FVEG_13271_Orf_F	CTCCTTTCAGTGCGAGTAATAG
HP1/52	FVEG_13271_Orf_R	AGCCGTCTTAGCAGATATATAAAG
HP1/53	FVEG_13322_OSC1	GGGGACAGCTTTCTTGTACAAAGTGGAAACTTACAGAAGTATGTATCTGAGC
HP1/54	FVEG_13322_OSC2	GGGGACTGCTTTTTTGTACAAACTTGTGAGGCTTCGTCACTTAACTATAA
HP1/55	FVEG_13322_OSC3	GGGGACAACTTTGTATAGAAAAGTTGTTCATTCAGTTGGCAGATTCATTTAC

HP1/56	FVEG_13322_OSC4	GGGGACAACTTTGTATAATAAAGTTGTGAAGTTATCTGGAAGAGCCTTAAT
HP1/57	FVEG_13322_Orf_F	GTATATAAAGGCTAATCCGCAATG
HP1/58	FVEG_13322_Orf_R	GATGATGACGTCTAGCTTAGTAAT
HP1/59	FVEG_17422_OSC1	GGGGACAGCTTTCTTGTACAAAGTGGAACCTGTTAACACTTCCTTGTTAGA
HP1/60	FVEG_17422_OSC2	GGGGACTGCTTTTTTGTACAAACTTGTCAGAAACCTCATAAACTTCAACTC
HP1/61	FVEG_17422_OSC3	GGGGACAACTTTGTATAGAAAAGTTGTTATATTCCGTCGCTCTAATAACTAC
HP1/62	FVEG_17422_OSC4	GGGGACAACTTTGTATAATAAAGTTGTCATCATAGTCCTGTTACTCAATCT
HP1/63	FVEG_17422_Orf_F	CTGCATGGGATAACAGGTAAG
HP1/64	FVEG_17422_Orf_R	CTCTCTCAAAGGCGCAATAG
HP1/65	FVEG_17625_OSC1	GGGGACAGCTTTCTTGTACAAAGTGGAAGTACTTGAAGATTATCGACCTAGAG
HP1/66	FVEG_17625_OSC2	GGGGACTGCTTTTTTGTACAAACTTGTGTGGAGTCCGAATATAACTGATTA
HP1/67	FVEG_17625_OSC3	GGGGACAACTTTGTATAGAAAAGTTGTTGACGATGGTGGGTAAATATCTATG
HP1/68	FVEG_17625_OSC4	GGGGACAACTTTGTATAATAAAGTTGTCTAGATTGAGACATGAACGTAACA
HP1/69	FVEG_17625_Orf_F	CAAGCGCTCTACCTAGTTTC
HP1/70	FVEG_17625_Orf_R	GCCTCATTCGTGTACTTTACT

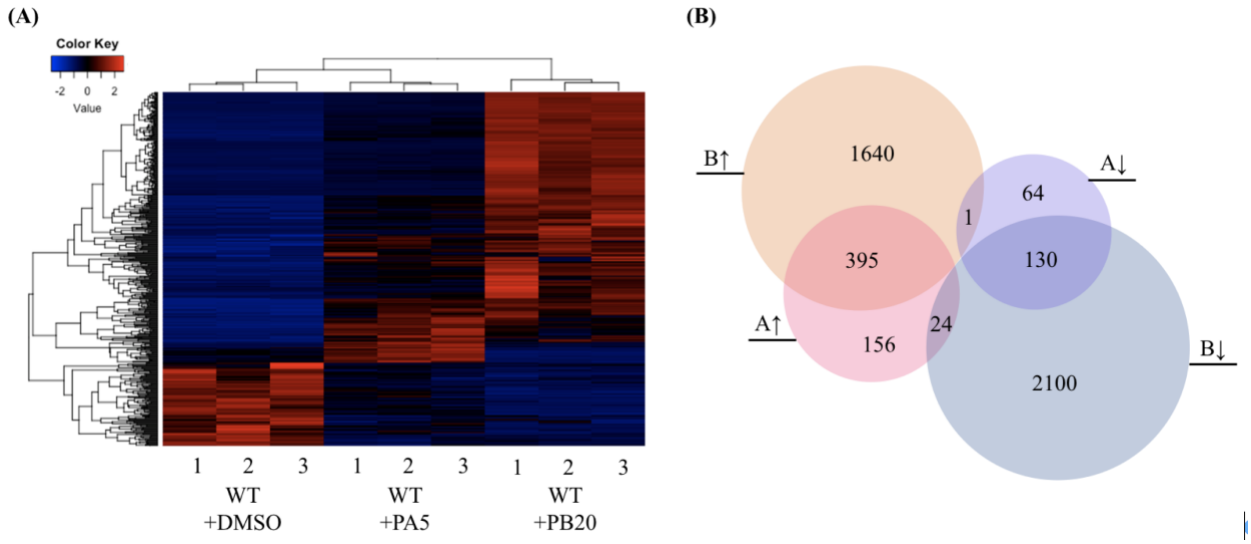

Figure 3.1 Pyrrocidine A and B elicit differential gene expressions. (**A**) Heatmaps showing transcription levels of 4510 differentially expressed genes upon exposure to pyrrocidine A (PA, 5µg/mL) or pyrrocidine B (PB, 20µg/mL). The Y-axis represents genes that are clustered and colored by the z-score. See the colored key. The X-axis shows the 3 biological replicates of each treatment. FPKM refers to Fragments Per Kilobase of transcript per Million mapped reads. (**B**) Venn diagram shows the number of genes with altered expression due to pyrrocidine A and/or B exposure. Each circle represents up- or down-regulation by pyrrocidine A or B, which is denoted by up/down arrows and A/B, respectively. Intersected regions represent genes regulated in both treatments, while the direction of regulation may vary.

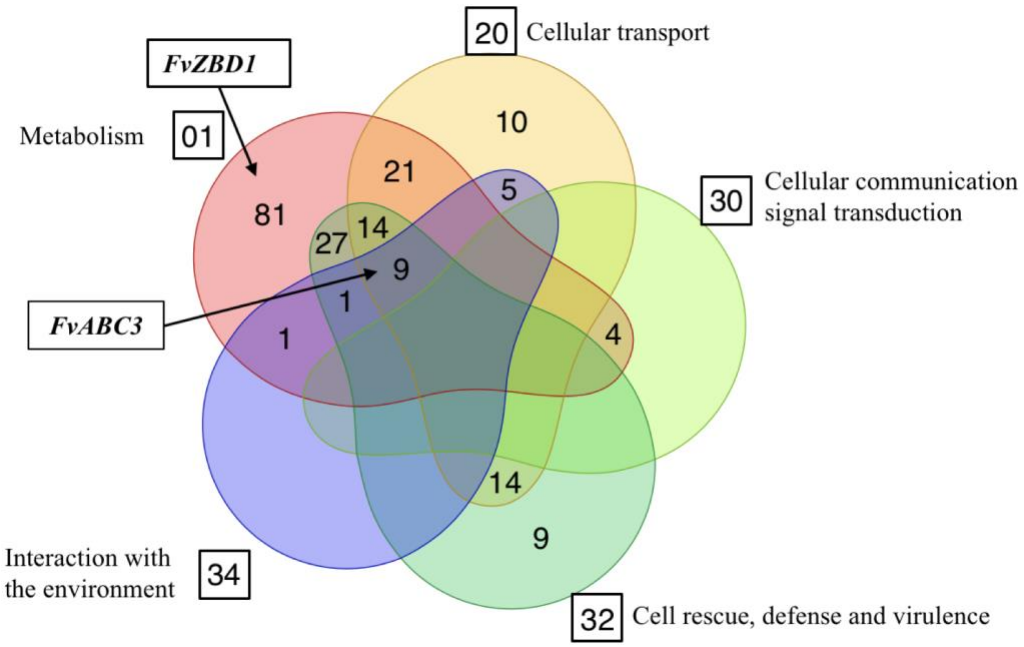

Figure 3.2 Functional catalog of pyrrocidine-responsive genes. Function enrichment analysis was conducted with MIPS FunCat Server (http://mips.helmholtz-muenchen.de/funcatDB/) (Ruepp et al., 2004). The five club shapes correspond to the following MIPS functional categories: metabolism (01), cellular transport (20), cellular communication/signal transduction mechanism (30), cell rescue, defense and virulence (32), and interaction with the environment (34). The numbers of genes functionally enriched in the different categories are included, and genes with multifunctional enrichment are shown in overlapping regions. Of 525 pyrrocidine-responsive genes, 196 genes were functionally enriched in these five different categories after applying a filter of p-value < 0.05. *FvABC3* is one of nine genes that functionally span four different enriched categories (01, 20, 32, 34), and *FvZBD1* is functionally enriched only in metabolism along with another 80 genes.

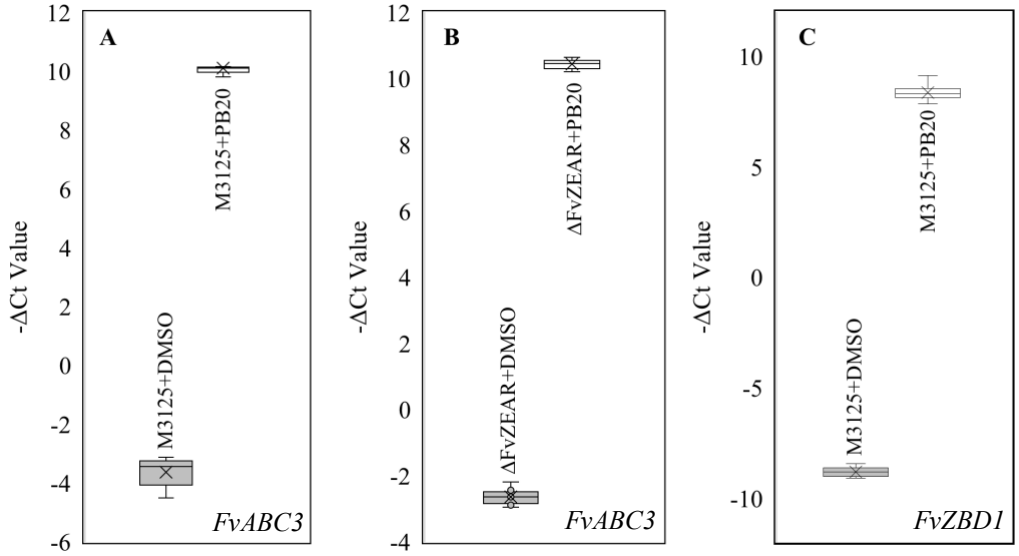

Figure 3.3 qRT-PCR results validated the pyrrocidine B induced up-regulation of *FvABC3* and *FvZBD1*, and that induction of *FvABC3* was independent of Δ*FvZEAR*. qRT-PCR was performed with M3125 exposed or not exposed to 20 μg/mL pyrrocidine B. The Y-axis of the box plots shows the -ΔCt value, which was calculated by subtracting the Ct value of the β-tubulin reference gene from the Ct value of each gene of interest. Expression of *FvABC3* in (**A**) wild-type M3125 and (**B**) the Δ*FvZEAR*-1 mutant. (**C**) Induction of *FvZBD1* in wild type upon exposure to pyrrocidine B. Three biological replicates, each with 3 technical replicates were assessed. All nine data points of each treatment were shown in the box plots. The range of -ΔCt values is shown with error bars, and each box indicates first and third quartile. Mean and median are marked with an "×" and a line in each of the boxes.

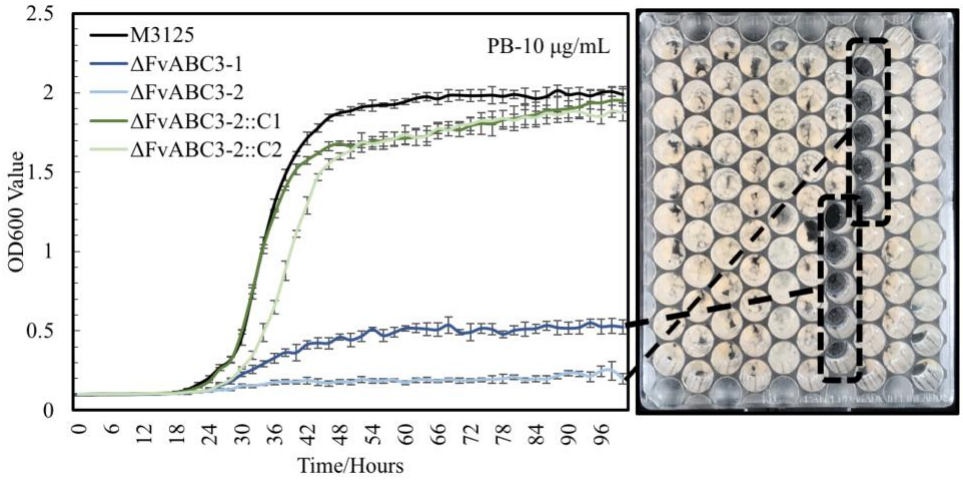

Figure 3.4 Deletion of *FvABC3* in *F. verticillioides* elevated its sensitivity to pyrrocidine B. Strains were monitored for 100 hours in PDB medium amended with pyrrocidine B at 10 μg/mL. OD_{600} measurements taken every 2 hours were plotted (mean ± standard deviation). FRC M3125 serves as the control (black curve). Two Δ*FvABC3* deletion mutants are shown in light and dark blue, and 2 complemented strains in light and dark green. Corresponding growth inhibition phenotypes of the Δ*FvABC3* deletion mutants are highlighted in the honeycomb plate after 100-hour incubation.

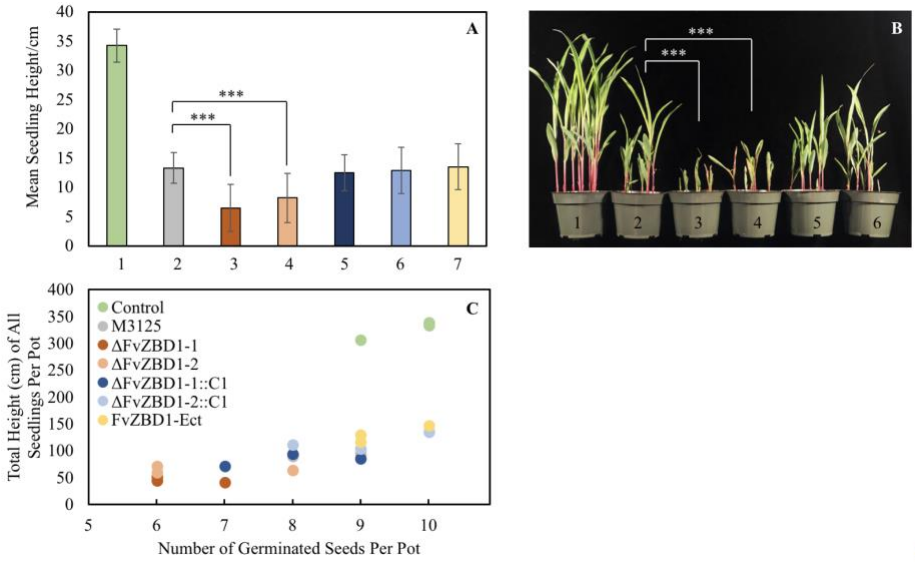

Figure 3.5 Deletion of *FvZBD1* in *F. verticillioides* significantly enhanced virulence on maize seedlings. Fifty Silver Queen® maize seeds were inoculated with 10^4/mL conidial suspensions for each of the five different *F. verticillioides* strains prior to planting. Seeds treated with sterile water served as a control. Plants were grown for 14 days before measuring their heights and assessing numbers of germinated seeds. Three biological replicates were conducted. Results are shown from one representative trial. The other two trials showed the same overall trends. (**A**) Histogram showing the mean height of seedlings. Numbers on the X-axis correspond to the following treatments: **1**, sterile water control; **2**, M3125; **3**, Δ*FvZBD1*-1; **4**, Δ*FvZBD1*-2; **5**, Δ*FvZBD1*-1::C-1; **6**, Δ*FvZBD1*-2::C-1; **7**, *FvZBD1*-Ect. Statistical analysis was conducted with two-tailed Mann Whitney Wilcoxon test (***, p-value < 0.001). (**B**) Visualization of seedling growth among treatments. Numbers on the pots correspond to those in (A). (**C**) Two-dimensional visualization of seedling growth among different treatments. Each dot represents a technical replicate of a particular treatment. Total height (cm) of all seedlings per pot is denoted on the Y-axis, and the X-axis shows the number of germinated seeds per pot.

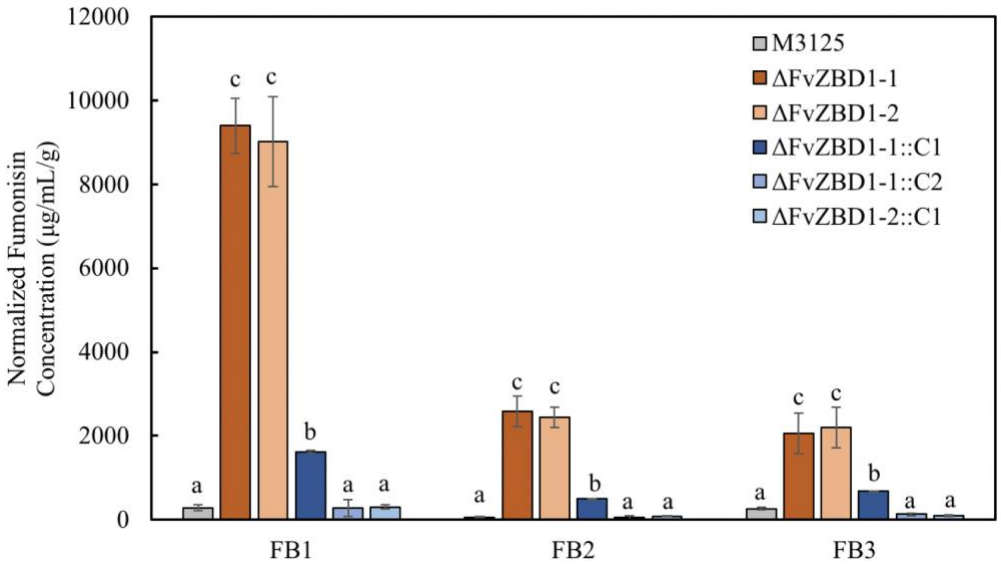

Figure 3.6 Deletion of *FvZBD1* dramatically increased fumonisin productions in GYAM liquid cultures. Two milliliters of GYAM liquid medium in snap-cap tubes were inoculated with 10^4 spores of each strain and cultured in the dark at 27 °C, 250 rpm for 7 days. Fumonisin concentrations were determined by LC-MS and normalized to the vacuum-desiccated fungal mass weight, as indicated on the Y-axis. The experiment was conducted three times, with 3 technical replicates each. The two trials showed similar patterns, and one representative trial is plotted. Statistical differences (p-value < 0.05) were estimated with two-tailed Mann Whitney Wilcoxon test and denoted with lower case letters for each fumonisin group. Strains sharing the same letters are not significantly different. FB1/FB2/FB3 represent fumonisin B1/B2/B3.

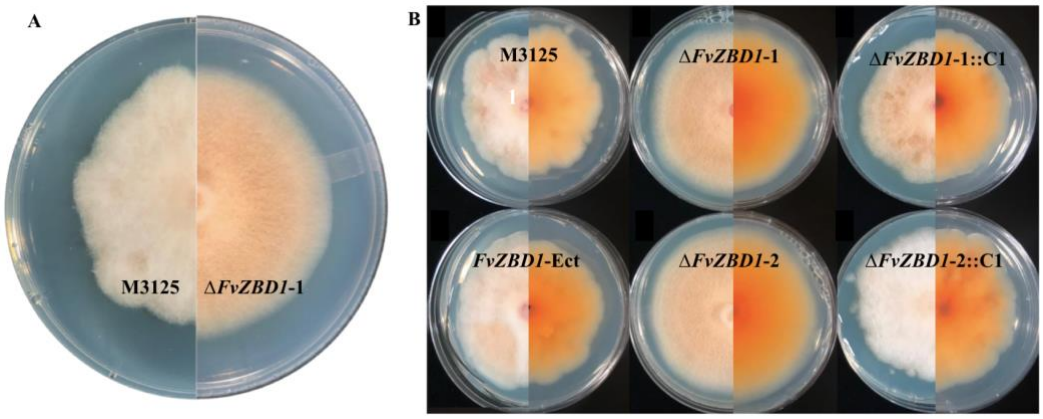

Figure 3.7 Δ*FvZBD1* mutants displayed more uniform growth morphology on GYAM plates. (A) Seven-day-old GYAM agar cultures displayed different growth phenotypes of M3125 (left) and Δ*FvZBD1*-1 (right), both shown from the front view. **(B)** Growth phenotypes of nine-day-old GYAM cultures for the *F. verticillioides* strains with both front and reverse views (left and right halves, respectively, of the split images). Genotypes are labeled as shown.

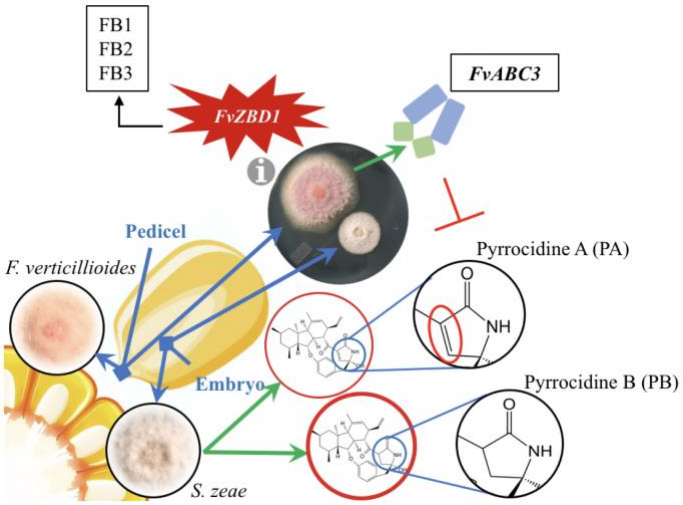

Figure 3.8 Illustration of biological antagonism between two maize seed endophytes, *F. verticillioides* and *S. zeae* in the endosperm. *F. verticillioides* is primarily confined to the pedicel of the maize kernel, while *S. zeae* is more frequently isolated from embryonic tissue. Pyrrocidine A and B, two lactam-containing antibiotics produced by *S. zeae*, are postulated to contribute to an allelopathic antagonism between the two fungi. The chemical structures of pyrrocidines differ by a double (red circle) or single bond within lactam ring, resulting in higher toxicity of pyrrocidine A than B. Detailed analyses were carried out for an ABC transporter encoding gene, *FvABC3*, and a zinc-binding dehydrogenase encoding gene, *FvZBD1*. We hypothesize that *FvABC3* facilitates persistence of *F. verticillioides* in maize seeds when encountering pyrrocidines, while *S. zeae* induces the expression of *FvZBD1* in *F. verticillioides*, a gene negatively impacting the production of fumonisins and virulence in maize seedlings. Actually, *FvZBD1* is the most highly induced gene in both pyrrocidine A and B treatments, and its impact on fumonisin production provides evidence for allelochemical activity and response.

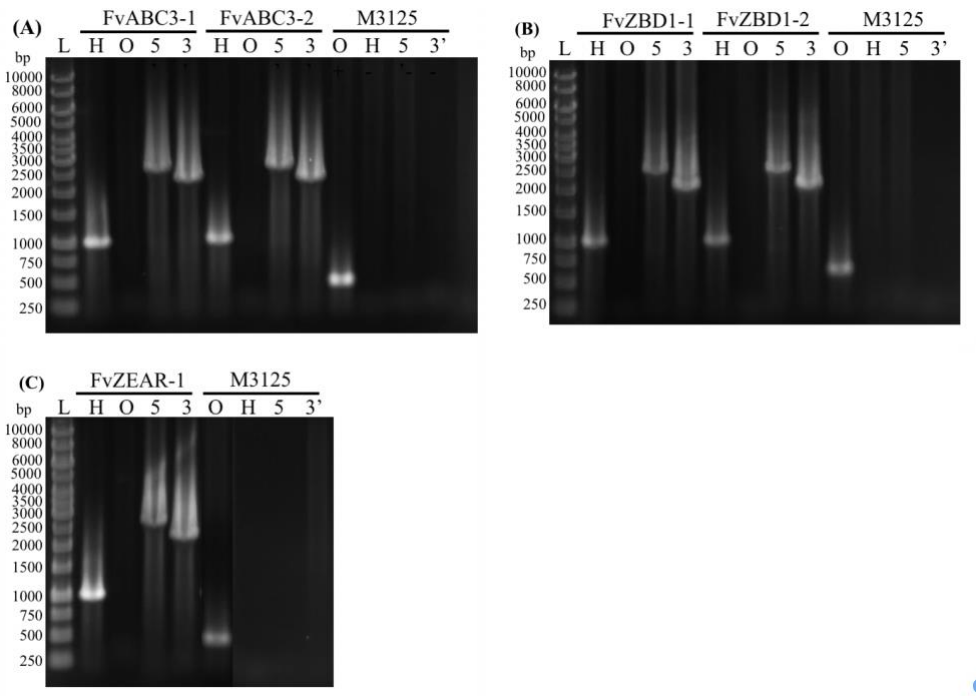

Supplemental Figure 3.1 Deletion of genes in this study was confirmed by PCR. To confirm the deletion of target genes, four PCR reactions were performed for each mutant to determine 1) the presence of hygromycin resistance cassette (HRC); 2) the absence of the open reading frame (ORF); 3) the homologous recombination at the 5' flank; 4) the homologous recombination at the 3' flank. L: 1kb ladder (New England BioLabs Inc.); O: target gene ORF; H: HRC; 5': 5' flank; 3': 3' flank. Verification was performed for (**A**) Δ*FvABC3* (FVEG_11089) mutants, (**B**) Δ*FvZBD1* (FVEG_00314) mutants, and (**C**) the Δ*FvZEAR* (FVEG_11090) mutant; M3125 genomic DNA, molecular grade water (data not shown), and ectopic transformed strains (data not shown) served as the control DNA templates.

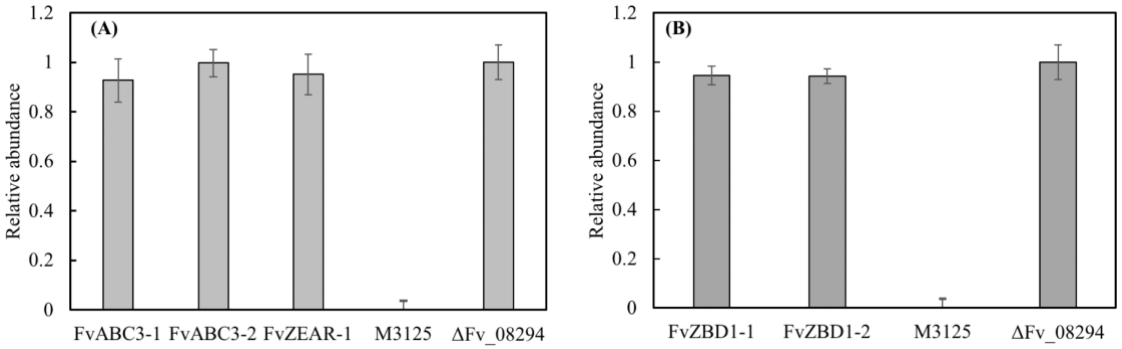

Supplemental Figure 3.2 Deletion mutants possessed a single genomic copy of the hygromycin resistance cassette. The copy number of the hygromycin resistance cassette (HRC) in the mutants was determined by qPCR of extracted genomic DNA. M3125 and ΔFVEG_08294 served as null and single-copy controls, respectively. ΔFVEG_08294 is a deletion mutant with only a single HRC as previously determined using Southern hybridization. The data were normalized to the reference β-tubulin gene (FVEG_04081) and calculated via the $2^{-\Delta\Delta Ct}$ method (Livak and Schmittgen, 2001). The ΔCt standard error is indicated by error bar. Copy number determination was performed for (A) Δ*FvABC3* and Δ*FvZEAR*, and (B) Δ*FvZBD1* mutants. Three technical replicates were prepared for each strain. There were no significant differences in abundance levels for the HRC among Δ*FvABC3,* Δ*FvZEAR,* Δ*FvZBD1*, and the ΔFVEG_08294 single-copy control (two-tailed Mann Whitney Wilcoxon test, p-value < 0.05).

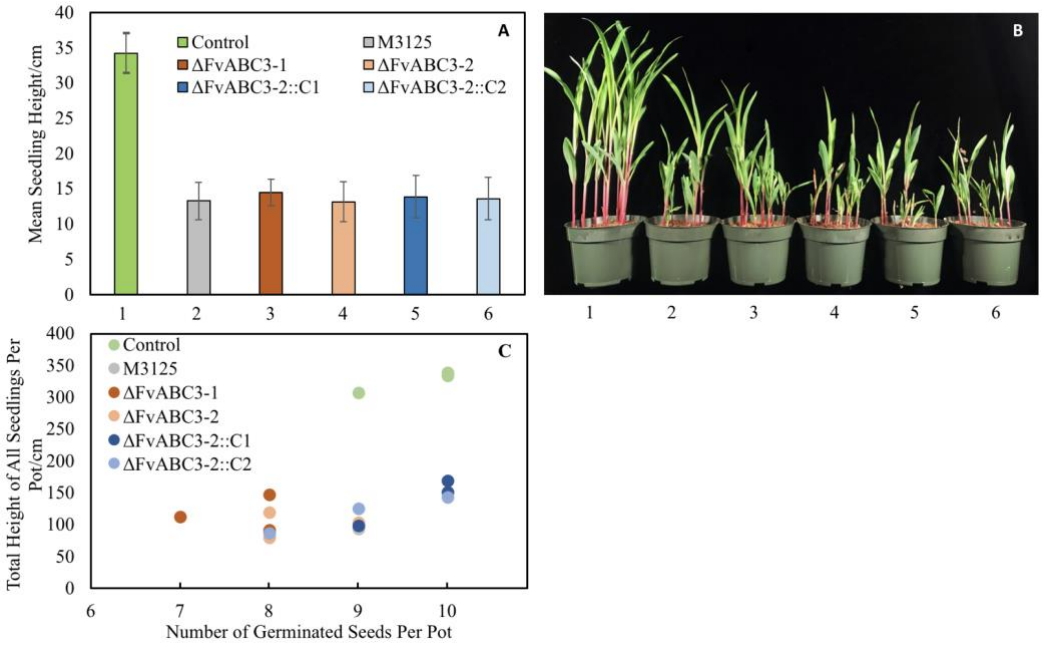

Supplemental Figure 3.3 Deletion of *FvABC3* in *F. verticillioides* did not alter fungal virulence on maize seedlings. Fifty Silver Queen® maize seeds were inoculated with 10^4/mL conidial suspensions for each of the five different *F. verticillioides* strains prior to planting. An uninoculated control treated with sterile water was also included. Plants were grown for 14 days before measuring their heights and counting germinated seeds. The experiment was repeated three times with three technical replicates each. Trials consistently showed no differences in virulence between M3125 and the *FvABC3* deletion mutants. Data from one trial was plotted for representation. (**A**) Histogram showing the mean height of seedlings. Numbers on X-axis correspond to the following treatments: **1**, sterile water control; **2**, M3125; **3**, Δ*FvABC3*-1; **4**, Δ*FvABC3*-2; **5**, Δ*FvABC3*-1::C-1; **6**, Δ*FvABC3*-1::C-1. Statistical analysis was conducted with the two-tailed Mann Whitney Wilcoxon test. (**B**) Phenotypic representation of seeding growth among treatments. Numbers on the pots correspond to those in (A). (**C**) Two-dimensional visualization of seedling growth among different treatments. Each dot represents a technical replicate of a particular treatment. Total height (cm) of all seedlings per pot is denoted on the Y-axis, and the X-axis shows the number of germinated seeds per pot.

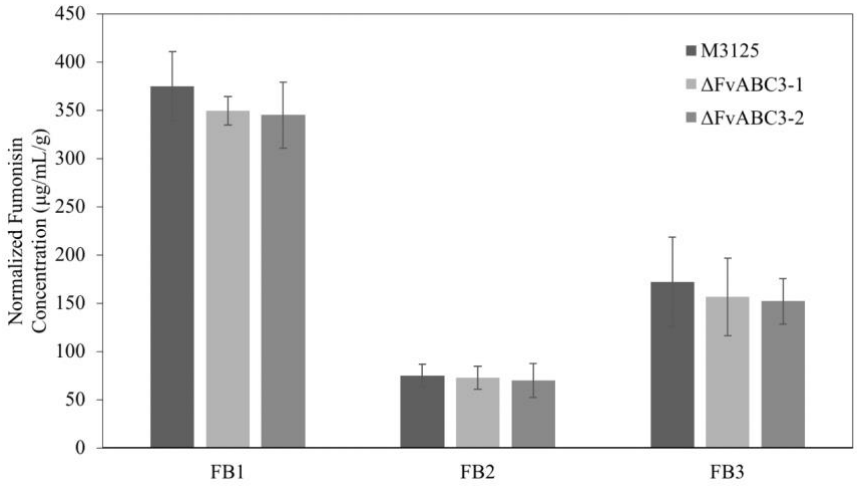

Supplemental Figure 3.4 Deletion of *FvABC3* did not impact fumonisin production in GYAM liquid cultures. Two milliliters of GYAM liquid medium in snap-cap tubes with loose caps were inoculated with 10^4 spores of each strain and cultured in dark at 250 rpm, 27 °C for 7 days. Fumonisin concentrations were determined by LC-MS and normalized to the vacuum-desiccated fungal mass weight, as indicated on the Y-axis. Statistical analyses performed with two-tailed Mann Whitney Wilcoxon test showed no significant differences (p-value < 0.05), in terms of fumonisin production, between deletion mutants and M3125. FB1/FB2/FB3 represent fumonisin B1/B2/B3.

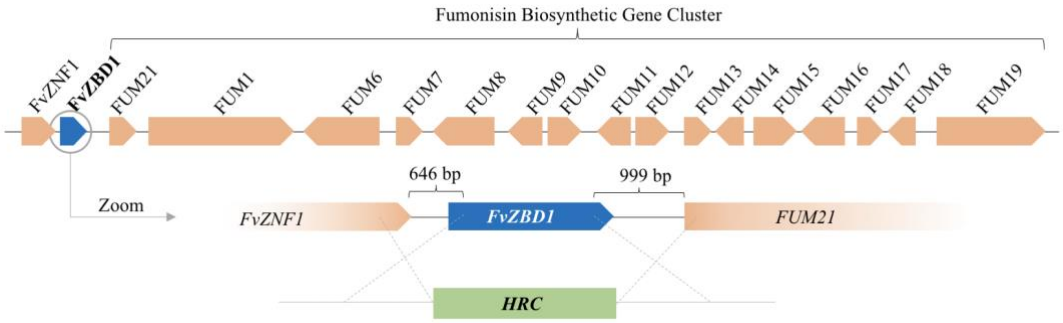

Supplemental Figure 3.5 *FvZBD1* is adjacent to the well-characterized *FUM* cluster. Genes are represented by colored arrows with labels. The direction of arrows denotes the orientation of genes. A zoom-in section of the *FvZBD1* locus indicates the deletion occurs at 646 bp downstream of *FvZNF1* and 999 bp upstream of *FUM21* when generating Δ*FvZBD1* mutants. *FvZBD1* is replaced with the hygromycin resistance cassette (HRC).

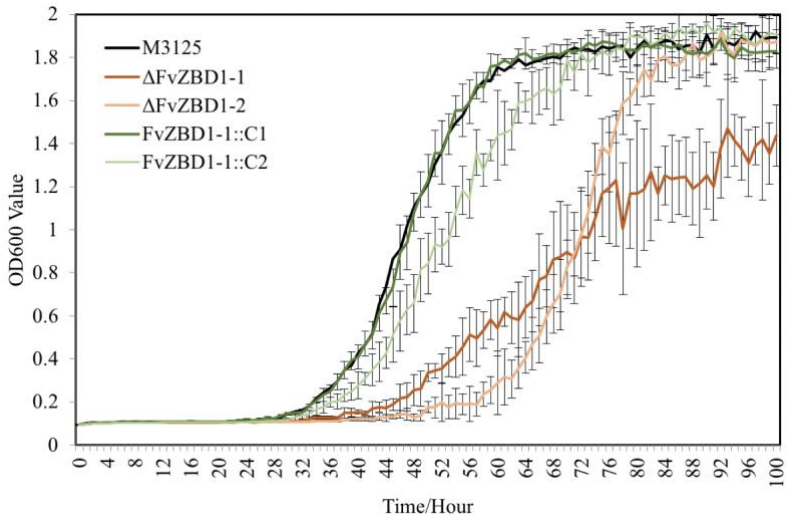

Supplemental Figure 3.6 Deletion of *FvZBD1* resulted in increased sensitivity to pyrrocidine B. Strains were monitored for 100 hours in PDB media amended with pyrrocidine B at 10 μg/mL. OD_{600} measurements taken every 2 hours were plotted (mean ± standard deviation). FRC M3125 serves as the control (black curve). Two *FvZBD1* deletion mutants are shown in orange, and two complemented strains in green.

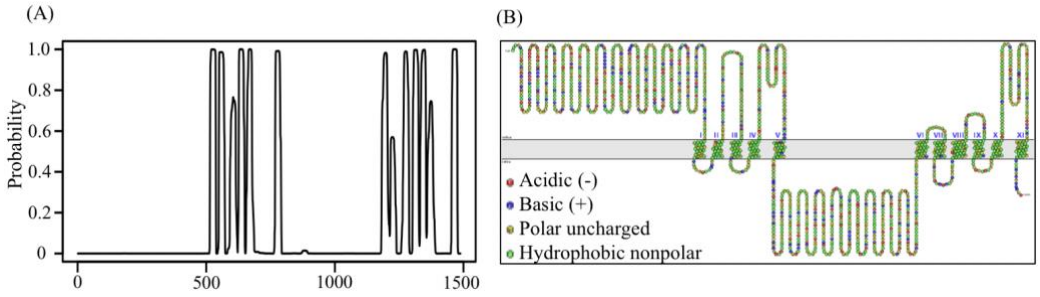

Supplemental Figure 3.7 FvABC3 shows typical ABC transporter transmembrane domain arrangement. (A) Eleven transmembrane domains were predicted with the TMHMM web server (http://www.cbs.dtu.dk/services/TMHMM/). The X-axis refers to the position of amino acid sequences, and the Y-axis corresponds to the probability of being a transmembrane domain. (B) The predicted transmembrane topology of FvABC3 amino acid sequence by the CAMPS (Computational Analysis of the Membrane Protein Space) database (http://webclu.bio.wzw.tum.de:18080/CAMPS2.0/index.jsp) (Neumann et al., 2012). The polarity of amino acids is marked by the color index.

CHAPTER 4

TRANSCRIPTOMIC RESPONSES TO BENZOXAZOLINONE-LIKE COMPOUNDS IN *FUSARIUM VERTICILLIOIDES*

Gao, M., Glenn, A. E., Gu, X., Duke, M. V., Scheffler, B. E., & Gold, S. E. For submission to Genes, Genomes, Genetics

ABSTRACT

The important cereal crops of maize, rye, and wheat constitutively produce precursors to 2-benzoxazolinone, a phytochemical having antifungal effects towards many *Fusarium* species. However, *Fusarium verticillioides* can tolerate 2-benzoxazolinone by converting it into non-toxic metabolites through the synergism of two previously identified gene clusters, *FDB1* and *FDB2*. Inspired by the induction of these two clusters upon exposure to 2-benzoxazolinone, the particular chemical structure of 2-benzoxazolinone with both lactam and lactone moieties, and the presence of lactamase encoding genes within the clusters, RNA sequencing experiments were carried out by challenging *F. verticillioides* with 2-benzoxazolinone and three related compounds, 2-oxindole, 2-coumaranone, and chlorzoxazone. The latter compound is a chlorinated 2-benzoxazolinone. Besides *FDB1* and *FDB2*, four additional gene clusters were identified as induced by 2-benzoxazolinone exposure, including a cluster thought to be responsible for biosynthesis of pyridoxine (vitamin B6), a known antioxidant providing tolerance to reactive oxygen species. Three putative gene clusters were identified as induced by challenging *F. verticillioides* with 2-oxindole, two with 2-coumaranone, and two with chlorzoxazone. Interestingly, 2-benzoxazolinone and 2-oxindole each induced two specific gene clusters with similar composition of enzymatic functions. Exposure to 2-coumranone elicited the expression of the fusaric acid biosynthetic gene cluster. Another gene cluster that may encode enzymes responsible for degrading intermediate catabolic metabolites with carboxylic ester bonds was induced by 2-benzoxazolinone, 2-oxindole, and chlorzoxazone. Also, the induction of a dehalogenase encoding gene during chlorzoxazone exposure suggested its role in the removal of the chlorine atom. Together, this work identifies genes and putative gene clusters responsive to

the 2-benzoxazolinone-like compounds with metabolic inferences, and interesting targets for future functional analyses are discussed.

INTRODUCTION

Plants have adopted various defensive mechanisms against microbial pathogens. One of the most notable mechanism is the production of antimicrobial secondary metabolites. These phytochemicals may be constitutively produced by the healthy plant (phytoanticipins) or synthesized *de novo* when encountering pathogens (phytoalexins) (VanEtten et al., 1995). However, some plant pathogens are capable of detoxifying these bioactive phytochemicals, which complicates plant disease management and poses a threat to the health of agricultural crops (Osbourn, 1999).

As one of the phytoanticipins found in select members of the Poaceae, 2-benzoxazolinone (BOA) is known for its *in vitro* antagonistic effect against a wide range of microbes (Glenn et al., 2001; Niemeyer, 1988). BOA is the spontaneous degradation product of its unstable precursor, 2,4-dihydroxy-2*H*-1,4-benzoxazin-3(4*H*)-one (DIBOA), which is also a defensive compound known for inhibiting bacteria, fungi, and insect feeding (Bravo et al., 1997; Corcuera et al., 1978; Glenn et al., 2001; Hashimoto and Shudo, 1996; Niemeyer, 1988; Woodward et al., 1978).

Fusarium verticillioides is one of the most prevalent seed- and soil-borne fungal pathogens on maize and is capable of causing severe ear rot with dangerous fumonisin mycotoxin contamination. Alternative to its pathogenic effect, *F. verticillioides* often exists as a symptomless endophyte (Blacutt et al., 2018). Living inside maize tissues, *F. verticillioides* has to cope with antimicrobial phytochemicals, such as the benzoxazinones and benzoxazolinones. *F. verticillioides* can tolerate BOA at concentrations that are inhibitory to other fungi. In fact, only a

limited number of *Fusarium* species can tolerate BOA, with *F. verticillioides* and *F. subglutinans* being the most tolerant (Glenn et al., 2001; Vilich et al., 1999). BOA tolerance is due to hydrolysis of the five-membered oxazole ring of BOA and loss of the carbonyl group, followed by an additional modification yielding the non-toxic metabolite, N-(2-hydroxyphenyl) malonamic acid (HPMA) (Glenn et al., 2002, 2003, 2016; Glenn and Bacon, 2009). It is worth mentioning that the oxazole ring consists of moieties for both a γ-lactam and γ-lactone.

Glenn et al. (2016) characterized a metallo-beta-lactamase gene (*MBL1*) in *F. verticillioides* essential for BOA tolerance, and deletion of this gene rendered *F. verticillioides* incapable of metabolizing BOA (Glenn et al., 2016). Its orthologs in *F. graminearum* and *F. pseudograminearum* also demonstrated indispensable roles in BOA hydrolysis (Kettle et al., 2015). Collectively, these studies represented the first functional characterization of fungal lactamases. Additional questions of interest are *i*) how and in what order the lactam and lactone moieties are hydrolyzed during BOA degradation and *ii*) is there a substrate preference for these hydrolases? To address these knowledge gaps, comparative transcriptomic studies in *F. verticillioides* were designed with BOA-like compounds to gain insights on the unique genes responsive to different moieties.

Four compounds were selected for the comparative transcriptomic response analyses, BOA, 2-oxindole (OXD), 2-coumaranone (CMN), and chlorzoxazone (CZX) (Fig. 4.1). OXD is an aromatic heterocyclic organic compound consisting of a six-membered benzene ring fused to a γ-lactam ring. OXD differs from BOA in that it contains only the lactam moiety. An entomopathogenic bacterium, *Xenorhabdus hominickii*, produces OXD, which suppresses host insect responses by inhibiting eicosanoid biosynthesis, and oxindole alone can inhibit the hemocytic nodule formation of *Spodoptera exigua*, an entomopathogenic nematode species, in a

dose-dependent manner (Sadekuzzaman et al., 2017). In contrast to OXD, CMN contains only the lactone moiety (Fig. 4.1). There have been no reports so far describing biological functions of CMN. CZX has been prescribed as a muscle relaxant to treat spasms and the resulting pain or discomfort (Dong et al., 2006). The chemical structure of CZX is the same as BOA except for the addition of a chlorine on the benzene ring (Fig. 4.1).

The *MBL1* lactamase gene in *F. verticillioides* was identified through transcriptomic analysis after exposure to BOA (Glenn et al., 2016). To further explore additional genes responsive to other BOA-like compounds and to gain insight into hydrolytic activities associated with specific moieties, comparative RNA-seq experiments were designed to get clues about the degradation of BOA. Herein are described the transcriptomic responses of *F. verticillioides* upon individual exposure to BOA, OXD, CMN, and CZX and possible inferences regarding the degradation of those compounds.

RESULTS

BOA, OXD, CMN, and CZX elicited differential gene responses in *F.verticillioides*.

Wild-type *F. verticillioides* FRC M3125 liquid cultures were individually treated with 50 μg/mL BOA, OXD, CMN, or CZX compounds prior to obtaining RNA. To gain insight into the transcriptional responses of *F. verticillioides* upon exposure to these compounds, the sequenced transcriptomes were compared to a DMSO control (untreated) and each other. The raw RNA-seq reads of each BOA, OXD, and CZX biological replicate ranged from 14.6 to 19.7 million, of which 14.5 to 19.5 million reads were mapped to the reference genome of *F. verticillioides* (Supplemental Table 4.1) (Ma et al., 2010). We obtained 69.3 – 84.0 million raw reads for the CMN treated samples. Above 96% of raw reads in each library were mapped to the *F. verticillioides* reference genome (Supplemental Table 4.1).

In the BOA treatment, 587 differentially expressed genes were identified (false discovery rate adjusted p-value < 0.05, $\log_2$ fold change > 1 for up-regulated and $\log_2$ fold change < -1 for down-regulated), with 422 up-regulated and 165 down-regulated genes, respectively, when compared to the DMSO only treated control (Fig. 4.2A). The down-regulated genes generally exhibited a low level of expression before BOA challenge and a minor fold change (< 6.5 fold down-regulation) after BOA challenge. RNA-seq results corroborated previous findings (Glenn et al., 2016) that two BOA-hydrolysis associated gene clusters, *FDB1* in chromosome 10 (FVEG_08287 – FVEG_08295) and *FDB2* in chromosome 3 (FVEG_12625 – FVEG_12641), were significantly induced. Individual gene responses in both clusters ranged from no change to 2234-fold increase following exposure to BOA (Table 4.1). The core metallo-beta-lactamase gene *MBL1* (FVEG_08291) in the *FDB1* cluster exhibited greater induction levels (761-fold) than its paralog FVEG_12637 (32-fold, FPKM = 0.36 before induction and 13 after induction) in *FBD2* cluster, which was also observed in previously reported microarray data (Glenn et al., 2016). In addition, RNA-seq results also identified another highly up-regulated gene FVEG_12642 (236-fold) adjacent to the *FDB2* cluster, which was not up-regulated in the previous microarray data. Interestingly, four new putative gene clusters were identified in the RNA-seq results following BOA exposure, including FVEG_03387 – FVEG_03405, FVEG_06020 – FVEG_06024, FVEG_16700 – FVEG_09978, and FVEG_13976 – FVEG_13979 (Table 4.1). The induction levels ranged for cluster contained genes was from 2.6- to 208-fold compared to the DMSO treated control.

OXD exposure in RNA-seq experiments elicited 164 significantly up-regulated genes and 37 down-regulated genes, compared to the DMSO only treated control (Fig. 4.2B). Amongst the 164 up-regulated genes, three highly induced putative clusters were identified (FVEG_06533 –

FVEG_06536, FVEG_08763 – FVEG_08774, and FVEG_13976 – FVEG_13979) (Table 4.2). The induction levels ranged from 8- to 760-fold.

Upon exposure to CMN, 4335 genes demonstrated significant differential expression compared to the control treatment, with 1857 genes up- and 2478 genes down-regulated (Fig. 4.2C). Two distinctive putative gene clusters spanning genomic regions from FVEG_11952 to FVEG_11959 and FVEG_12519 to FVEG_12534 were significantly up-regulated (Table 4.3). The last cluster exhibited a high level of induction and transcript abundance (FPKM from approximately 400 to 6000) upon exposure to CMN, among which an alpha-beta hydrolase (FVEG_12519) gene and a serine hydrolase (FVEG_12520) demonstrated the greatest fold changes, 304- and 344-fold, respectively. The gene cluster contains two fungal Zn(2)-Cys(6) transcription factor encoding genes (FVEG_12532 and FVEG_12534), which may be involved in regulating the expression of neighboring genes.

In the CZX treatment, 3331 genes were differentially expressed, including 1270 up-regulated and 2061 down-regulated (Fig. 4.2D). A close inspection of fold changes and levels of significance identified two putative gene clusters, which are FVEG_16699 – FVEG_09978 and FVEG_13976 – FVEG_13979 (Table 4.4). FVEG_16700 and FVEG_09974 – FVEG_09978 demonstrated highest fold changes (>512 fold) and lowest p-values (< 1.16E-121). It's worth noting that FVEG_16700 is an ATP-binding cassette (ABC) transporter, and its adjacent transcription factor FVEG_16699 was also induced (8-fold, FPKM = 98/787 before/after induction) upon exposure to CZX. Interestingly, FVEG_16700 also exhibited a 20-fold change in expression following BOA treatment. However, FVEG_16699 was not differentially expressed in any other treatments other than CZX.

Shared induced genes among chemical treatments.

Inspired by previous functional analyses of up-regulated genes responding to BOA treatment and the similarity of other chemical structures to BOA, we were particularly interested in induced genes shared among the different chemical treatments shown in the Venn diagram (Fig. 4.3). The 22 significantly induced genes shared among all four compounds are detailed in Table 4.5. BOA and CZX both contain lactam and lactone moieties, while OXD and CMN contain either a lactam or a lactone, respectively. We further examined shared genes to gain insight into induced genes associated with either moiety. BOA, CZX, and OXD together exclusively induce 16 genes (Fig. 4.3; Table 4.6). Analogously, BOA, CZX, and CMN induced a unique set of 58 genes (Fig. 4.3, Table 4.7).

Shared induced gene clusters were observed between BOA and BOA-like compound treatments.

A three-gene cluster, consisting of FVEG_13976, FVEG_13977, and FVEG_13979 was highly up-regulated in BOA, CZX, and OXD treatments, ranging from 10- to 724-fold induction compared to the DMSO control treatment (Tables 4.1, 4.2, 4.4, and 4.6). However, FVEG_13976 and FVEG_13977 were not significantly induced upon exposure to CMN. Compared to the extremely high levels of induction in BOA, CZX, and OXD treatments (> 120-fold change, FPKM > 2000 after induction), a nominal induction of FVEG_13979 was seen in CMN treatment, with approximately 3-fold change and FPKM values less than 10 after induction.

Interestingly, both BOA and CZX treatments shared a highly induced six-gene cluster, with accession numbers ranging from FVEG_16700 to FVEG_09978 (Table 4.1, 4.4). Genes in the cluster were up-regulated from 20- to 68-fold when exposed to BOA, while the level of induction was even higher in CZX treatment, ranging from 541- to 4608-fold for genes in the

cluster. However, exposure to OXD or CMN did not elicit differential expression of the cluster compared to the DMSO control treatment.

Differential expression of lactamase encoding genes was observed across chemical treatments.

Our previous studies functionally characterized the major role the metallo-beta-lactamase gene *MBL1* (FVEG_08291) plays in BOA degradation (Glenn et al., 2016). Considering that lactonases and lactamases are categorized under the same protein family, and that all the four tested compounds in this study possess lactam and/or lactone moieties, we wanted to explore the evidence of lactamase gene induction upon exposure to these four compounds. In addition to the previously validated up-regulation of *MBL1* (FVEG_08291) and *MBL2* (FVEG_12637) in BOA treatments (Glenn et al., 2016), we also observed the significant induction of two more lactamase encoding genes, FVEG_09854 and FVEG_12526 (Table 4.8). FVEG_12347 was the only down-regulated lactamase encoding gene upon exposure to BOA (Table 4.8). Exposure to CMN regulated the differential expression of ten lactamase encoding genes in total, with four up- and six down-regulated (Table 4.8). Exposing *F. verticillioides* to OXD did not down-regulate any of the lactamase encoding genes, and the previously noted FVEG_09854 was the only up-regulated lactamase encoding gene with a 2.5-fold induction. CZX elicited the differential expression of eight lactamase-encoding genes. Of four CZX up-regulated beta-lactamases (FVEG_03849, FVEG_05734, FVEG_09854, and FVEG_12457), FVEG_09854 alone was also induced by BOA, OXD and CMN treatments (Table 4.8). Exposure to CZX elicited an equal number of down-regulated lactamase encoding genes, and two of them (FVEG_13172 and FVEG_13253) were also repressed in the CMN treatment.

MIPS functional categorization reveals differential trends in genes responsive to BOA and BOA-like compounds.

To gain insight into the functional categories of genes responsive to the four chemical treatments, MIPS FunCat system was utilized with gene lists from differential expression analysis (Ruepp et al., 2004). Functional categories enriched under BOA were those involved in metabolism, energy, protein degradation, cell rescue, and interaction with the environment (Table 4.9). Similarly, OXD-responsive genes are putatively involved in the majority of the above categories with one additional gene associated with signal transduction. None of OXD-responsive genes were functionally enriched in energy metabolism. More enriched functional categories, including systemic development and biogenesis of cellular components, were observed in both CMN and CZX treatments, compared to BOA and OXD ones. Since there were more genes differentially expressed upon exposure to CMN and CZX than to BOA or OXD, each enriched category in the above two treatments contains a larger number of genes, compared to that in BOA or OXD treatments (Table 4.9). Despite the differences in the total number of induced genes among the four treatments, approximately 31% - 36% were enriched in the metabolism category. Surprisingly, CMN and CZX treatments demonstrated a significantly higher correlation between metabolism with down-regulation, compared to BOA or OXD treatments. Approximately 15 – 19% of induced genes in BOA, CMN, and CZX treatments were enriched for cellular transport, but less than 10% was reflected in OXD treatment.

DISCUSSION

OXD, CMN, and CZX are three lactam and/or lactone-containing compounds with similar chemical structures to the maize phytoanticipin, BOA. Inspired by transcriptional and functional analyses of lactamase gene-containing gene clusters in BOA degradation by *F.*

verticillioides, additional transcriptional inferences were explored by exposing *F. verticillioides* to BOA, OXD, CMN, and CZX, with a focus on induced genes of interest and putative clusters. Interestingly, a number of putative degradative gene clusters were elicited during chemical exposure, and these clusters were either exclusive to a particular compound treatment or shared between various treatments. This work provides insight into the co-regulatory expression patterns upon exposure to lactam/lactone compounds, which directs future functional characterization.

Putative hydrolytic genes and gene clusters were identified upon exposure to BOA.

The RNA-seq results were fairly consistent to the previous microarray data (Glenn et al., 2016). Compared to the previous microarray data, the RNA-seq experiment identified a larger number of genes differentially expressed by BOA challenge, among which FVEG_12642 exhibited a 236-fold induction upon exposure to BOA. This gene putatively encodes a NmrA-like protein of 301 amino acids in length, which possibly functions as a transcription regulator and NADPH sensor. FVEG_12642 is located adjacent to the previously characterized *FDB2* cluster, but it was not previously described in the microarray data. The induction level is comparable to other induced genes in the *FDB2* cluster. The orthologs to FVEG_12642 are widely present in other *Fusarium* species with over 98% sequence identities (data not shown) as opposed to the limited range of the *FDB2* cluster.

In addition to the two previously characterized BOA-induced gene clusters (Glenn et al., 2002, 2016; Glenn and Bacon, 2009), here we identified two additional gene clusters (Table 4.1). The FVEG_03387 – FVEG_03405 cluster contains a fumarylacetoacetate hydrolase (FVEG_03394), which was previously studied in human clinical research for its role in tyrosine catabolism in liver and kidney (Awata et al., 1994). Fumarylacetoacetate hydrolase is thought to

be involved in the catabolism of phenylalanine, and the chemical structure of phenylalanine is reminiscent of N-(2-hydroxyphenyl)malonamic acid (HPMA), which is the metabolic product of BOA hydrolysis and malonylation (Glenn et al., 2016; Glenn and Bacon, 2009). It is possible that FVEG_03394 is regulated by a break-down product of BOA and contributes to further catabolic activity. Interestingly, the FVEG_03387 – FVEG_03405 cluster is also located directly adjacent to the bikaverin (BIK) biosynthesis gene cluster (FVEG_03379 – FVEG_03384) (Linnemannstöns et al., 2002), but the genes in the BIK biosynthesis gene cluster did not demonstrate differential expression upon exposure to BOA. It may be worth pursuing the impact of the BOA-induced FVEG_03387 – FVEG_03405 cluster on BIK biosynthesis.

The FVEG_06020 – FVEG_06024 cluster putatively codes for the biosynthesis of pyridoxine, also known as vitamin B6, which is an efficient singlet oxygen quencher and antioxidant that contributes to resistance to reactive oxygen species (Bilski et al., 2000). It's been shown that *Cercospora nicotianae* can protect itself against $^1O_2$-mediated damage by $^1O_2$-scanvenger vitamin B6 (Ehrenshaft et al., 1999). FVEG_06020 encodes a homolog of PDX2, a glutamine amidotransferase, and FVEG_06021 encodes a homolog of PDX1, a pyridoxal 5'-phosphate synthase. These are the core enzymes for biosynthesis of pyridoxine (Tambasco-Studart et al., 2007; Titiz et al., 2006). Lastly, FVEG_06024 putatively encodes a 1-aminocyclopropane-1 carboxylate deaminase, which is a pyridoxal phosphate (PLP)-dependent enzyme that degrades 1-aminocyclopropane-1-carboxylate (ACC), which in plants is a precursor of the ripening hormone ethylene, to ammonia and alpha-ketoglutarate (Van de Poel and Van Der Straeten, 2014). ACC synthase is a member of the PLP-dependent enzymes, which utilizes vitamin B6 as a co-factor for its enzymatic function (Boller et al., 1979).

BOA and OXD exposure revealed specific clusters with functional similarity.

Another BOA- and CZX-inducing gene cluster, FVEG_09969 – FVEG_09978, was identified with genes encoding an amidohydrolase (FVEG_09970), a SnoaL-like domain (FVEG_ 09974), a NAD-binding domain (FVEG_09975), and additional hydrolases, which presumably function in hydrolyzing specific chemical moieties (Table 4.1). Interestingly, exposure to OXD also elicited the expression of a gene cluster containing genes encoding an amidohydrolase (FVEG_06533), a SnoaL-like domain (FVEG_06534), and a NAD-binding domain (FVEG_06535) (Table 4.2). The one-atom difference between BOA and OXD chemical structures apparently contributes to the specific induction of gene clusters containing genes of similar functions. Although both clusters contain three genes with similar functional annotations, the amino acid sequences of similarly annotated genes possess low sequence similarities (< 5%) (data not shown).

CMN exposure induced the fusaric acid biosynthetic gene cluster in *F. verticillioides*.

As is shown in Table 4.3, exposure to CMN induces a gene cluster from FVEG_12519 to FVEG_12534. This is the fusaric acid biosynthetic gene cluster (*FUB*) (Brown et al., 2015). Deletion of a global regulator gene *lae1* in *F. verticillioides* results in a significant down-regulation of this *FUB* cluster (Butchko et al., 2012), and it is interesting to observe a significant up-regulation of the same cluster upon exposure to the lactone-containing compound, CMN. Thus, exposure to CMN may impact the production of fusaric acid production by *F. verticillioides*. Interestingly, a metallo-beta-lactamase encoding gene FVEG_12526 is located within the cluster. FVEG_12526 is neither down-regulated in the absence of *lae1*, nor is it induced in the presence of CMN. Future analyses will investigate the impact of CMN on fusaric acid production.

A dehalogenase encoding gene may be involved in the removal of the chlorine in CZX.

CZX exposure elicited more than 81-fold induction of FVEG_02350, which putatively encodes a dehalogenase. With CZX being the only compound of the four possessing a halogen atom in the chemical structure, we did not observe the induction of FVEG_02350 in BOA, OXD, or CMN treatments. As the functional prediction indicates, FVEG_02350 may be involved in catalyzing the removal of the chlorine atom from CZX. This will be evaluated as part of a series of future studies.

We did not observe the induction of *FDB1* or *FDB2* clusters upon exposure to CZX when the only difference of its chemical structure from BOA is the additional chlorine. It's probably an artifact of the experimental design that the *FDB* clusters may not be responsive at one-hour after CZX induction. Removal of the chlorine atom may need to take place ahead of the degradation of its lactam/lactone ring structure.

FVEG_16700 may possess substrate specificity as a putative membrane transport protein.

When challenging *F. verticillioides* with BOA and CZX, we noticed a significant induction of a membrane transporter encoding gene, FVEG_16700, with 20- and 1200-fold up-regulation, respectively. The putative membrane transporter protein encoded by FVEG_16700 belongs to the major facilitator superfamily, which is a protein superfamily ubiquitously expressed across the different kingdoms of life, importing and transporting metabolites, drugs, amino acids, etc (Marger and Saier, 1993). Interestingly, the induction of FVEG_16700 was not observed in either OXD or CMN treatment, which respectively contain only a lactam or lactone bond in their chemical structures, as opposed to the tandem arrangement of both moieties in BOA and CZX. This suggests that the lactam/lactone bond juxtaposition common to these molecules may be inductive and/or may be an excreted cargo signature.

BOA, OXD, and CZX share a common induced gene cluster.

Although specific gene clusters were induced upon each compound treatment, we observed a common gene cluster shared among BOA, OXD, and CZX treatments, composed of three genes FVEG_13976, FVEG_13977, and FVEG_13979. FVEG_13976 putatively encodes a protein containing NAD(P)-binding Rossmann-like domain, which often contributes to substrate binding. FVEG_13977 putatively encodes carboxymethylenebutenolidase, which belongs to a family of hydrolases, specifically those potentially acting on lactone carboxylic ester bonds (Schmidt and Knackmuss, 1980). Carboxymethylenebutenolidase typically catalyzes the hydrolysis of 4-carboxymethylenebut-2-en-4-olide and breaks it down to 4-oxohex-2-enedioate (Schmidt and Knackmuss, 1980). The substrate of the enzyme, 4-carboxymethylenebut-2-en-4-olide, contains carboxylic ester bond that is present in BOA, CMN, and CZX. This is fairly interesting because we did not see the induction of FVEG_13977 in the CMN treatment but rather in the OXD treatment. A possible explanation is FVEG_13977 may not function in the very first step of breaking open the lactone ring but perhaps work later on intermediate metabolites with carboxylic ester bonds. FVEG_13979 encodes a putative short chain dehydrogenase, and most of short chain dehydrogenases are NAD- or NADP-dependent oxidoreductases. It would be interesting to pursue functional analyses by generating cluster knock-out strains and examining changes in degradation products.

In sum, exposure to BOA, CMN, OXD, or CZX elicited the differential expression of genes and putative gene clusters that are either exclusive to a particular treatment or shared among them. It's likely that certain genes or gene clusters may not have a direct role on catabolizing BOA, CMN, OXD, or CZX. Instead, they may be responding to their degradation intermediates or the pyridoxine biosynthetic cluster, which indicates that the fungus may be

making compounds, such as antioxidants, to respond to other physiological challenges, such as ROS being generated as a result of the xenobiotic challenge. The induction of the fusaric acid biosynthesis gene cluster by CMN and the putative cluster adjacent to the BIK biosynthetic gene cluster by BOA may suggest a link between BOA/BOA-like compound exposure and production of mycotoxins and other secondary metabolites. Meanwhile, the predicted putative gene clusters will direct future functional characterization of genes potentially involved in targeting specific moieties of BOA-like compounds and provide insights into their biochemical roles during xenobiotic exposure and importance into compound exposure.

MATERIALS AND METHODS

Culture preparation and reagents

Two milliliters of PDB (potato dextrose broth; Neogen Food Safety, Lansing, MI, USA) cultures in sterile 15 mL snap-cap tubes (Falcon, Corning, NY, USA), with caps loose, were inoculated with 10^4 FRC M3125 wild-type *F. verticillioides* conidia and grown at 27 °C, 250 rpm for 47 hours, at which time 5 µL DMSO containing 100 µg (final concentrations of 50 µg/mL) of BOA (Sigma-Aldrich, St. Louis, MO, USA), OXD (Sigma-Aldrich), CMN (Sigma-Aldrich), or CZX (Sigma-Aldrich), respectively, were added to the respective treatments. Five microliters of DMSO was added to negative control samples. All culture tubes were incubated for a final one-hour induction. Three biological replicates were each prepared for BOA, OXD, CMN, and CZX treatments and a DMSO only (no treatment) control. After the final hour, 1 mL liquid culture from each tube was pelleted by centrifugation at 8000xg for 5 min at 4 °C, resuspended in 1 mL ice cold lysis buffer, and transferred to lysing matrix D tubes (MP Biomedicals, LLC, Santa Ana, CA, USA). The tubes were homogenized with a FastPrep-24™

5G instrument (MP Biomedicals) at 6 m/s with 2 pulses of 30 s and a 1 min intervening pause at room temperature.

RNA extraction, library preparation and sequencing

Total RNA was extracted from the homogenized samples with a PureLink® RNA Mini Kit (Thermo Fisher Scientific Inc., MA, USA) following the manufacturer's protocol. RNA quality was checked with an Agilent 2100 Bioanalyzer (Agilent Technologies, Palo Alto, CA, USA). Sequencing libraries were constructed with Illumina Truseq DNA LT sample prep kit (Illumina Inc., San Diego, CA, USA) following the manufacturer's protocol. Illumina library size validation was performed using the Agilent Tapestation 2200 High Sensitivity D1000 Assay (Part No. 5067-5584, Agilent Technologies, Santa Clara, CA, USA). Prior to equimolar library pool preparation, individual libraries were assayed for concentration by an Illumina library quantification kit (Product number KK4854, Kapa Biosystems, Inc, Wilmington, MA, USA) on a qPCR instrument (LightCycler 96, Roche Applied Science, Indianapolis, IN, USA). Each pool was clustered onboard an Illumina HiSeq2500 DNA sequencer with SR Rapid v2 flowcell clustering kits (Product number GD-402-4002, Illumina, San Diego, CA, USA). Single-end 50 bp sequencing was carried out with Rapid SBS v2 (Product number FC-402-4022, Illumina) reagents. Approximately 15 million reads were collected for BOA, OXD, and CZX libraries, and over 69 million reads were collected for CMN libraries.

Sequencing data analysis

Sequencing reads were processed by Cutadapt 1.9.dev1 (Martin, 2011), Trimmomatic 0.32 (Bolger et al., 2014) and custom scripts to remove adapters, low-quality reads, rRNA and organellar sequences, which were obtained from National Center for Biotechnology Information (NCBI) Gene Database (https://www.ncbi.nlm.nih.gov/). Reads were mapped to *F. verticillioides*

7600 genome by Tophat 2.0.13 (Kim et al., 2013; Ma et al., 2010), alignment sorted by Samtools 1.2 (Li et al., 2009), and read count and expression estimation obtained by HTseq 0.6.1p1 (Anders et al., 2015) and DESeq2 (Love et al., 2014).

Public availability of data

RNA-seq data were deposited in NCBI's Gene Expression Omnibus (GEO) and are accessible through GEO Series accession GSE116351 (http://www.ncbi.nlm.nih.gov/geo/). The reference genome *Fusarium verticillioides* 7600 (ASM14955V1) was obtained from NCBI genome database (https://www.ncbi.nlm.nih.gov/genome/) (Ma et al., 2010).

REFERENCES

Anders, S., Pyl, P. T., and Huber, W. (2015). HTSeq-A Python framework to work with high-throughput sequencing data. *Bioinformatics* 31, 166–169. doi:10.1093/bioinformatics/btu638.

Awata, H., Endo, F., Tanoue, A., Kitano, A., Nakano, Y., and Matsuda, I. (1994). Structural organization and analysis of the human fumarylacetoacetate hydrolase gene in tyrosinemia type I. *BBA - Mol. Basis Dis.* 1226, 168–172. doi:10.1016/0925-4439(94)90025-6.

Bilski, P., Li, M. Y., Ehrenshaft, M., Daub, M. E., and Chignell, C. F. (2000). Vitamin B6 (pyridoxine) and its derivatives are efficient singlet oxygen quenchers and potential fungal antioxidants. *Photochem. Photobiol.* doi:10.1562/0031-8655(2000)0710129SIPVBP2.0.CO2.

Blacutt, A. A., Gold, S., Voss, K. A., Gao, M., and Glenn, A. E. (2018). *Fusarium verticillioides* : Advancements in understanding the toxicity, virulence, and niche adaptations of a model mycotoxigenic pathogen of maize. *Phytopathology*, PHYTO-06-17-0203-RVW. doi:10.1094/PHYTO-06-17-0203-RVW.

Bolger, A. M., Lohse, M., and Usadel, B. (2014). Trimmomatic: A flexible trimmer for Illumina sequence data. *Bioinformatics* 30, 2114–2120. doi:10.1093/bioinformatics/btu170.

Boller, T., Herner, R. C., and Kende, H. (1979). Assay for and enzymatic formation of an ethylene precursor, 1-aminocyclopropane-1-carboxylic acid. *Planta*. doi:10.1007/BF00454455.

Bravo, H. R., Copaja, S. V, and Lazo, W. (1997). Antimicrobial Activity of Natural 2-Benzoxazolinones and Related Derivatives. *J. Agric. Food Chem.* 45, 3255–3257. doi:doi: 10.1021/jf9608581.

Butchko, R. A., Brown, D. W., Busman, M., Tudzynski, B., and Wiemann, P. (2012). Lae1 regulates expression of multiple secondary metabolite gene clusters in *Fusarium verticillioides*. *Fungal Genet. Biol.* 49, 602–612. doi:10.1016/j.fgb.2012.06.003.

Corcuera, L. J., Woodward, M. D., Helgeson, J. P., Kelman, A., and Upper, C. D. (1978). 2,4-Dihydroxy-7-methoxy-2H-1,4-benzoxazin-3(4H)-one, an inhibitor from *Zea mays* with differential activity against soft rotting *Erwinia* species. *Plant Physiol.* 61, 791–795.

doi:10.1104/pp.61.5.791.
Dong, D.-L., Luan, Y., Feng, T.-M., Fan, C.-L., Yue, P., Sun, Z.-J., et al. (2006). Chlorzoxazone inhibits contraction of rat thoracic aorta. *Eur. J. Pharmacol.* 545, 161–166. doi:10.1016/J.EJPHAR.2006.06.063.
Ehrenshaft, M., Bilski, P., Li, M. Y., Chignell, C. F., and Daub, M. E. (1999). A highly conserved sequence is a novel gene involved in *de novo* vitamin B6 biosynthesis. *Proc. Natl. Acad. Sci. U. S. A.* doi:10.1073/pnas.96.16.9374.
Glenn, A. E., and Bacon, C. W. (2009). *FDB2* encodes a member of the arylamine N-acetyltransferase family and is necessary for biotransformation of benzoxazolinones by *Fusarium verticillioides*. *J. Appl. Microbiol.* 107, 657–671. doi:10.1111/j.1365-2672.2009.04246.x.
Glenn, A. E., Davis, C. B., Gao, M., Gold, S. E., Mitchell, T. R., Proctor, R. H., et al. (2016). Two horizontally transferred xenobiotic resistance gene clusters associated with detoxification of benzoxazolinones by *Fusarium* species. *PLoS One* 11, e0147486. doi:10.1371/journal.pone.0147486.
Glenn, A. E., Gold, S. E., and Bacon, C. W. (2002). *Fdb1* and *Fdb2*, *Fusarium verticillioides* loci necessary for detoxification of preformed antimicrobials from corn. *Mol. Plant. Microbe. Interact.* 15, 91–101. doi:10.1094/MPMI.2002.15.2.91.
Glenn, A. E., Hinton, D. M., Yates, I. E., and Bacon, C. W. (2001). Detoxification of corn antimicrobial compounds as the basis for isolating *Fusarium verticillioides* and some other *Fusarium* species from corn. *Appl Env. Microbiol* 67, 2973–2981. doi:10.1128/AEM.67.7.2973-2981.2001.
Glenn, A. E., Meredith, F. I., Morrison, W. H., and Bacon, C. W. (2003). Identification of intermediate and branch metabolites resulting from biotransformation of 2-benzoxazolinone by *Fusarium verticillioides*. *Appl. Environ. Microbiol.* 69, 3165–3169. doi:10.1128/AEM.69.6.3165-3169.2003.
Hashimoto, Y., and Shudo, K. (1996). Chemistry of biologically active benzoxazinoids. *Phytochemistry* 43, 551–559. doi:10.1016/0031-9422(96)00330-5.
Kettle, A. J., Carere, J., Batley, J., Benfield, A. H., Manners, J. M., Kazan, K., et al. (2015). A γ-lactamase from cereal infecting *Fusarium* spp. catalyses the first step in the degradation of the benzoxazolinone class of phytoalexins. *Fungal Genet. Biol.* 83, 1–9. doi:10.1016/j.fgb.2015.08.005.
Kim, D., Pertea, G., Trapnell, C., Pimentel, H., Kelley, R., and Salzberg, S. L. (2013). TopHat2: Accurate alignment of transcriptomes in the presence of insertions, deletions and gene fusions. *Genome Biol.* 14. doi:10.1186/gb-2013-14-4-r36.
Li, H., Handsaker, B., Wysoker, A., Fennell, T., Ruan, J., Homer, N., et al. (2009). The Sequence Alignment/Map format and SAMtools. *Bioinformatics* 25, 2078–2079. doi:10.1093/bioinformatics/btp352.
Linnemannstöns, P., Schulte, J., Del Mar Prado, M., Proctor, R. H., Avalos, J., and Tudzynski, B. (2002). The polyketide synthase gene *pks4* from *Gibberella fujikuroi* encodes a key enzyme in the biosynthesis of the red pigment bikaverin. *Fungal Genet. Biol.* doi:10.1016/S1087-1845(02)00501-7.
Love, M. I., Huber, W., and Anders, S. (2014). Moderated estimation of fold change and dispersion for RNA-seq data with DESeq2. *Genome Biol.* 15. doi:10.1186/s13059-014-0550-8.
Ma, L. J., Van Der Does, H. C., Borkovich, K. A., Coleman, J. J., Daboussi, M. J., Di Pietro, A.,

et al. (2010). Comparative genomics reveals mobile pathogenicity chromosomes in *Fusarium*. *Nature* 464, 367–373. doi:10.1038/nature08850.
Marger, M. D., and Saier, M. H. (1993). A major superfamily of transmembrane facilitators that catalyse uniport, symport and antiport. *Trends Biochem. Sci.* 18, 13–20. doi:10.1016/0968-0004(93)90081-W.
Martin, M. (2011). Cutadapt removes adapter sequences from high-throughput sequencing reads. *EMBnet.journal* 17, 10. doi:10.14806/ej.17.1.200.
Niemeyer, H. M. (1988). Hydroxamic acids (4-hydroxy-1,4-benzoxazin-3-ones), defence chemicals in the gramineae. *Phytochemistry* 27, 3349–3358. doi:10.1016/0031-9422(88)80731-3.
Osbourn, A. E. (1999). Antimicrobial phytoprotectants and fungal pathogens: A commentary. *Fungal Genet. Biol.* 26, 163–168. doi:10.1006/fgbi.1999.1133.
Ruepp, A., Zollner, A., Maier, D., Albermann, K., Hani, J., Mokrejs, M., et al. (2004). The FunCat, a functional annotation scheme for systematic classification of proteins from whole genomes. *Nucleic Acids Res.* 32, 5539–5545. doi:10.1093/nar/gkh894.
Sadekuzzaman, M., Park, Y., Lee, S., Kim, K., Jung, J. K., and Kim, Y. (2017). An entomopathogenic bacterium, *Xenorhabdus hominickii* ANU101, produces oxindole and suppresses host insect immune response by inhibiting eicosanoid biosynthesis. *J. Invertebr. Pathol.* 145, 13–22. doi:10.1016/j.jip.2017.03.004.
Schmidt, E., and Knackmuss, H. J. (1980). Chemical structure and biodegradability of halogenated aromatic compounds. Conversion of chlorinated muconic acids into maleoylacetic acid. *Biochem. J.* 192, 330–339. doi:10.1042/bj1920339.
Tambasco-Studart, M., Tews, I., Amrhein, N., and Fitzpatrick, T. B. (2007). Functional analysis of *PDX2* from *Arabidopsis*, a Glutaminase involved in vitamin B6 biosynthesis. *Plant Physiol.* 144, 915–925. doi:10.1104/pp.107.096784.
Titiz, O., Tambasco-Studart, M., Warzych, E., Apel, K., Amrhein, N., Laloi, C., et al. (2006). *PDX1* is essential for vitamin B6 biosynthesis, development and stress tolerance in *Arabidopsis*. *Plant J.* doi:10.1111/j.1365-313X.2006.02928.x.
Van de Poel, B., and Van Der Straeten, D. (2014). 1-aminocyclopropane-1-carboxylic acid (ACC) in plants: more than just the precursor of ethylene! *Front. Plant Sci.* doi:10.3389/fpls.2014.00640.
VanEtten, H. D., Sandrock, R. W., Wasmann, C. C., Soby, S. D., McCluskey, K., and Wang, P. (1995). Detoxification of phytoanticipins and phytoalexins by phytopathogenic fungi. *Can. J. Bot.* 73, 518–525. doi:10.1139/b95-291.
Vilich, V., Löhndorf, B., Sikora, R. A., and Friebe, A. (1999). Metabolism of benzoxazolinone allelochemicals of *Zea mays* by *Fusarium subglutinans*. *Mycol. Res.* 103, 1529–1532. doi:10.1017/S0953756299008862.
Woodward, M. D., Corcuera, L. J., Helgeson, J. P., and Upper, C. D. (1978). Decomposition of 2,4-dihydroxy-7-methoxy-2H-1,4-benzoxazin-3(4H)-one in aqueous solutions. *Plant Physiol.* 61, 796–802. Available at: http://www.plantphysiol.org/cgi/content/abstract/61/5/796.

Table 4.1 Gene clusters with differential expression upon exposure to BOA

Gene #	log_2(FC[a])	p-value[b]	Annotation
FVEG_03387	6.204	6.13E-70	NAD(P)-binding Rossmann-like domain
FVEG_03388	NS[c]	NS	C2H2-type zinc finger
FVEG_03389	NS	NS	Retinal pigment epithelial membrane protein
FVEG_03390	NS	NS	Hypothetical protein
FVEG_03391	NS	NS	Cutinase transcription factor
FVEG_03392	NS	NS	Hypothetical protein
FVEG_03393	NS	NS	C6 transcription factor
FVEG_03394	2.340	2.26E-25	Fumarylacetoacetate hydrolase family
FVEG_03395	NS	NS	Cutinase
FVEG_03396	3.465	3.43E-13	Hypothetical protein
FVEG_03397	2.578	2.14E-43	Fungal specific transcription factor
FVEG_03398	1.401	3.09E-08	Secretory lipase
FVEG_03399	4.078	1.19E-34	FAD binding domain
FVEG_03400	6.794	2.77E-33	Cupin domain
FVEG_03401	NS	NS	Aldehyde dehydrogenase
FVEG_03402	2.931	1.70E-07	Sugar (and other) transporter
FVEG_03403	NS	NS	Hypothetical protein
FVEG_03404	NS	NS	Allantoate permease
FVEG_03405	1.905	0.01614446	UbiD family decarboxylases
FVEG_06020	4.636	1.07E-115	SNO glutamine amidotransferase family, *PDX2*
FVEG_06021	6.230	0	Pyridoxal 5'-phosphate synthase, *PDX1*
FVEG_06022	NS	NS	Hypothetical protein
FVEG_06023	NS	NS	Uncharacterized protein
FVEG_06024	4.747	0	1-aminocyclopropane-1-carboxylate deaminase
FVEG_08287	10.910	0	NmrA-like family
FVEG_16285	10.257	4.59E-95	Amidase
FVEG_08290	NS	NS	Dienelactone hydrolase
FVEG_08291	9.573	0	Metallo-beta-lactamase superfamily, MBL1
FVEG_08292	3.145	5.31E-75	Transmembrane amino acid transporter protein
FVEG_08293	10.909	7.63E-159	FAD binding domain
FVEG_08294	5.871	0	Fungal specific transcription factor
FVEG_08295	9.687	2.48E-105	Amidase
FVEG_08296	2.714	4.63E-39	Hypothetical protein
FVEG_09969	1.421	2.75E-05	Cytochrome P450
FVEG_09970	2.324	0.001	Amidohydrolase
FVEG_09971	NS	NS	Cytochrome P450
FVEG_09972	NS	NS	Isoflavone reductase
FVEG_16699	NS	NS	Fungal specific transcription factor
FVEG_16700	4.355	9.12E-41	ABC transporter
FVEG_09974	5.183	1.39E-98	SnoaL-like domain
FVEG_09975	5.679	1.62E-221	NAD dependent epimerase/dehydratase family
FVEG_09976	4.736	1.28E-21	Putative cyclase
FVEG_09977	5.699	5.09E-34	Transketolase, C-terminal domain
FVEG_09978	6.094	9.47E-50	Short chain dehydrogenase
FVEG_12625	9.143	3.21E-109	Dienelactone hydrolase family
FVEG_12626	NS	NS	Monocarboxylate transporter
FVEG_12627	NS	NS	Uncharacterized protein

FVEG_12628	NS	NS	3-Hydroxyacyl-CoA dehydrogenase
FVEG_12629	10.322	8.02E-141	CoA-transferase family III
FVEG_12630	4.142	1.15E-24	Salicylate hydroxylase
FVEG_17313	NS	NS	Fatty-acid amide hydrolase
FVEG_12633	9.616	0	AMP-binding enzyme
FVEG_12634	10.679	6.92E-181	Carboxylesterase family
FVEG_12635	6.069	0	Fungal specific transcription factor
FVEG_12636	9.523	0	Arylamine N-acetyltransferase
FVEG_12637	4.989	9.67E-30	Metallo-beta-lactamase, MBL2
FVEG_17314	6.353	6.76E-26	Hypothetical protein
FVEG_12638	11.126	8.26E-206	Aldo/keto reductase family
FVEG_12639	7.908	0	Protein of unknown function
FVEG_12640	7.805	5.69E-161	Transmembrane amino acid transporter protein
FVEG_12641	9.504	0	2Fe-2S iron-sulfur cluster binding domain
FVEG_12642	7.880	7.29E-44	NADH(P)-binding
FVEG_13976	7.100	1.43E-126	L-lysine 6-monooxygenase
FVEG_13977	3.350	7.36E-131	Carboxymethylenebutenolidase
FVEG_13978	NS	NS	Activator of stress protein
FVEG_13979	7.707	9.84E-51	Short chain dehydrogenase

[a] FC, fold change

[b] p-value refers to the false discovery rate adjusted p-value

[c] NS, not significant induction

Clusters are highlighted in alternate shadings.

Table 4.2 Gene clusters with differential expression upon exposure to OXD

Gene #	log_2(FC[a])	p-value[b]	Annotation
FVEG_06533	9.362	0	Amidohydrolase family protein
FVEG_06534	6.964	0	SnoaL-like domain
FVEG_06535	9.350	6.43E-80	NAD(P)-binding Rossmann-like domain
FVEG_06536	2.981	1.86E-165	Fungal specific transcription factor
FVEG_08763	4.365	1.75E-250	FAD dependent oxidoreductase
FVEG_08764	4.345	3.63E-93	Alpha/beta hydrolase family
FVEG_08765	NS[c]	NS	Hypothetic protein
FVEG_08766	NS	NS	Nitrosoguanidine resistance protein
FVEG_08767	NS	NS	Glucose 1-dehydrogenase 2
FVEG_08768	NS	NS	Cercosporin resistance protein
FVEG_08769	NS	NS	Aromatic peroxygenase
FVEG_08770	3.567	9.62E-144	Carboxypeptidase
FVEG_08771	4.330	1.36E-280	Fungal specific transcription factor
FVEG_08772	6.753	4.02E-275	Alpha/beta hydrolase family
FVEG_08773	7.248	0	CAIB/BAIF family enzyme
FVEG_08774	6.195	0	Catechol dioxygenase N terminus
FVEG_13976	9.572	5.53E-230	L-lysine 6-monooxygenase
FVEG_13977	NS	NS	Carboxymethylenebutenolidase
FVEG_13978	5.800	0	Activator of stress protein
FVEG_13979	8.955	4.08E-68	Short chain dehydrogenase

[a] FC, fold change
[b] p-value refers to the false discovery rate adjusted p-value
[c] NS, not significant induction
Clusters are highlighted in alternate shadings.

Table 4.3 Gene clusters with differential expression upon exposure to CMN

Gene #	log_2(FC[a])	p-value[b]	Annotation
FVEG_11952	1.325	1.28E-10	Family description
FVEG_11953	2.783	5.51E-20	Uncharacterized protein
FVEG_11954	1.570	5.05E-43	Uncharacterized protein
FVEG_11955	2.341	3.16E-124	Catalase
FVEG_11956	2.085	8.94E-90	Mo-co oxidoreductase dimerization domain
FVEG_11957	1.782	9.35E-43	Methyltransferase domain
FVEG_11958	5.539	1.23E-46	C4-dicarboxylate transporter
FVEG_11959	3.401	7.26E-24	Uncharacterized protein
FVEG_12519	8.249	1.78E-231	Acetyltransferase
FVEG_12520	8.427	0	Serine hydrolase (FSH1)
FVEG_12521	7.539	0	Amino acid kinase
FVEG_12522	6.758	4.70E-195	YCII-related domain
FVEG_12523	7.016	0	Polyketide synthase
FVEG_12524	NS[c]	NS	Esterase
FVEG_17290	NS	NS	Acyl-CoA dehydrogenase
FVEG_17291	NS	NS	Hypothetical protein
FVEG_12526	NS	NS	Metallo-beta-lactamase
FVEG_12527	2.566	4.51E-06	Aldolase
FVEG_12528	6.750	0	Dehydrogenase
FVEG_12529	6.858	0	Sulfhydrylase
FVEG_12530	6.619	0	Dehydrogenase
FVEG_12531	5.662	0	Oxidase
FVEG_12532	2.848	1.08E-64	Fungal specific transcription factor
FVEG_12533	2.818	2.44E-84	Major facilitator superfamily
FVEG_12534	2.293	4.82E-77	Fungal specific transcription factor

[a] FC, fold change
[b] p-value refers to the false discovery rate adjusted p-value
[c] NS, not significant induction
Clusters are highlighted in alternate shadings.

Table 4.4 Gene clusters with differential expression upon exposure to CZX

Gene #	log_2(FC[a])	p-value[b]	Annotation
FVEG_09969	1.645	2.55E-08	Cytochrome P450
FVEG_09970	5.300	9.81E-22	Amidohydrolase
FVEG_09971	1.233	0.006	Cytochrome P450
FVEG_09972	NS	NS	Isoflavone reductase
FVEG_16699	2.996	0	Fungal specific transcription factor
FVEG_16700	10.229	1.02E-230	ABC transporter
FVEG_09974	9.087	0	SnoaL-like domain
FVEG_09975	9.590	0	NAD dependent epimerase/dehydratase family
FVEG_09976	10.893	1.16E-121	Putative cyclase
FVEG_09977	11.459	1.84E-141	Transketolase, C-terminal domain
FVEG_09978	12.179	5.34E-203	Short chain dehydrogenase
FVEG_13976	5.965	2.43E-89	L-lysine 6-monooxygenase
FVEG_13977	4.337	1.21E-219	Carboxymethylenebutenolidase
FVEG_13978	NS	NS	Activator of stress protein
FVEG_13979	7.731	1.32E-51	Short chain dehydrogenase

[a] FC, fold change
[b] p-value refers to the false discovery rate adjusted p-value
[c] NS, not significant induction
Clusters are highlighted in alternate shadings.

Table 4.5 Shared induced genes among BOA, OXD, CMN, and CZX treatments

Gene #	BOA		OXD		CMN		CZX		Annotation
	log_2(FC)[a]	p-value[b]	log_2(FC)	p-value	log_2(FC)	p-value	log_2(FC)	p-value	
FVEG_00314	1.280	9.06E-03	2.048	5.85E-06	1.656	1.92E-04	1.523	2.90E-04	Zinc binding dehydrogenase
FVEG_01806	4.267	3.74E-197	3.318	1.61E-117	1.231	1.93E-21	1.863	4.91E-36	Thiolase, C-terminal domain
FVEG_03295	2.129	4.33E-21	1.464	2.67E-09	3.297	6.59E-62	2.397	1.66E-27	Hypothetical protein
FVEG_04214	1.183	9.83E-05	1.829	7.24E-11	2.271	5.16E-19	1.322	1.68E-06	Hypothetical protein
FVEG_05017	3.989	3.94E-211	1.747	3.79E-39	2.506	2.41E-64	3.698	7.69E-181	Coenzyme A transferase
FVEG_05278	1.401	7.17E-12	1.270	2.18E-09	1.830	6.66E-26	2.646	1.20E-42	Hypothetical protein
FVEG_06463	1.224	8.47E-05	1.019	3.08E-03	1.401	9.84E-09	3.272	5.30E-36	Aromatic ring-opening dioxygenase
FVEG_07389	5.517	4.22E-280	1.717	1.92E-25	1.869	3.26E-38	3.712	3.42E-125	Nitroreductase
FVEG_07493	2.608	6.35E-39	3.212	2.09E-59	3.186	2.44E-61	3.383	1.15E-66	NmrA-like family
FVEG_09320	1.342	4.66E-02	1.687	1.27E-02	1.684	6.28E-03	2.472	3.37E-06	Heterokaryon incompatibility protein
FVEG_09854	1.499	1.68E-18	1.337	2.69E-14	1.353	1.75E-19	1.115	3.78E-11	Beta-lactamase
FVEG_11329	1.106	9.70E-22	1.005	1.74E-17	3.161	6.18E-253	1.744	1.25E-56	Lysine N-acyltransferase
FVEG_11958	1.509	8.69E-04	1.382	4.86E-03	5.539	1.23E-46	2.054	2.54E-07	C4-dicarboxylate transporter
FVEG_12238	1.555	2.44E-26	1.003	1.23E-10	3.346	2.12E-150	2.688	2.95E-79	FAD binding domain
FVEG_12499	1.432	2.13E-24	1.701	6.39E-35	1.744	1.03E-50	2.591	1.66E-85	Methyltransferase domain
FVEG_12866	1.169	1.64E-23	1.621	4.99E-45	3.108	2.60E-225	3.515	1.87E-216	Drug resistance protein
FVEG_13057	5.150	4.07E-219	2.685	1.42E-57	2.508	3.94E-61	4.708	2.93E-182	Amidohydrolase
FVEG_13686	1.590	6.19E-36	1.571	7.88E-35	2.076	1.72E-82	3.749	7.75E-223	Methyltransferase domain
FVEG_13687	1.035	1.83E-06	1.131	2.40E-07	1.452	4.49E-17	3.235	1.61E-67	NmrA-like family
FVEG_13979	7.707	9.84E-51	8.955	4.08E-68	1.807	2.05E-03	7.731	1.32E-51	Short chain dehydrogenase
FVEG_15235	1.884	2.88E-05	1.348	1.02E-02	2.807	1.19E-11	1.889	5.84E-06	Uncharacterized protein
FVEG_16505	1.184	1.23E-03	1.091	5.97E-03	2.571	4.30E-20	1.105	1.03E-03	Uncharacterized protein

[a] FC, fold change
[b] p-value refers to the false discovery rate adjusted p-value
Treatments are highlighted in alternate shadings

Table 4.6 Shared induced genes among BOA, OXD, and CZX treatments

Gene #	BOA		OXD		CZX		Annotation
	log_2(FC)[a]	p-value[b]	log_2(FC)	p-value	log_2(FC)	p-value	
FVEG_03387	6.204	6.13E-70	10.150	1.75E-187	7.909	4.93E-114	NAD(P)-binding Rossmann-like domain
FVEG_04841	2.522	4.86E-17	1.830	2.95E-08	2.250	6.33E-14	Hypothetical protein
FVEG_06534	1.305	3.80E-12	6.964	0.00E+00	1.035	3.57E-08	Hypothetical protein
FVEG_08763	1.885	3.45E-42	4.365	1.75E-250	1.116	3.32E-14	FAD dependent oxidoreductase
FVEG_08878	2.770	2.08E-07	9.345	6.25E-89	2.907	6.93E-09	Neutral amino acid permease
FVEG_09220	1.836	1.03E-34	1.158	6.99E-13	1.307	1.68E-17	Hemerythrin HHE cation binding domain
FVEG_09322	1.340	4.39E-08	1.183	6.46E-06	1.385	3.48E-09	Fungal specific transcription factor
FVEG_09414	4.184	2.73E-38	1.910	9.64E-08	1.318	8.22E-05	1,2-Dioxygenase
FVEG_10517	1.152	2.37E-09	1.226	4.02E-10	1.151	3.97E-10	3-Hydroxyacyl-CoA dehydrogenase
FVEG_10905	5.394	1.57E-68	6.424	3.99E-97	4.603	3.92E-50	Related to integral membrane protein PTH11
FVEG_12220	5.566	0.00E+00	5.954	0.00E+00	5.143	3.29E-278	SnoaL-like domain
FVEG_12508	2.478	1.81E-31	2.132	1.30E-22	2.797	7.27E-41	Thiamine pyrophosphate enzyme
FVEG_12509	5.420	3.83E-42	4.056	2.13E-22	3.301	3.33E-15	Acyl-CoA reductase (LuxC)
FVEG_13976	7.100	1.43E-126	9.572	5.53E-230	5.965	2.43E-89	L-lysine 6-monooxygenase
FVEG_13977	3.350	7.36E-131	5.800	0.00E+00	4.337	1.21E-219	Carboxymethylenebutenolidase
FVEG_13979	7.707	9.84E-51	8.955	4.08E-68	7.731	1.32E-51	Short chain dehydrogenase

[a] FC, fold change

[b] p-value refers to the false discovery rate adjusted p-value

Treatments are highlighted in alternate shadings

Table 4.7 Shared induced genes exclusively among only BOA, CMN, and CZX treatments

Gene #	BOA		CMN		CZX		Annotation
	$log_2(FC)^a$	p-value[b]	$log_2(FC)$	p-value	$log_2(FC)$	p-value	
FVEG_00022	2.588	5.87E-33	2.094	5.00E-23	2.943	1.10E-43	Zinc-binding dehydrogenase
FVEG_00023	4.022	2.13E-104	2.753	6.87E-50	2.919	9.96E-53	Cytochrome P450
FVEG_00094	1.410	1.31E-06	2.829	1.19E-31	1.350	7.16E-07	Hypothetical protein
FVEG_00201	1.149	6.09E-04	2.848	4.54E-32	1.678	6.66E-09	ADP-ribose pyrophosphatase
FVEG_00220	1.180	2.61E-04	1.363	5.61E-08	1.124	1.47E-04	Hypothetical protein
FVEG_01737	2.439	3.04E-05	2.551	1.08E-03	1.589	6.36E-03	Flavin-binding monooxygenase-like
FVEG_01983	1.063	4.05E-17	1.836	5.91E-70	1.822	7.35E-52	Putative pantothenate kinase
FVEG_02001	1.933	4.35E-13	1.737	1.57E-11	1.683	2.22E-10	Hypothetical protein
FVEG_02121	1.428	2.88E-34	1.868	3.35E-80	2.057	3.14E-72	3,4-dihydroxy-2-butanone 4-phosphate synthase
FVEG_02122	1.073	2.52E-37	1.337	1.49E-84	1.424	8.97E-67	Ribosomal protein L11 methyltransferase
FVEG_02231	1.828	1.75E-45	1.327	2.87E-32	1.314	4.93E-24	Histidine phosphatase superfamily
FVEG_03096	1.107	3.98E-14	1.557	2.71E-39	1.044	4.42E-13	Domain of unknown function (DUF4009)
FVEG_03434	1.076	4.81E-13	1.774	2.74E-39	2.099	9.17E-53	Thioesterase-like superfamily
FVEG_03678	1.330	8.89E-26	1.048	2.44E-20	1.890	8.31E-53	Fungal specific transcription factor
FVEG_03712	1.105	2.90E-09	1.773	2.56E-27	1.092	9.10E-10	NAD(P)-binding Rossmann-like domain
FVEG_05402	1.042	4.62E-08	1.387	1.23E-21	1.189	3.77E-11	Ribosomal protein
FVEG_05486	3.159	7.60E-187	1.288	5.63E-28	1.512	1.52E-41	Flavin reductase like domain
FVEG_06021	6.230	0.00E+00	2.137	2.58E-46	2.164	3.79E-39	Pyridoxal 5'-phosphate synthase
FVEG_06355	1.327	2.61E-23	2.119	1.86E-74	2.575	1.40E-88	PPR repeat family
FVEG_06356	1.222	8.75E-15	2.064	3.59E-55	2.438	1.06E-60	Helicase conserved C-terminal domain
FVEG_07842	1.518	2.43E-13	1.157	4.10E-10	1.667	7.58E-17	Hypothetical protein
FVEG_08287	10.910	0.00E+00	1.510	3.59E-06	1.966	4.99E-10	NmrA-like protein
FVEG_08293	10.909	7.63E-159	1.457	4.81E-04	1.836	1.76E-05	FAD binding domain
FVEG_08296	2.714	4.63E-39	1.419	1.00E-12	2.048	1.22E-21	Major facilitator superfamily
FVEG_08301	1.250	3.71E-08	1.859	6.66E-26	1.359	2.67E-10	Glycosyl hydrolases family

FVEG_08506	1.046	6.54E-14	1.665	1.18E-45	2.042	9.12E-54	Hypothetical protein
FVEG_08507	1.161	4.04E-14	2.344	3.16E-73	1.817	4.10E-36	Phospholipid methyltransferase
FVEG_09401	4.016	1.14E-24	1.770	5.11E-05	1.184	1.18E-02	Zinc-binding dehydrogenase
FVEG_09796	2.428	3.68E-96	2.055	4.18E-93	1.217	1.39E-23	Serine hydrolase (FSH1)
FVEG_09813	1.494	1.20E-46	1.957	6.60E-112	1.356	1.56E-38	Amidohydrolase
FVEG_09841	4.083	1.31E-20	4.746	3.71E-12	4.276	2.35E-23	MmgE/PrpD family
FVEG_09842	2.299	1.56E-03	4.286	1.70E-03	2.226	6.51E-04	SP: MFS transporter, sugar porter (SP) family
FVEG_09878	1.778	4.57E-03	2.215	1.30E-03	1.889	5.92E-04	Xylose isomerase-like TIM barrel
FVEG_10067	1.209	9.72E-08	1.325	1.67E-11	1.679	7.36E-16	Hypothetical protein
FVEG_10938	1.487	9.13E-25	1.912	4.83E-58	1.706	2.64E-33	FAD binding domain
FVEG_11172	1.336	6.31E-54	1.031	3.53E-44	1.693	2.23E-87	GTP cyclohydrolase II
FVEG_11330	1.194	2.39E-25	2.834	2.02E-197	2.530	8.23E-117	AMP-binding enzyme
FVEG_11398	1.118	1.10E-28	1.662	9.11E-85	1.718	2.19E-68	Adenylate kinases
FVEG_11439	4.487	2.03E-50	3.093	5.10E-21	2.082	4.97E-10	Endoribonuclease L-PSP
FVEG_11507	1.931	2.21E-04	2.922	3.53E-10	1.951	4.44E-05	Hypothetical protein
FVEG_12174	1.729	5.54E-50	1.462	8.89E-47	1.297	4.94E-27	Terpene synthase family, metal binding domain
FVEG_12625	9.143	3.21E-109	4.080	7.37E-17	3.136	9.24E-13	Dienelactone hydrolase family
FVEG_12634	10.679	6.92E-181	2.236	1.05E-08	1.941	1.63E-06	Carboxylesterase family
FVEG_12635	6.069	0.00E+00	1.733	2.13E-91	1.788	2.64E-85	Fungal specific transcription factor
FVEG_12636	9.523	0.00E+00	1.273	1.13E-16	2.430	1.55E-49	Arylamine N-acetyltransferase
FVEG_13006	5.246	6.76E-55	1.829	3.07E-06	1.966	2.63E-07	Hypothetical protein
FVEG_13056	1.120	1.43E-06	1.783	9.47E-24	1.738	1.10E-16	Fungal specific transcription factor
FVEG_13061	1.054	2.37E-02	1.939	2.21E-07	2.181	8.83E-10	Hypothetical protein
FVEG_13807	2.339	4.63E-04	2.395	2.02E-02	1.595	1.30E-02	KR domain
FVEG_13808	1.678	4.62E-07	1.148	1.43E-04	2.263	8.37E-14	SnoaL-like domain
FVEG_13989	2.865	2.08E-18	2.147	7.72E-12	1.147	1.88E-03	SMP-30/Gluconolaconase/LRE-like region
FVEG_14011	1.620	3.82E-02	2.835	4.37E-02	2.023	1.70E-03	Alpha amylase, catalytic domain
FVEG_14160	4.321	4.01E-111	1.445	9.04E-15	1.336	4.77E-10	Glycosyl hydrolase family
FVEG_14949	1.107	3.22E-02	1.384	6.26E-04	1.175	7.59E-03	Hypothetical protein

FVEG_15086	2.421	3.35E-04	2.822	5.89E-03	1.468	2.50E-02	Hypothetical protein
FVEG_15221	1.032	4.05E-06	2.081	2.16E-32	1.623	7.52E-16	Hypothetical protein
FVEG_15302	3.254	9.58E-11	2.353	2.82E-05	3.100	1.70E-10	Short chain dehydrogenase
FVEG_16409	1.551	3.60E-02	2.193	2.91E-02	2.173	2.86E-04	Berberine and berberine like
FVEG_17021	1.282	5.36E-03	2.235	8.69E-07	1.070	9.34E-03	Hypothetical protein

[a] FC, fold change

[b] p-value refers to the false discovery rate adjusted p-value

Treatments are highlighted in alternate shadings.

Table 4.8 Lactamase genes differentially expressed upon exposure to BOA, CMN, OXD, and CZX

Group	Gene#	Mean FPKM		$log_2(FC)$[a]	p-value[b]
		w/o Induction	w/ Induction		
BOA-up	FVEG_08291	3.199	2765.573	9.573	0.000E+00
	FVEG_09854	78.535	225.985	1.499	1.680E-18
	FVEG_12526	0.114	0.607	1.704	2.069E-02
	FVEG_12637	0.359	13.138	4.989	9.670E-30
BOA-down	FVEG_12347	1.263	0.411	-1.366	1.007E-02
CMN-up	FVEG_08291	3.151	5.917	1.035	1.763E-07
	FVEG_09854	77.331	194.239	1.353	1.751E-19
	FVEG_10996	2.166	5.186	1.297	7.105E-15
	FVEG_12159	9.454	65.409	2.737	6.898E-156
CMN-down	FVEG_04555	9.133	3.657	-1.282	1.142E-17
	FVEG_05854	8.558	0.288	-4.986	2.743E-71
	FVEG_09904	4.591	1.972	-1.274	3.837E-07
	FVEG_12637	0.353	0.088	-2.039	2.123E-03
	FVEG_13172	348.896	1.585	-7.794	3.726E-220
	FVEG_13253	0.839	0.279	-1.539	2.664E-04
OXD-up	FVEG_09854	78.535	201.618	1.337	2.69E-14
CZX-up	FVEG_03849	64.211	142.193	1.141	5.046E-38
	FVEG_05734	1.310	4.433	1.690	1.324E-09
	FVEG_09854	78.535	201.619	1.337	2.686E-14
	FVEG_12457	0.455	1.620	1.608	1.114E-04
CZX-down	FVEG_09904	4.662	0.642	-2.585	1.433E-14
	FVEG_12347	1.263	0.146	-2.142	1.647E-05
	FVEG_13172	354.235	71.106	-2.205	1.548E-15
	FVEG_13253	0.851	0.091	-2.131	8.939E-05

[a] FC, fold change

[b] p-value refers to the false discovery rate adjusted p-value.

Differentially expressed lactamase genes are highlighted in alternate shadings by treatment.

Table 4.9 MIPS functional categorization reveal differential trends in genes responsive to BOA, OXD, CMN, and CZX compounds

Functional Category	BOA		OXD		CMN		CZX	
	Up-regulated (422)	Down-regulated (165)	Up-regulated (164)	Down-regulated (37)	Up-regulated (1857)	Down-regulated (2478)	Up-regulated (1270)	Down-regulated (2061)
01 Metabolism	153	29	58	16	587	582	394	503
02 Energy	30				127	51		
12 Protein synthesis								31
14 Protein fate (folding, modification, destination)				2			33	
16 Protein with binding function or cofactor requirement	28		15		139	5	268	89
20 Cellular transport, transport facilities and routes	71	39	26	3	308	361	253	297
30 Cellular communication/signal transduction				1				
32 Cell rescue, defense and virulence	52	6	33		199	216	150	216
34 Interaction with the environment	6			3	57		81	6
41 Systemic development						5		
42 Biogenesis of cellular components					35		36	

Treatments are highlighted in alternate shadings.

Supplemental Table 4.1 Summary of RNA-seq mapping results

Sample treatment	Raw reads #	Mapped reads #	Mapping rates
Control-1	17239023	17042978	98.90%
Control-2	17788944	17377585	97.70%
Control-3	15630242	15186301	97.20%
BOA-1	16088932	15906235	98.90%
BOA-2	14644527	14500927	99.00%
BOA-3	15013010	14838938	98.80%
CMN-1	69300901	68189682	98.40%
CMN-2	69418371	68145812	98.17%
CMN-3	83976794	81331723	96.85%
OXD-1	15672040	15481366	98.80%
OXD-2	15532169	15354578	98.90%
OXD-3	15556372	15400751	99.00%
CZX-1	19650453	19475090	99.10%
CZX-2	14598789	14469840	99.10%
CZX-3	15322677	15167178	99.00%

Treatments are highlighted in alternate shadings.

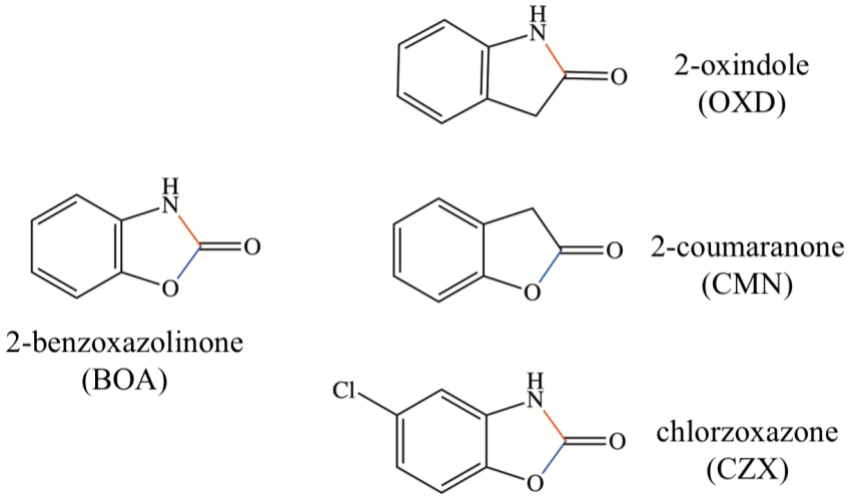

Figure 4.1 Chemical structures of BOA, OXD, CMN, and CZX.
Lactam bonds are highlight in red and lactone in blue.

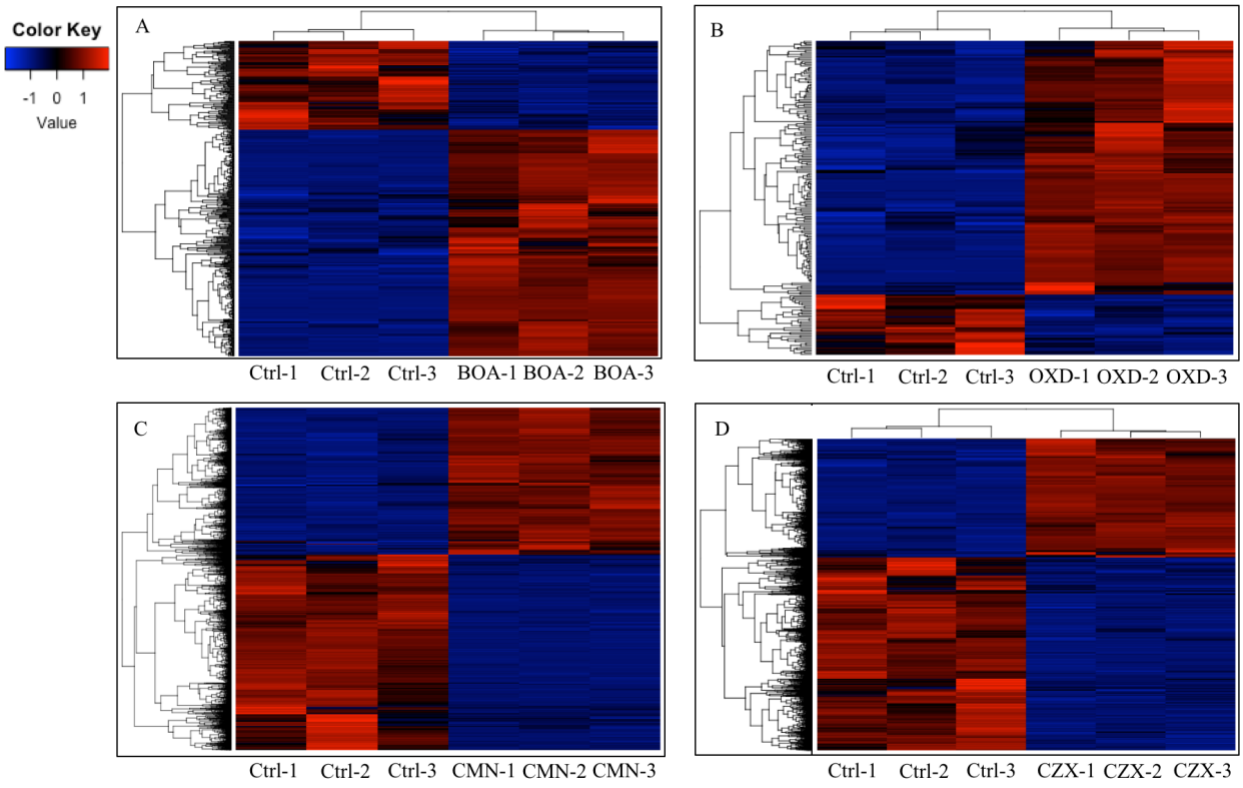

Figure 4.2 BOA, OXD, CMN, and CZX elicit differential gene expression. Heatmaps showing transcription levels of differentially expressed genes upon exposure to BOA (A), OXD (B), CMN (C), and CZX (D). The Y-axis represents genes that are clustered and colored by the similarity of $\log_2$(FPKM values). See the colored key. The X-axis shows the 3 biological replicates of each treatment. FPKM refers to Fragments Per Kilobase of transcript per Million mapped reads.

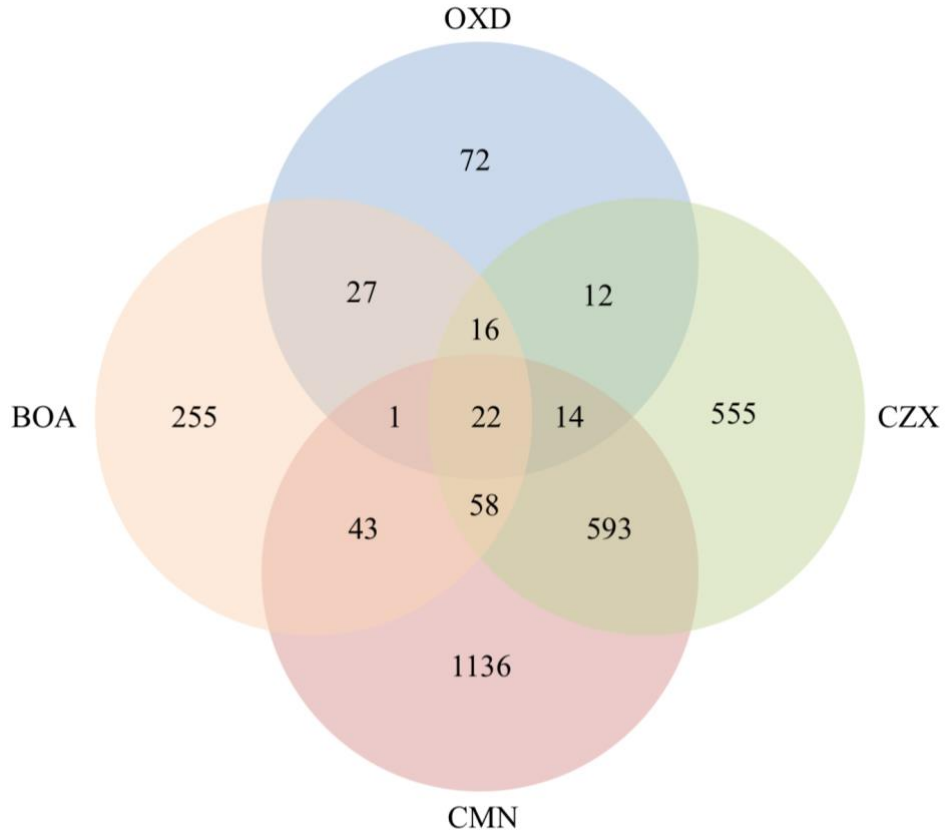

Figure 4.3 Co-upregulated genes were observed among BOA, OXD, CMN, and CZX treatments. Venn diagram shows the number of genes with altered expression due to BOA, OXD, CMN, or CZX exposure. Each circle represents one chemical treatment. Overlaps represent up-regulated genes shared between corresponding treatments.

CHAPTER 5

CONCLUSIONS

This dissertation explores the topic of xenobiotic degradation in *F. verticillioides*. The work presented here is a continuation of work by Glenn et al. (2016), in which a fungal β-lactamase was found responsible for *in vitro* resistance to the maize phytochemical 2-benzoxazolinone (BOA). The β-lactamases are important in bacteria for conferring degradative resistance to bactericidal β-lactam antibiotics. The substrates, β-lactams, disrupt biosynthesis of the bacterial peptidoglycan cell wall and have been a cornerstone of modern medicine. However, fungal cell walls are structurally unrelated to those of bacteria, and β-lactam antibiotics generally have no effect on fungal growth. This raised several interesting questions: how wide-spread and abundant are fungal lactamases across the kingdom; why do fungi possess β-lactamase genes in their genomes when β-lactams generally have no effect upon them; what might be the functions of the fungal lactamases and; what are their molecular characteristics? To address these questions, I conducted a detailed bioinformatic study to explore the molecular characteristics of lactamases in fungi with a particular focus on selected *Fusarium* species (which are very rich in lactamase genes) and conjecture on their possible ecological functions (Chapter 2). Inspired by the differing toxicities of pyrrocidine A and pyrrocidine B resulting from the presence or absence of a double bond within their lactam ring, respectively. I further identified and functionally characterized ten genes highly induced upon exposure to both pyrrocidines by RNA sequencing. Amongst other interesting findings, a PDR5-like ABC transporter-encoding gene, when deleted, increased the sensitivity of *F. verticillioides* dramatically to pyrrocidine B and was therefore identified as a

major tolerance locus (Chapter 3). Additional efforts were made to describe the transcriptomic responses of *F. verticillioides* upon individual exposure to 2-benzoxazolinone, 2-oxindole, 2-coumaranone, and chlorzoxazone (Chapter 4). Together, the work detailed in this dissertation pioneered the systematic studies of lactamases in fungi and elucidated the mechanism of resistance and transcriptional response to lactam compound-mediated antagonism by *Sarocladium zeae*, a co-inhabitant of maize seed with *F. verticillioides*. Finally, I generated biochemical inferences from transcriptomic changes in *F. verticillioides* after exposure to BOA and BOA-like chemicals.

Research Objective 1: Bioinformatically characterize beta-lactamase-encoding genes in fungi, with *F. verticillioides* serving as a paradigm

As absorptive feeders, fungi must colonize and ramify through their substrate to survive. Inevitably, soil fungi are exposed to numerous xenobiotic compounds produced and employed by other soil competitors as offensive molecular weapons. One prominent mechanism to combat the disadvantageous xenobiotics is through the production of corresponding degradative enzymes. In this research, through inferences from the classic example of "β-lactamases vs. β-lactams" in bacteria I described the abundance and potential roles for lactamases in soil fungi. In this research project, many fungal genes were identified exhibiting a high degree of similarity to β-lactamases. An overview of fungal genomes suggested a strong positive correlation between environmental niche complexity and the number of fungal lactamase encoding-genes, with soil-borne fungi showing dramatic amplification of lactamase genes compared to those fungi found in less biologically complex environments. It was hypothesized that many fungal hydrolytic lactamases are responsible for the degradation of plant or microbial xenobiotic lactam compounds. Most of the lactamase-encoding genes in *F. verticillioides* demonstrated traits of vertical inheritance while two may have a history of horizontal gene transfer. Structural predictions of *F. verticillioides*

lactamases also suggested similar catalytic mechanisms to those of their bacterial counterparts. Overall, this work was the first in-depth analysis of both "metallo-β-lactamases" (PF00753) and "serine-based β-lactamases" (PF00144) in fungi and addressed their fundamental and unexplored role as lactam hydrolases in soil microbiology.

Research Objective 2: Assess the impact of pyrrocidine lactam challenge on the *F. verticillioides* transcriptome and functionally characterize select interesting induced genes

S. zeae and *F. verticillioides* share the same ecological niche, the maize kernels. Pyrrocidine A and B, two lactam-containing compounds produced by *S. zeae* in maize kernels, demonstrated growth inhibitory effects against *F. verticillioides*. To speculate on possible mechanisms by which *F. verticillioides* survives in the presence of pyrrocidines, I explored the transcriptional responses via RNA sequencing in *F. verticillioides* upon exposure to pyrrocidine A or B at sub-inhibitory concentrations. A pleiotropic-drug resistance (PDR)-type ABC-transporter gene, *FvABC3* (FVEG_11089), was identified with the crucial role in contributing to pyrrocidine tolerance. Deletion of *FvABC3*'s adjacent transcription factor, *FvZEAR* (FVEG_11090), did not impact pyrrocidine tolerance during *in vitro* drug screening assays, though the induced expression of *FvZEAR* was observed in both pyrrocidine A and B treatments. Structural predictions of *FvABC3* suggested its role as a molecular pump in the cell membrane, excreting pyrrocidines. *FvZBD1* (FVEG_00314), a zinc-binding dehydrogenase encoding gene, was also identified due to its dramatic induction in transcriptomic analyses. Interestingly, deletion of *FvZBD1* significantly enhanced maize seeding virulence, which was corroborated by the remarkable increase in fumonisin production by *FvZBD1* mutants. The close proximity of *FvZBD1* to the well-known fumonisin biosynthetic gene cluster suggested a link between pyrrocidine

exposure and fumonisin production by *F. verticillioides*. It is also proposed to incorporate *FvZBD1* as part of the fumonisin biosynthetic cluster.

Research Objective 3: Compare the transcriptomic responses of lactam or lactone-containing benzoxazolinone-like compounds in *F. verticillioides*

2-oxindole (OXD), 2-coumaranone (CMN), and chlorzoxazone (CZX) are three lactam and/or lactone-containing compounds with similar chemical structures to the maize phytoanticipin, 2-benzoxazolinone (BOA). Inspired by transcriptional and functional analyses of lactamase gene-containing gene clusters in BOA degradation by *F. verticillioides*, I attempted to generate inferences regarding biochemical degradation of BOA through exposing *F. verticillioides* to BOA, OXD, CMN, and CZX. The primary focus was placed on induced genes of interest and putative clusters. In addition to corroborating the observed induction of *FDB1* and *FDB2* gene clusters, I identified an additional highly induced putative transcriptional regulator encoding gene (FVEG_12642) directly adjacent to the *FDB2* cluster. Four additional gene clusters were also identified with putative hydrolytic functions. Exposing *F. verticillioides* to OXD elicited the expression of three putative degradative gene clusters, one of which (FVEG_06533 – FVEG_06535) exhibited functional similarities to a newly identified gene cluster (FVEG_09969 – FVEG_09978) upon exposure to BOA. Exposure to CMN provoked the expression of three interesting gene clusters in *F. verticillioides*, one of which was previously identified as the fusaric acid biosynthetic gene cluster (FVEG_12519 to FVEG_12534). Interestingly, CZX exposure elicited over 81-fold induction of a dehalogenase, which is not surprising in that CZX has the same structure as BOA with an additional chlorine modification to the benzene ring. In addition, three putative hydrolytic gene clusters were also turned on by CZX exposure, one of which (FVEG_13976 to FVEG_13979) was also observed as induced in BOA and OXD treatments.

Genes associated with degradation of either lactam or lactone moieties were also identified, which may be targeted for future functional analyses.

The work described in this dissertation serves as the first in-depth analysis of both "metallo-β-lactamases" and "serine-based β-lactamases" in fungi and their potential relevance to resistance to antimicrobials in the environment. Transcriptional and functional characterization of *F. verticillioides* genes responding to lactam-containing pyrrocidine compounds revealed molecular defensive mechanisms and established a link between xenobiotic exposure and mycotoxin production. The putative gene clusters identified through BOA-like compound exposure will guide future directions for studying their functions in lactam and/or lactone hydrolysis.